INTRINSIC RESPONSE

PROPERTIES

OF AUDITORY THALAMIC

NEURONS IN THE

GERBIL (Meriones unguiculatus)

MICHAEL REID

AUS NEW JERSEY, U.S.A.

JOHANN WOLFGANG GOETHE

UNIVERSITÄT

FRANKFURT AM MAIN

2007

SUMMARY (in German)

Der Nucleus geniculatum mediale (MGB, medial geniculate body) ist in der aufsteigenden Hörbahn der Säuger die Umschaltstation auf der Ebene des Diencephalon (Zwischenhirn), nach den Kerngebieten Ganglion ciliare (dessen Fasern den Hörnerven bilden), dem Nucleus cochlearis, dem oberen Olivenkomplexes, dem Colliculus inferior und dem Lemniscus laterale. Vom MGB aus wird die Erregung zu den auditorischen Arealen des Cortex cerebri (Hörkortex) weitergeleitet. Der MGB ist aber Teil der absteigenden Hörbahn. Er erhält direkte Eingänge vom Hörkortex und hat selbst Afferenzen zum Colliculus inferior. Diese absteigende Hörbahn reicht über den Olivenkomplex bis einer Innervation des Innenohrs, wo die Erregung der (äußeren Haarsinneszellen) beeinflusst werden kann. Der MGB ist damit sehr wahrscheinlich in unterschiedliche funktionelle Verarbeitungsschritte eingebunden.

Die Einbindung in mehrere Funktionen deutet sich auch in der internen Struktur des MGB an. Der ventrale Bereich des MGB (vMGB) ist tonotop organisiert, d.h. enthält eine systematische Frequenzanordnung, und ist ein Teil der primären Hörbahn. Neurone im vMGB sind damit Teil einer systematischen Frequenzrepräsentation, haben meist eine schmale Frequenzabstimmung und zeigen eine kurze Antwortlatenz bei akustischer Reizung. Der dorsale Bereich des MGB (vMGB) ist eine dagegen nicht tonotop organisierte Struktur, die sehr wahrscheinlich abgeleitete Funktionen bei der Hörverarbeitung hat, wie zum Beispiel die Integration der Hörinformation mit anderen Sinnessystemen. Neurone im dMGB sind nicht Teil einer systematischen Frequenzabbildung, haben meist eine breite Frequenzabstimmung und zeigen lange Antwortlatenzen bei der Reizung mit Reintönen (Calford & Webster 1981, Webster 1983).

Neuronen aus dem dMGB und dem vMGB, die jeweils an unterschiedlichen Verarbeitungsschritten im neuronalen Verbund beteiligt sind, zeigen möglicherweise auch

Unterschiede in ihren elektrophysiologischen Eigenschaften als Einzelneurone. Dies könnte wesentlich zu Unterschieden in der Verarbeitung beitragen. Solche Unterschiede können bei grundlegenden neuronalen Eigenschaften wie Ruhemembranpotenzial, Erregungsschwelle oder Antwortlatenz vorhanden sein. Solche Unterschiede sind zum Beispiel zwischen den Typ I- und Typ II- Neuronen des Ganglion ciliare zu finden (Reid et al. 2004). Es können aber auch abgeleitete Eigenschaften sein, wie z.B. den Fähigkeiten Erregung räumlich oder zeitlich zu integrieren. Der Vergleich der Neurone aus vMGB und dMGB eignet sich gut um mögliche Unterschiede in den intrinsischen elektrophysiologischen Eigenschaften der Nervenzellen mit unterschiedlichen Aufgaben bei der Hörverarbeitung zu korrelieren. Deshalb wurde dieser Vergleich zum zentralen Thema der vorliegenden Arbeit gemacht.

Für die Untersuchungen wurden lebende, frontal orientierte Hirnschnitte (200 µm Dicke) des Thalamus von 4 bis 5 Wochen alten Wüstenrennmäusen präpariert. Mit der patch clamp-Technik wurde elektrophysiologisch Potenziale von Neuronen des dorsalen und ventralen Bereichs des MGB abgeleitet. Es wurden sowohl die Reaktionen der Zellen auf hyper- als auch depolarisierende Strominjektion untersucht. Die dabei notwendigen Parameter für einen gute physiologischen Zustand der Hirnschnitte und eine stabile patch-clamp-Ableitung wurden in umfangreichen Vorversuchen ermittelt. Bereits in der Ableitapparatur war eine genaue Positionierung der Elektrode im dMGB oder vMGB unter optischer Kontrolle möglich. Zusätzlich wurden nach erfolgreicher Ableitung die Hirnschnitte fixiert, gegen Nissl gefärbt und zur Bestätigung der Ableitposition lichtmikroskopisch untersucht.

Insgesamt wurden 73 Neurone (vMGB: 34 Neurone, dMGB: 39 Neurone) vollständig untersucht. Deren Ruhepotenzial lag zwischen -79 mV und -45 mV. Dabei gab es keine Unterschiede zwischen vMGB-Neuronen und dMGB-Neuronen (vMGB: 62.9 mV; dMGB: 60.1 mV; Abb. 3.2). Wurden die Neurone vom Ruhepotenzial aus durch zunehmende

Strominjektion überschwellig depolarisiert, dann antworteten sie mit einer zunehmenden Anzahl von Aktionspotenzialen (Abb. 3.1). Diese wurden bei zunehmender Reizstärke in immer schnellerer Folge und mit immer kürzerer Latenz ausgelöst wurden. Allerdings gab es ein Potenzialniveau (zwischen -35 mV und -25 mV) bei dem eine maximale Feuerrate erreicht wurde. Bei noch höherer Depolarisation blieb diese maximale Feuerrate gleich oder nahm wieder ab.

Bei Stimulation von einem hyperpolarisierten Haltepotenzial aus (z.B. -90 mV) kam es zusätzlich zu Beginn der Antwort zu einem kleinen initialen Gipfel, dem eine schnelle Repolarisation (durch offensichtlichen Einstrom) folgte (Abb. 3.0). Nach deren Abklingen kam es zum Potenzialanstieg mit einer schnellen Folge von Aktionspotenzialen. Die Feuerschwellen zum Auslösen von Aktionspotenzialen im MGB lagen zwischen -54 mV und -32 mV. Die mittleren Schwellenwerte im vMGB (42.9 mV) und dMGB (44.3 mV) waren nicht signifikant verschieden. Die Dauer der an der Schwelle ausgelösten Aktionspotenziale wurde bei halber Höhe gemessen und verglichen. Auch dieser Wert war im Mittel zwischen vMGB (2.04 ms) und dMGB (1.95 ms) nicht verschieden. Diese Werte änderten sich bei höherer Stimulation kaum.

Außerdem wurden der Membranwiderstand (d.h. der "Eingangswiderstand") der Neurone bei Potenzialen um das Ruhepotenzial ("niedriges Potenzial") und bei Potenzialen oberhalb der Feuerschwelle ("hohes Potenzial") gemessen. Die Membranwiderstände in beiden Bereichen des MGB waren im Mittel bei niedrigem Potenzial deutliche höher (vMGB: 307.0 MΩ; dMGB: 237.5 MΩ) als bei hohem Potenzial (vMGB: 61.0 MΩ; dMGB: 64.2 MΩ) und in beiden Zuständen zwischen vMGB und dMGB nicht signifikant unterschiedlich.

Da aufgrund der Literatur mögliche Unterschiede zwischen ventralem und dorsalem Bereich des MGB bei der Fähigkeit der Neurone zur Integration über mehrere Eingänge zu

erwarten waren, wurden zusätzlich Zeitparameter und die Dynamik der Reizantworten untersucht, die besonders für die zeitliche Integration wichtig sind. Dabei fiel besonders auf, dass die Neurone teilweise eine starke Adaptation (Abnahme) der Aktionspotenzial-Rate über die Dauer des Reizes (200 ms) hinweg zeigten. Dieses Verhalten wurde bei maximaler Aktionspotenzial-Rate (siehe oben) näher untersucht.

Zum einen zeigte sich, dass die Neurone unterschiedliche schnelle Adaptations-Raten zeigten (Abb. 3.3a,b). Quantifiziert wurde das mit der Anzahl der Aktionspotenziale während des Reizes von 200 ms Dauer (Adaptationsrate). Die Neurone zeigten maximal zwischen 1 und 23 Aktionspotenziale (Abb. 3.4). Sie wurden entweder in schnell adaptierende Neurone (bis max. 4 Aktionspotenziale) oder langsam adaptierende Neurone (5 und mehr Aktionspotenziale während der Reizdauer) eingeteilt. In schnell adaptierenden Neuronen war gleichzeitig auch die Folge von Aktionspotenzialen (max. 5 APs; siehe Abb. 3.4) vor Ende des Reizes beendet (Beispiel in Abb. 3.3B), während das bei langsam adaptierenden Neuronen (bis zu 23 APs) nicht der Fall war (Beispiel in Abb. 3.3A). Dieses Kriterium hatte sich schon im peripheren Hörsystem bewährt (Adamson et al. 2002; Reid et al. 2004). Die meisten Neurone im MGB der Wüstenrennmaus waren schnell adaptierend (76.5%; n = 56; Fig. 3.4).

Beim Adaptationsverhalten gab es klare Unterschiede zwischen vMGB und dMGB. Der Anteil langsam adaptierender Neurone im dMGB war deutlich höher (33%) als im vMGB (11%; Abb. 3.3D). Entsprechend war die mittlere Anzahl an ausgelösten Aktionspotenzialen bei vergleichbarem Haltepotenzial im dMGB deutlich höher (6.0 APs) als im vMGB (2.0 APs; Abb. 3.3C). Die große Mehrheit der langsam adaptierenden Neuronen (in absoluten Zahlen) wurde im dMGB gefunden (13 von 17 Neuronen). Ein Teil der langsam adaptierenden Neurone zeigte außerdem spontane Erregung (Aktionspotentiale) schon auf dem Niveau des Ruhepotenzials (n= 4; Beispiel in Abb. 3.5). Diese Neurone wurden alle im

dMGB gefunden. Die Spontane Rate lag dabei zwischen 12 und 15 Hz. Der Anteil an den langsam adaptierenden Neuronen betrug dabei 24%).

Um das Adaptationsverhalten noch genauer an analysieren wurden die Abstände der Aktionspotenziale gemessen und gegen den Zeitverlauf des Reizes aufgetragen. Es zeigte sich, dass das Adaptationsverhalten unabhängig von der absoluten Feuerrate war (Abb. 3.6). Nur die ersten Intervalle schwankten stark, danach pendelte sich meist das Verhalten auf einen mittleren Wert ein. Dieser blieb bei langsam adaptierenden Neuronen sehr konstant (Abb. 3.7, hier als Verhältnis der Intervalle zw. Aktionspotenzialen (I_{n+1}/I_n), das um 1 herum schwankte). Das mittlere Verhältnis der Intervalle war im vMGB 1.04 und im dMGB 1.08.

Entscheidend für den Grad der zeitlichen Erregungsintegration ist auch die Geschwindigkeit des Erregungsanstiegs beim Einsetzen des Reizes (sog. Anstiegskinetik). Dadurch werden zwei eng miteinander zusammenhängende Parameter bestimmt: die Latenz bis zum Auftreten des ersten Aktionspotenzials und die Zeitkonstante des Potenzialanstiegs bei depolarisierenden Strominjektionen. Diese Parameter waren massiv von der Reizstärke abhängig und wurden mit zunehmender Reizstärke deutlich kürzer (Beispiele in Abb. 3.8).

Bei beiden Parametern zeigten sich außerdem signifikante Unterschiede zwischen Neurone des vMGB und des dMGB. Ventrale Neurone antworteten im Mittel mit deutlich kürzeren Latenzen bis zum ersten Aktionspotenzial (vMGB: 41.5 ms) als dorsale Neurone (dMGB :128.4 ms), letztere betrugen im Mittel das dreifache der Latenzen im vMGB. Neurone im vMGB zeigten dabei Latenzen in einem viel größeren Bereich (29 – 250) als Neurone im dMGB (130 – 260). Verlängerte Latenzen blieben über den ganzen Potenzialbereich bei Depolarisation erhalten: Neurone die an der Schwelle eine längere Latenz hatten, zeigten auch bei stärkerer Depolarisation eine längere Latenz (Abb. 3.9). Entsprechend zeigte auch die Gruppe der langsam adaptierenden Neurone längere Latenzen (137 ms) als die schnell adaptierenden (54 ms).

Die Zeitkonstanten des Potenzialanstiegs bei depolarisierenden Reizen wurden ermittelt, indem eine Exponentialfunktion an den Potenzialverlauf (Bereich Ruhepotenzial bis erstes Aktionspotenzial, Abb. 3.10) angepasst wurde. Die Zeitkonstanten dieser Funktionen betrugen im Mittel bei Neuronen des vMGB 6.9 ms, bei Neuronen des dMGB 116.7 ms. Auch die Zeitkonstanten wurden mit stärkerer Depolarisation kürzer (Abb. 3.12). Die Unterschiede zwischen vMGB und dMGB, und die Abhängigkeit von der Reizstärke bei den Zeitkonstanten waren bei den Neuron sehr eng mit dem Verhalten bei den Latenzen korreliert.

Neurone des vMGB sind hauptsächlich für die Fortleitung von primären auditorischen Eingängen verantwortlich, die Neurone des dMGB integrieren dagegen verschiedene multimodale Eingänge. Ein Vergleich der hier gefundenen Unterschiede mit den peripher gelegenen Neuronen des Hörnerven, den Fasern des Spiralganglion vom Typ I und Typ II, erbrachte ein vergleichbares Muster. Neurone vom Typ I vermitteln primäre auditorische Eingänge und haben kurze Antwortlatenzen sowie schnelle Zeitkonstanten im Antwortpotenzial auf elektrische Reizung. Neurone vom Typ II integrieren dagegen über viele Eingänge, auf elektrische Reizung hin zeigen sie langsame Erregung und vielfach eine langsame Adaptation.

Zusammenfassen ergibt sich als generelles Muster für die physiologischen Eigenschaften der beiden Zelltypen in der peripheren und der zentralen Hörbahn, dass Grad der Adaptation, Antwortlatenz und Zeitkonstanten in der Erregung in direktem Zusammenhang zur Anzahl der Eingänge steht, über welche die Neurone integrieren müssen. Hohe Integration korreliert dabei mit langsamer Adaptation, deutlich längerer Antwortlatenz und verzögertem Erregungsanstieg. Umgekehrt korreliert die präzise Weitergabe einzelner Eingänge mit schneller Adaptation, sowie kurzer Antwortlatenz und schneller Anstiegskinetik der Erregung.

ABSTRACT

Neurons in the medial geniculate body (MGB) have the complex task of processing the auditory ascending information from the periphery and a more extensive descending input from the cortex. Differences in the pattern of afferent and efferent neuronal connections suggest that neurons in the ventral and dorsal divisions of the MGB take different roles in this complex task. The ventral MGB (vMGB) is the primary, tonotopic, division and the dorsal MGB (dMGB) is one of the higher order, nontonotopic divisions. The vMGB neurons are arranged tonotopically, have sharp tuning properties, and a short response delay to acoustic stimuli. The dMGB neurons are not tonotopically arranged, have broad tuning properties, and a long response delay to acoustical stimuli.

These two populations of neurons, with inherently different tasks, may display differences in intrinsic physiological properties, e.g. the capacity to integrate information on a single cell level. Neurons of the ventral and dorsal divisions of the MGB offer an ideal system to explore and compare the intrinsic neuronal properties related to auditory processing.

Coronal slices of 200 μm thicknesses were prepared from the thalamus of 4 - 5 week old gerbils. The current-clamp configuration of the patch-clamp technique was used to do experiments on the dorsal and ventral divisions of the medial geniculate body. Slices were subsequently Nissl stained to verify the location of recording.

Recordings from the dorsal and ventral divisions exhibited differences in response to depolarizing current injections. The ventral division responded with significantly shorter first spike latency (vMGB = 41.50 ± 7.7, dMGB = 128.43 ± 16.28; ($p < 0.01$)) and rise time constant (vMGB = 6.95 ± 0.90, dMGB = 116.67 ± 0.13; ($p < 0.01$)) than the dMGB.

Neurons in the dorsal division possessed a larger proportion of slowly accommodating neurons (rapidly accommodating: vMGB: 89%, dMGB: 64%), including a subpopulation of neurons that fired at resting membrane potential.

Neurons in the vMGB are primarily responsible for relaying primary auditory input. Dorsal MGB neurons relay converging multimodal input. A comparative analysis with the primary auditory neurons, the Type I and Type II spiral ganglion neurons, reveals a similar pattern. Type I neurons relay primary auditory input and exhibit short first spike latencies and rise time constants. The Type II neurons relay converging input from many sources, while possessing significantly slower response properties and a greater subpopulation of slowly accommodating neurons. Hence, accommodation, first spike latency, and rise time constant are suggested to be a reflection of the amount of input that must be integrated before an action potential can be fired. More converging input correlates to slower accommodation, a longer first spike latency and rise time. Conversely, a greater capacity to derive discrete input is associated with rapid accommodation, along with a short first spike latency and rise time.

E R K L Ä R U N G

Ich erkläre hiermit, dass ich mich bisher keiner Doktorprüfung unterzogen habe.

Frankfurt am Main, den........22 Oktober 2007...........................

....

(Unterschrift)

Eidesstattliche Versicherung

Ich erkläre hiermit an Eides Statt, dass ich die vorgelegte Dissertation über

INTRINSIC RESPONSE PROPERTIES OF AUDITORY THALAMIC NEURONS IN

THE GERBIL (Meriones unguiculatus)

selbständig angefertigt und mich anderer Hilfsmittel als der in ihr angegebenen nicht bedient habe, insbesondere, dass aus Schriften Entlehnungen, soweit sie in der Dissertation nicht ausdrücklich als solche mit Angabe der betreffenden Schrift bezeichnet sind, nicht stattgefunden haben.

Frankfurt am Main, den...................................... ....
(Unterschrift)

ACKNOWLEDGEMENTS

I am also indebted to many individuals outside of the lab for making this thesis possible. First and foremost, I acknowledge my mother, **Amelia Chandler Reid**, who contributed tremendously to this effort. She was the single most significant factor responsible for my educational and professional progress. She has also been a positive role model, as a paragon of integrity, wisdom, and steadfastness. Her emotional support and guidance has given me vision, wherewithal, and strength. My gratefulness exceeds expression and can only be measured by a greater Force. Thanks.

I also thank and acknowledge my wife, **Zephaniah Nixon-Reid**, for her material and emotional support throughout, along with our daughter, **Zaire**. Both have sacrificed and endured more than I could have ever anticipated or could have expected during this endeavour. Their stalwart love and support ensured that I bring this project to completion and shall never be forgotten.

I also thank my aunt**, Jane Harris,** who has consistently and unquestionably supported my efforts at various critical points. She has been the common denominator over the decades for my mother, me, and many others. Without her nothing would have been possible.

Family and friends, particularly **Ken, Karen, and KJ Ellis**; **Byron, Nadine, and Nina Wiley; The Murphys; Tyrone Thomas, Eddie Harris, Shannon Pridgen, Lemont Streeter**, **Dan Falcon,** and, most importantly and at many critical moments, my brother, **Victor Larry Reid,** have supported me in spirit and oft times financially throughout this arduous endeavour. I sincerely thank them and maintain an eternal debt of gratitude.

I also thank the German state of Hessen and the Johann Wolfgang Goethe Universität Frankfurt Am Main for the investment in my education and the quality of life afforded to my family during our stay in Deutschland. The German government and people have shown graciousness and humanity to us, particularly the **Raabe Family** and the **Bouchon Family**, which have given me a new awareness of the potential kindness within human nature.

I must also acknowledge the consistent and critical support that I have received from friends within the field, especially **Dr. Jonathon D. Victor**, of Cornell University Medical College. His sincere concern and guidance, intellectually and more importantly personally, over the years will forever be appreciated by my family. **Drs. Veronica Nwosu, Eugene Eaves, Lana Henderson, and Ja'net Chappelle,** of my alma mater, have been of enormous support and have shown great courage and integrity. Without them so much would have been impossible. Also, **Drs. Dale Purves**, of Duke University; **Dr. Gordon Silverman**, of Rockefeller University; **Dr. Paul Glimcher**, of New York University; **Dr. Aziz Hafidi**, of Universite Victor Segalen Bordeaux 2; and **Dr. Rodolfo Llinas**, of New York University have individually and consistently extended themselves in support of this effort. Thanks.

Let it not go without being said that the aforementioned's support over the years constitutes the majority of all support received. The significance of producing an African American scientist would be difficult to overstate. Despite the heroic efforts of the United States government and private industry, expending over 2 billion U.S. dollars, over 2 decades, to train over 250,000 "minority" students, there has been negligible success (less than 1% of scientists in the U.S. are African American). Therefore, I am compelled to clearly and unequivocally acknowledge the means and express the gratitude for this concerted effort. Thanks to all.

ABBREVIATIONS

ACSF	artificial cerebral spinal fluid
ADP	afterdepolarization
cAMP	cyclic adenosine monophosphate
CCD	charged-coupled device
dMGB	dorsal medial geniculate body
FRB	fast repetitive bursting/ chattering
FS	fast spiking
IB	intrinsically bursting
ICC	inferior colliculus
IHC	inner hair cells
IR-DIC	infra-red differential interference contrast
ISI	interspike interval
I_h	hyperpolarization-activated cation channel activity
I_T	voltage and time dependent inward Ca^{2+} current
LTS	low-threshold spiking
ms	millisecond
mV	millivolts
NMDA	N-methyl-D-aspartate
OHC	outer hair cells
pS	picosiemens
RMP	resting membrane potential
RS	regular spiking
RT	room temperature
SGN	spiral ganglion neurons
SOC	superior olivary complex
vMGB	ventral medial geniculate body

Table of Contents

1.0 INTRODUCTION

1.01 Sound

Encoding sound into the nervous system is a complex task. The underlying complexity of sound involves many intricate biological processes, beginning with the transduction of sound into a neural code within the peripheral auditory system. Sound produces an air pressure change that, upon entering the external ear, sets into motion middle ear mechanical machinations that culminate into neural signals in the cochlea. These neural signals are relayed with high temporal fidelity to the central nervous system for higher auditory processing. The focus herein is to gain a better understanding of the intrinsic neural mechanisms that are involved in the encoding of sound on the central auditory nervous system level, within the thalamus.

1.02 Mechano-electrical Transduction in the Auditory Periphery

Sound is a temporally varying phenomenon and the role of timing in neural encoding is more critical in encoding sound than in any of the other sensory systems. The auditory system has the nontrivial task of processing information about sound frequency and amplitude at precisely coordinated times. Thus a rigorous temporal regimen is necessary to encode and relay sounds from the auditory receptors, the hair cells in the cochlea, to the primary auditory cortex. Sound consists of frequency and amplitude components. Sound waves or the sound induced movement of air molecules that reach the ear are transformed through the outer and middle ear structures before reaching the cochlea in the inner ear (Figure 1.1). Within the cochlea the hair cells transduce sound induced movements as small as a nanometre into ion

conductance changes with microsecond resolution (Corey & Hudspeth, 1983). Conductance changes within the hair cells sum to generate a signal that follows the vibrations of sound waves, a cochlear microphonic potential, as high as 20 kHz in humans and 100 kHz in some bat species (Suga, 1988). These mechano-electrical transduction mechanisms initiate the neural response to sound by releasing neurotransmitters onto primary auditory neurons.
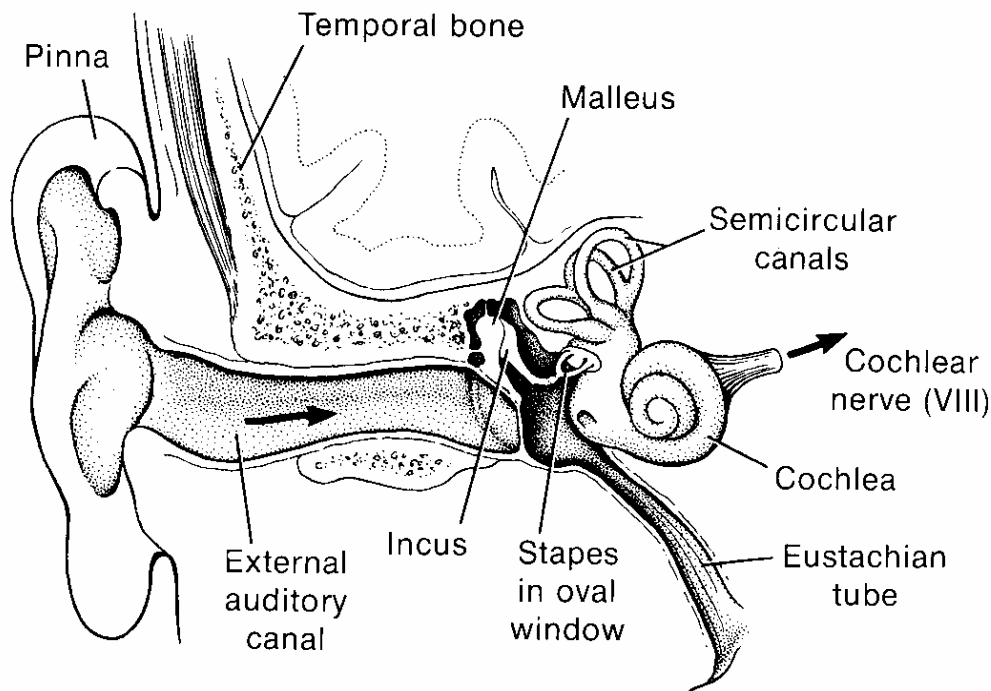
Figure 1.1. The cochlea in the inner ear houses the hair cells, which are connected to the neurons responsible for encoding sound. Sound travels through the outer ear and middle ear to reach the spiral ganglion neurons in the cochlea. The spiral ganglion neuron, the first step into the nervous system for sound, relays the signal to the brainstem nuclei along the VIII Cranial Nerve. (Adapted from Eckert & Randall, 1978).

1.03 Topographic Organization of the Auditory System

Functionally, another important process in the cochlea besides mechanoelectrical transduction is spectral decomposition. Sound is decomposed into component frequencies and encoded in the cochlea according to the frequency. In the auditory system the functional topography is organized tonotopically, according to frequency. High frequency sounds are encoded at the opposite end of the tonotopic axis as low frequency sounds, with intermediate

19

frequencies graded along this axis (Miller, 1997; Raphael & Altschuler, 2003). Different frequencies excite hair cells and spiral ganglion neurons at different places along the basilar membrane from the basal to the apical end. This introduces a spatial component. Hence, sound encoding is a spatio-temporal process. This organizational structure based upon frequency extends, beginning in the cochlea, along the entire primary auditory pathway to the cortex.

Several functional characteristics in the auditory periphery are related to the tonotopic gradient. The tonotopic organization is related to the timing of the latency of the initial spike in response to a depolarizing current injection (Adamson & Reid et al., 2002a,b; Reid et al., 2004). In general, current injection induced responses in the membrane potential of neurons located in the high frequency region of the cochlea are faster than those found in the low frequency region (Adamson & Reid et al., 2002a, b). Gradients of K^+ channel subtypes, i.e. $Kv_{3.1}, Kv_{1.4}$, BK, and $Kv_{1.1}$, that may be involved in shaping the kinetics of neuronal response properties were also found to be organized according to tonotopy (Adamson & Reid et al., 2002a,b). This shows that the tonotopic organization offers an additional layer of computational capacity.

In the cortex this capacity is expanded further as the tonotopic map is relayed onto multiple auditory cortical areas. An indication of the behavioural significance of hearing can be deduced by the extent of parcellation and cortical area dedicated to the auditory system. In the gerbil sound is relayed to at least 8 areas (Scheich et al., 1993; Thomas et al., 1993). Primates possess at least 20 interconnected auditory cortical areas (Kaas & Hackett, 2000). There are species whereby very few auditory areas may exist also, such as in the marsupials where only one auditory area exists (Gates & Aitkin 1982), or insectivores where only 3 or 4 exist, or approximately 6 in carnivores (Merzenich & Schreiner, 1992). The auditory system may differ between species but there are several commonalities that define all mammalian auditory systems.

1.04 Primary Auditory Processing

In the cochlea there are two types of auditory receptors, the inner hair cells (IHC) and the outer hair cells (OHC), and they transmit their signals to at least two types of neurons, Type I or Type II spiral ganglion neurons (SGN). All auditory information reaching the nervous system must travel along the spiral ganglion neurons. Sensory stimuli travels from the spiral ganglion neurons in the periphery to the cochlear nuclei (dorsal, posteroventral, and anteroventral cochlear nuclei) in the brainstem and then on to the inferior colliculus either along the lateral lemniscus or via the superior olivary complex. Neurons of the core and cortex of the inferior colliculus project to the ventral and dorsal medial geniculate body of the thalamus, respectively, which then innervates the auditory cortex (Figure 1.2).

The Type I and Type II SGNs play different specific roles in the encoding of sound but both adhere to a tonotopic organization, although their functional properties differ. The Type I neurons are responsible for encoding precise frequency information whereas the Type II neurons integrate converging information, which can be better understood upon consideration of the different innervation patterns. The Type I group receives input from individual IHCs and the Type II group receives input from many OHCs. Therefore one IHC receives innervation from many Type I neurons but each Type I neuron innervates only one IHC. Each Type II neuron innervates many OHCs, thereby acting as a convergent relay for the OHCs. Upon comparison of electrophysiological response properties, the Type II SGNs were found to have slower response properties than the Type I SGNs (Reid et al., 2004). Hence, slower response properties were found in neurons that receive a greater amount of synaptic input.

Once the information is encoded in the spiral ganglion neurons it is relayed into the brainstem and parceled into separate functional and spatial streams, following parallel afferent

routes. These parallel routes extend from the cochlear nucleus directly to the inferior colliculus but may also go to the inferior colliculus via routes relayed through the trapezoid body or the olivary complex (Casseday et al., 2000). In order for the auditory information to reach the cortex for higher processing it must be relayed through the inferior colliculus and the medial geniculate body of the thalamus.

1.05 Auditory Processing in the Thalamus

How is auditory information encoded in higher order processing in the central auditory nervous system? The thalamus was chosen to explore this question further. The term "thalamus" is commonly used to refer to the dorsal thalamus, which is only one of four portions of the diencephalon area of the brain. The diencephalon can be divided into the dorsal and ventral thalamus, the epithalamus, and the hypothalamus (Jones, 1985; Rose, 1958). In mammals the dorsal thalamus forms the largest part of the thalamus and is the source of the majority of subcortical input to the cerebral cortex. The dorsal thalamus contains two morphologically and functionally distinct classes of neurons, the relay neurons, which project outside of the thalamus, and interneurons, whose axons do not leave the thalamic nuclei in which they reside. This distinction was first recognized by Ramon y Cajal and later confirmed in electrophysiological and anatomical studies (Anderson et al., 1962). Immunocytochemical studies demonstrated that projection neurons in the dorsal thalamus use excitatory neurotransmission, while interneurons use the inhibitory neurotransmitter GABA (Jones, 1985, 2003; Penny & Diamond, 1984; Spreafico et al., 1983, 1994). Previous electrophysiological and neuroanatomical studies have consistently demonstrated that projection neurons provide excitatory output and GABAergic interneurons are a prominent source of intrathalamic inhibitory input (Jones, 1985). GABAergic interneurons are not present in all thalamic nuclei of every mammalian species. In primates and carnivores

GABAergic neurons are prevalent in the entire dorsal thalamus but they are virtually nonexistent in rodents, with the exception of the lateral geniculate nucleus (Barbaresi et al., 1986; Bentivoglio et al., 1991). Another major source of inhibition to the dorsal thalamus is the reticular nucleus of the ventral thalamus provides (Jones et al., 1975). There is also significant feedforward inhibition to the MGB from the inferior colliculus (Winer et al., 1996; Peruzzi et al., 1997).

The main auditory area of the dorsal thalamus is the medial geniculate body, which consists of three main areas: the ventral, dorsal, and medial divisions. The vMGB and dMGB divisions primarily relay auditory information whereas the medial division is primarily multisensory, integrating limbic and visceral information.

Figure 1.2. Connections in the auditory system. This cartoon depicts the entire auditory pathway. Auditory information enters at the spiral ganglion neuron level. Information is then relayed to the cochlear nucleus (AVCN, PVCN, DCN). Parallel routes are taken through the brainstem nuclei (LSO, MSO, MNTB, DNLL, VNLL) to reach the midbrain (ICc, ICp, ICdc, ICx). The primary auditory information is then relayed to the vMGB. Both pathways ultimately connect to the auditory cortex. Secondary auditory information is relayed to the dMGB. Information is processed and relayed to other cortical areas (temporal lobe, frontal lobe, parabelt, belt). The cortical connections are extensive and vary with species. Connections may be reciprocal, excitatory or inhibitory. The subcortical connections are generic for mammals. Abbreviations of subcortical nuclei: AVCN, anteroventral cochlear nucleus; PVCN, posteroventral cochlear nucleus; DCN, dorsal cochlear nucleus; LSO, lateral superior olivary nucleus; MSO, medial superior olivary nucleus; MNTB, medial nucleus of the trapezoid body; DNLL, dorsal nucleus of the lateral lemniscus; VNLL, ventral nucleus of the lateral lemniscus; ICc, central nucleus of the inferior colliculus; ICp, pericentral nucleus of the inferior colliculus; ICdc, dorsal cortex of the inferior colliculus; ICx, external nucleus of the inferior colliculus; MGv, ventral nucleus of the medial geniculate complex; MGd, dorsal nucleus of the medial geniculate complex; MGm, medial nucleus of the medial geniculate complex; Retic, reticular nucleus of the thalamus; Sg, suprageniculate nucleus; Lim, limitans nucleus; PM, medial pulvinar nucleus.

Association Cortex
Frontal
Lobe

Association Cortex
Temporal
Lobe

Auditory Cortex
Parabelt

Auditory Cortex
Belt

Auditory Cortex
Core

Thalamus

Midbrain

Lateral
Lemniscus

Superior
Olivary
Complex

Cochlear
Nucleus

Spiral
Ganglion

4 Areas

3 Areas

2 Areas

7 Areas

A I   R   RT

MG v   MG d   MG m   Retic   Sg/Lim

ICc   IC p   IC dc   IC x

DNLL   VNLL

LSO   MSO   MNTB

AVCN   PVCN   DCN

Auditory
Nerve
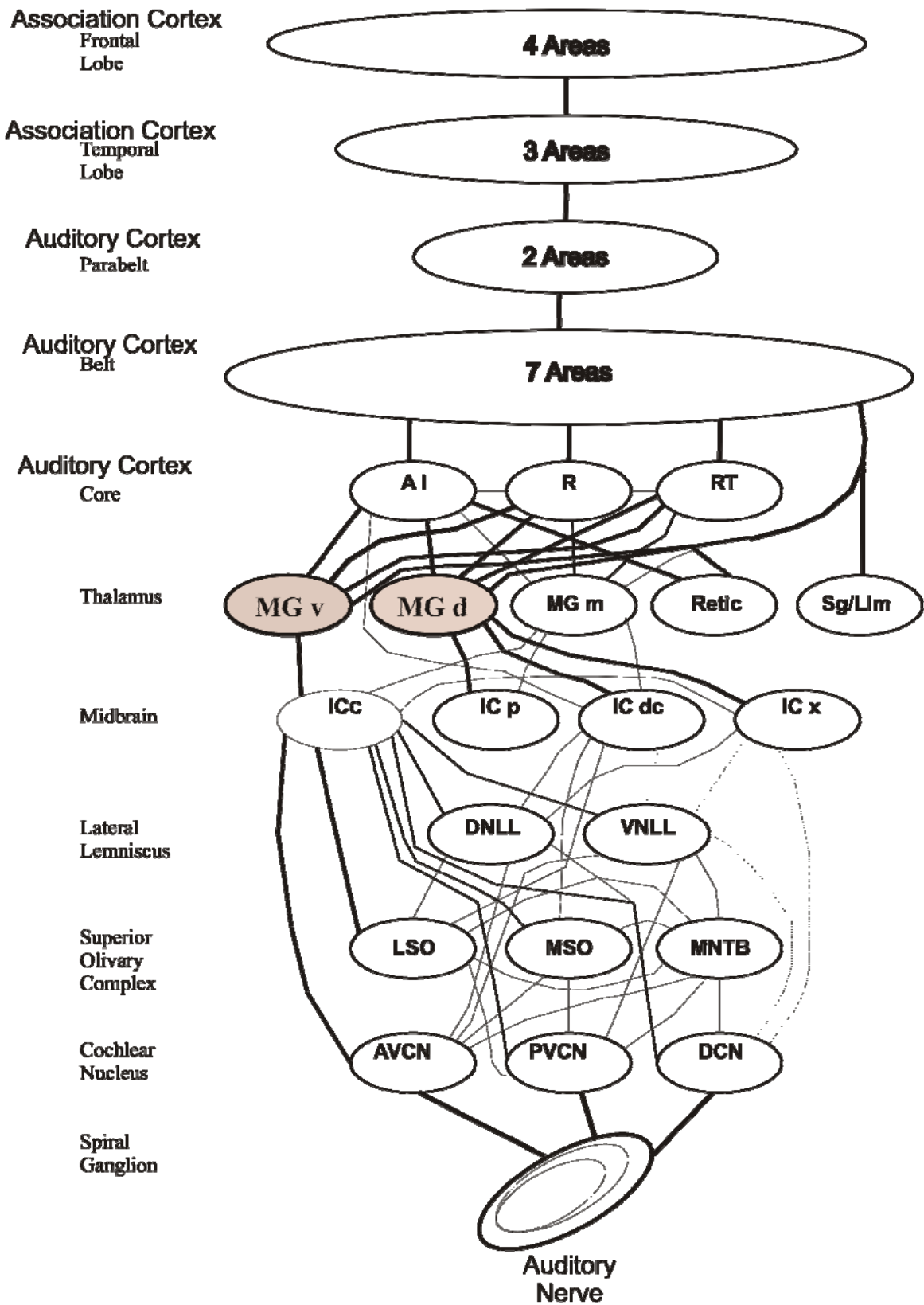
Neurons in the vMGB and dMGB share a similar distinction as the one found in the periphery. The vMGB neurons relay primary information, as done by the Type I SGNs. The dMGB neurons relay integrated information, as done by the Type II SGNs. Both the SGNs and the MGB neurons are part of mandatory pathways to the cortex, however at very different levels. This comparative observation is strictly based upon commonalities in innervation pattern and reported electrophysiological response properties.

As a mandatory pathway to the cortex, the thalamus has gained the name "gateway to the cortex" (Le Gros Clark, 1932). However, in recent years our understanding of the thalamus has been greatly enhanced and a more apt metaphor may be to consider the thalamus as a "courtyard" to the cortex, much like a courtyard may facilitate efficient movement between different parts of a building. It has been shown that the thalamus is enlisted extensively to relay information between different regions of the cortex (Jones, 1985), thereby maintaining a central role in cortical processing. The thalamus has historically received less focus than the other processing levels (Glimcher & Lau, 2005) but there have been studies that have offered useful insights on some of the important functional aspects of the thalamus (Sherman & Guillery, 1998; Jones, 1985, 2003).

Each area in the thalamus differs in connectivity (Calford, 1983; LeDoux et al., 1985; Doron & LeDoux, 1999; Morest et al., 1965, 1986), cell density (Winer et al., 1999; Morest, 1965), biochemistry (Jones, 1985, 2003), and functionality (Bordi & LeDoux, 1994). The primary auditory thalamic division, the vMGB, receives ascending input from the central nucleus of the inferior colliculus (ICC) (LeDoux et al., 1987). The higher order auditory division, the dMGB, receives input from the external cortex of the inferior colliculus (Aitkin, 1978; Jones, 1985; Kudo, 1984; Morest, 1964; Moore, 1963; Rose & Woosley, 1958; Winer et al., 1992). In addition to the feedforward excitatory input, a feedforward inhibitory input

exists (Winer et al., 1996) between the inferior colliculus with both the vMGB and the dMGB.

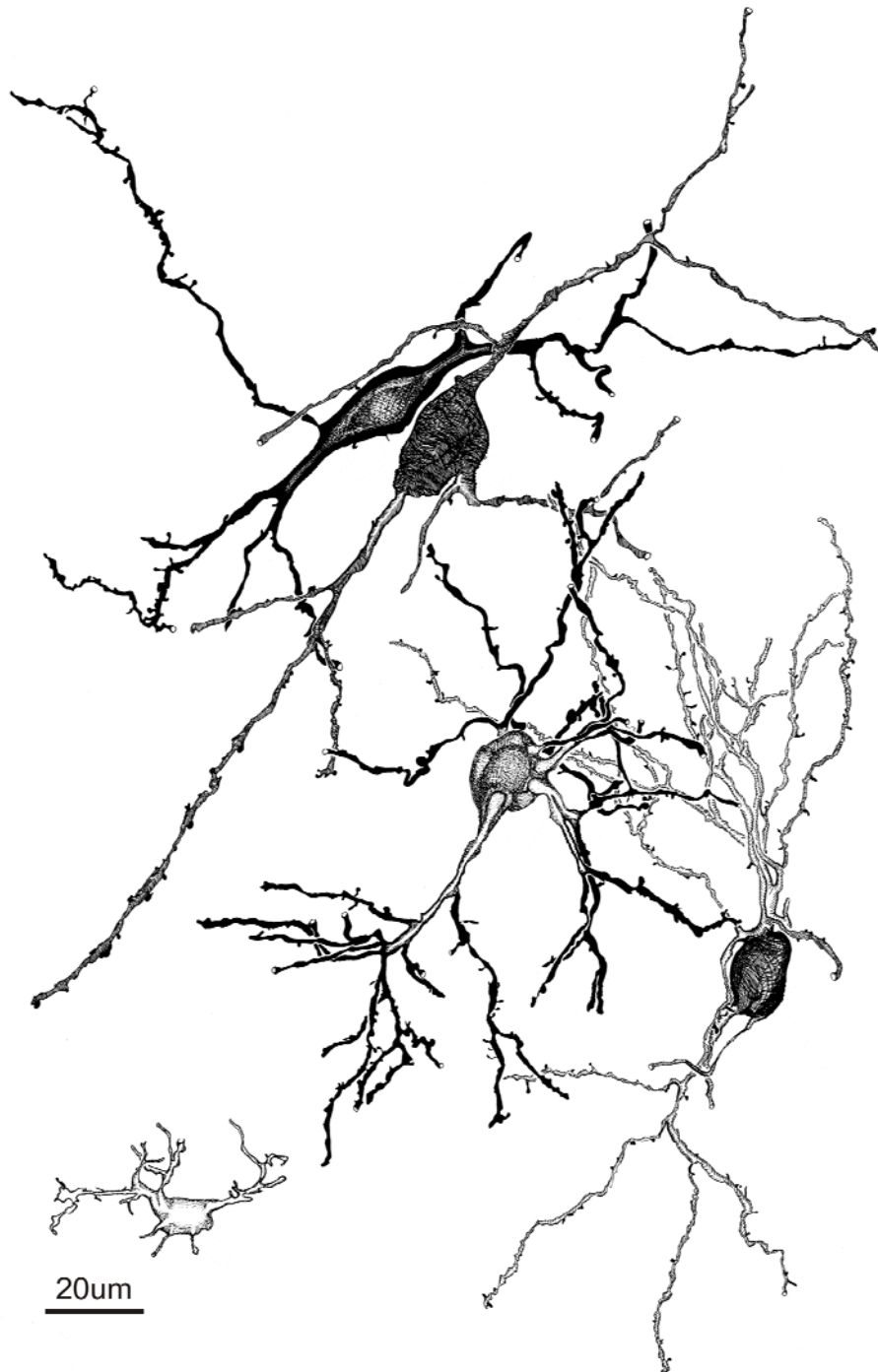**Figure 1.3. Cell morphology of neurons in the ventral division of the MGB.** Examples of bushy tufted neurons in the ventral MGB are shown, except for the small lower left neurons, which is a Golgi Type II neuron. (Reprinted from Winer 1999; Fig.3.)

In general, the nontonotopic pathways have prominent efferent projections to the limbic system (Shinonaga et al., 1994; Deschenes et al., 1998; Doron & Ledoux, 2000). Main

projections from the vMGB however, extend directly to layers III-IV (Scheel et al., 1988; Roger & Arnault, 1989; Romanski & Ledoux, 1993; Kimura et al., 2003) of the primary auditory cortex. Reciprocal innervation extends from layer VI, innervating the neurons in the vMGB with small boutons. Collaterals from the cortico-thalamic projections also innervate the thalamic reticular nucleus, which in turn relays inhibitory input to the vMGB nuclei (Liu, 1995, 1999). In contrast, the dMGB projects to the nonprimary auditory regions and receives large bouton projections from layer V neurons (Ojima et al., 1994; Rouiller et al, 1985a,b; Rouiller & Welker, 1991; Shi & Cassell, 1997; Bartlett et al., 1997).

1.06 Morphology of MGB Neurons

Neuronal morphology in the MGB is commonly described in terms of dendritic branching. MGB neurons have been morphologically characterized as either tufted, stellate, or radiate (Winer et al., 1999). Tufted refers to the particular ramification of the dendritic tree (Figures 1.3 and 1.4). Tufted neurons are in both divisions. The soma size and dendritic field dimensions vary between divisions. Small stellate neurons have also been identified in both divisions. Stellate cells have a small soma (~6 μm) with 3-4 primary dendrites with irregular projections (Figure 1.4). The radiate neuron is similar to the tufted neuron in soma size (8-10 μm) and dendritic field size, 80 by 80 μm. The distinction between radiate and tufted cell types is that the tufted cell has a more complex dendritic arbour whereas the radiate cell types are simpler with a dichotomous or bifurcated dendritic branching (Figure 1.4). The radiate neurons are also multi-dimensional in orientation. Surprisingly, intrinsic electrophysiological distinctions have not yet been reported based upon morphology in the MGB (Jahnsen & Llinas, 1984a,b; Bartlett & Smith, 1999).
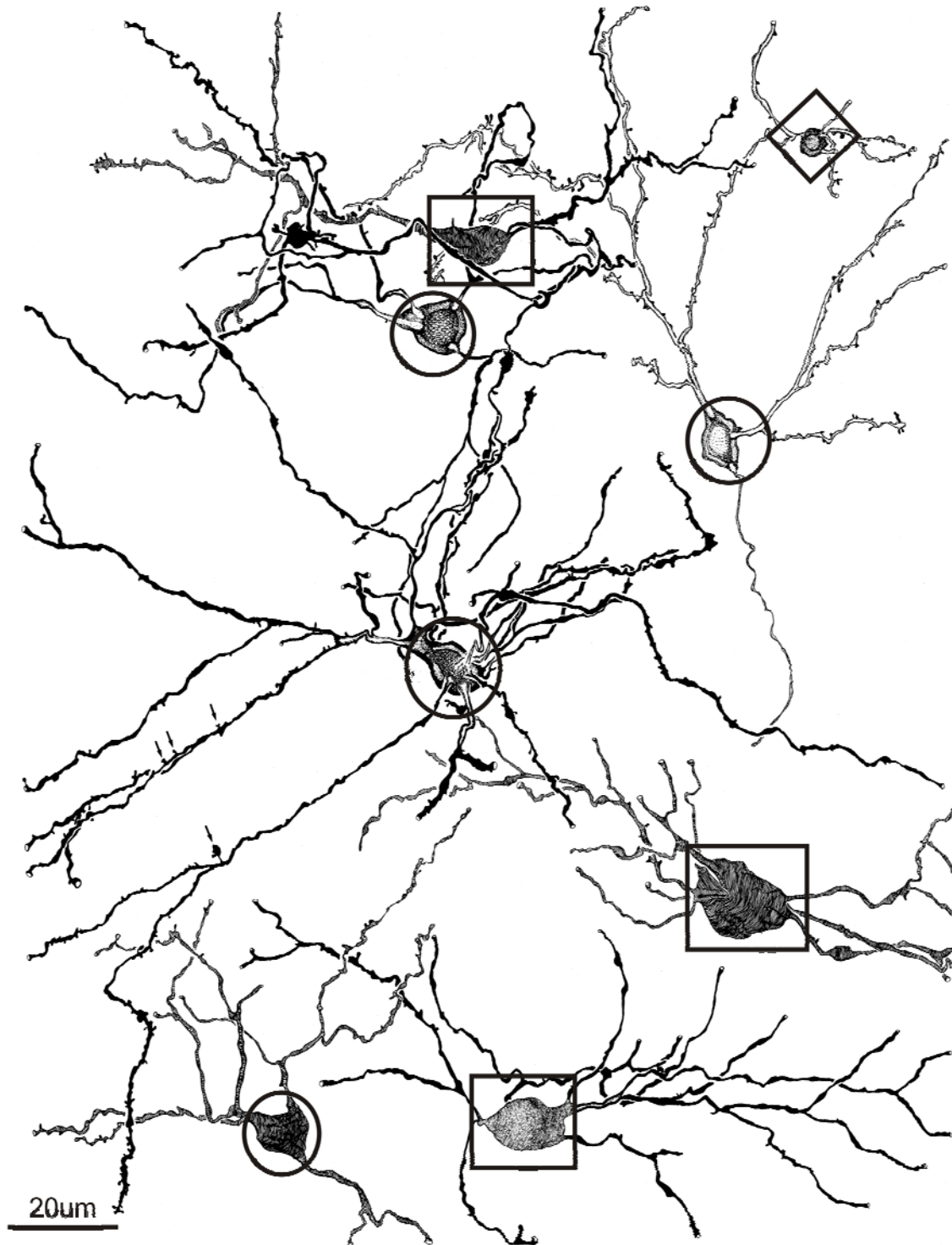
Figure 1.4. Cell morphology of neurons in the dorsal division of the MGB. Examples of tufted (enclosed in squares), radiate (enclosed in circles), and small stellate (enclosed in a diamond) morphologies in the dorsal division are shown. (Reprinted from Winer et al., 1999; Fig.4).

The neuronal population in the vMGB consists of stellate or tufted neurons (Figure 1.3). The tufted neurons that exist in the vMGB have profuse dendritic branching and are, therefore, called bushy tufted neurons (Figure 1.3). Bushy tufted neurons have an elongated dendritic field with a branching area of 50 by 100 μm.

The dMGB neuronal population consists of tufted, stellate, and radiate neurons (Figure 1.4). The tufted neurons that predominant in the dMGB are more polarized laterally, with a branching area of 200 by 100 μm, and are less profusely branched than the bushy tufted neurons of the vMGB (Figure 1.4).

1.07 Electrophysiology of MGB Neurons

Some of the first single-unit extracellular recordings of MGB neurons showed response differences between the ventral and dorsal pathways (Calford et al., 1983; Calford & Aitkin, 1983). Perhaps this was a first indication that an intrinsic distinction between the divisions of the MGB might exist. It is now recognized that the characteristic frequencies of neurons in the vMGB are tonotopically organized, have shorter tuning properties and possess shorter response times to sound stimulation (Miller & Schreiner, 2000; Miller et al., 2001a, b). Meanwhile, neurons in the dMGB are not tonotopically organized, have broad tuning properties and exhibit longer response latencies to sound stimulation (Hu, 2003). Intracellular studies in the rat MGB have reported that a minority subpopulation of neurons in the vMGB may exhibit a prominent inward rectifying "sag" in response to hyperpolarization, whereas no such subpopulation was found in the dMGB (Bartlett & Smith, 1999; Hu et al., 1995). These studies have led to the thought that the vMGB is responsible for rapidly relaying precise tonotopic information from the periphery while the dMGB is primarily responsible for greater integration and temporal pattern recognition (Winer, 1992). Those studies were pioneering in their focus but their analytical scope was limited to comparisons of a few parameters, i.e.

resting membrane potential, accommodation rates, inward rectification and rebound spikes in response to hyperpolarization, Ca^{2+} bursting, and input resistance (Bartlett & Smith, 1999). Since the focus in this study is on the intrinsic properties of these neurons, the scope has included a more extensive list of parameters, i.e. action potential latency and duration, afterhyperpolarization, onset and offset kinetics, and threshold level, in addition to the parameters compared by other groups.
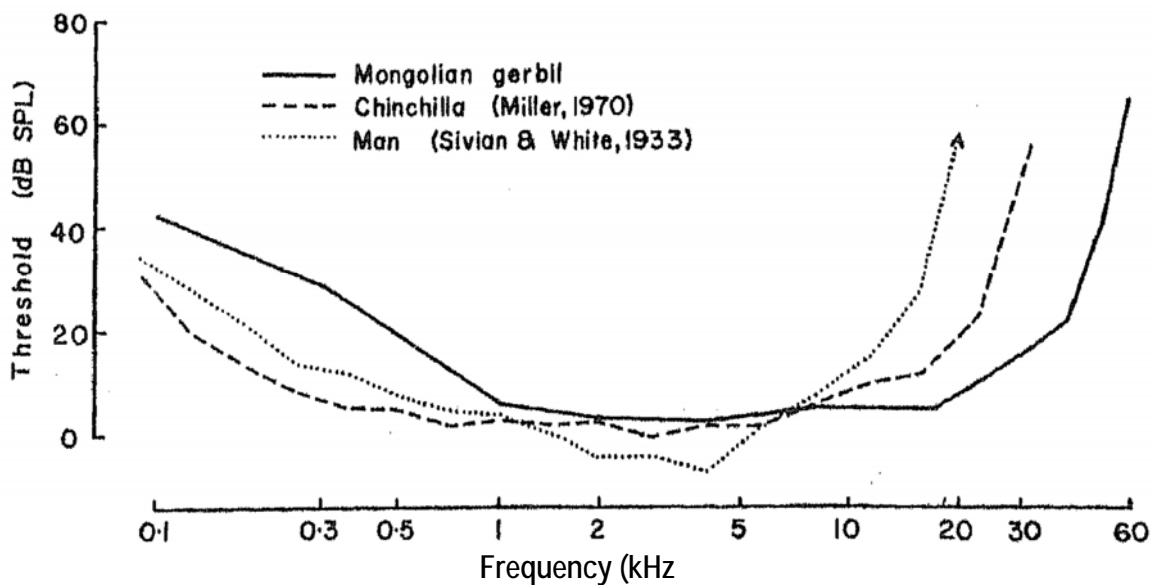
Figure 1.5. Gerbil hearing sensitivity spans human hearing sensitivity in the low frequency range. The figure shows average hearing thresholds for 3 species including man. Thresholds are based on behavioral performance in a tone detection task. Average hearing threshold in humans is similar to the recently revised standard ISO 226 (small differences in the low frequency range). The solid line represents the gerbil, the dots represent humans, and the line segments represent the chinchilla. (Reproduced from Ryan, 1976; Fig.6)

1.08 Gerbil Hearing Sensitivity

Early on it was observed that there is an inverse relationship between animal head size and hearing frequency range sensitivity (Masterton, 1969). This is due to head shadowing, the attenuation and filtering of sound by the head as it reaches the ears, and interaural timing differences, the difference in the arrival of sound between the two ears. Animals with smaller

31

heads would be predicted to have sensitivity to higher frequencies and, conversely, animals with larger heads should be more sensitive to lower frequency sounds. Webster and Webster (Webster & Webster, 1978) were able to show evidence that there are rodents with an expanded middle-ear cavity, indicative of low frequency sensitivity. It was then unequivocally shown that the gerbil did indeed possess hearing sensitivity comparable to humans in the low frequency range (Ryan, 1976) (Figure 1.5). Unlike most rodents, the gerbil has hearing sensitivity as low as 100 Hz but also as high as 60,000 Hz (Fay & Popper, 1994). This range of sensitivity spans much of the hearing sensitivity range of humans (20 - 20,000Hz). The low frequency hearing sensitivity of the gerbil makes the gerbil a more relevant animal model for understanding human hearing than most other rodents. Therefore the gerbil was chosen as the animal of choice to explore the auditory questions focused upon herein.

1.09 Gerbil Ecology

The subfamily Gerbillinae, commonly termed gerbils, inhabits as a particular ecological environment the arid desert areas. Physiological, anatomical, and behavioral adaptations permit the gerbil to survive in these harsh desert environments, which exhibit extremes in temperature and a sparse food supply. In fact, gerbils have more species of any mammals living in most of the deserts of the world. The desert environment is harsh. The summers are extremely hot and the winters are extremely cold. Not surprisingly, the gerbil has nocturnal habits. They forage for food during the night, while remaining in their 2-3 meters deep underground burrows during the days. Gerbils require little free water since they are able to survive on metabolic water and are either herbivorous or granivorous. The species of particular interest here is *Meriones unguiculatus*. It is granivorous. Gerbils are preyed upon by birds, cats, foxes, and reptiles to varying extents, which is partially dependant upon

the season of the year and the availability of other sources of sustenance for the predators. It can be argued that because they must forage on an open plain, without the cover of vegetation to hide from predators, it is especially useful to be able to hear a broad range of sounds to avoid predators (Lay, 1972).

Figure 1.6. Rapid developmental changes occur at young ages. Rapid changes in neuronal cell size and density in the MGB occur in early post-natal development. (top) Pruning of neurons and (bottom) cell growth is accelerated in the first 3 weeks of rat development, which is similar to the gerbil developmental time line (Blumberg-Feld-man & Eilam 1995). The onset of hearing in the gerbil coincides with the ending of the period of rapid development. It is not clear when develop-mental changes plateau but changes occur into adulthood. (Repro-duced from Clerici & Coleman, 1998; Fig. 8 and 9.)

Parallel evolution of low frequency sensitivity in other subfamilies of rodents, for example the desert ground squirrel, in different yet comparably harsh desert climates, suggests an adaptive preference for low-frequency sensitivity (Webster & Plassmann, 1991). Another palatable argument is that the low frequency hearing allows gerbils to communicate in their burrows by stomping their hind legs, conveying a low-frequency resonance through the labyrinthine network of tunnels to warn of predators, such as a snake. Gerbils

communicate fear or alarm with a staccato burst of thumping of their hind limbs, which drives all gerbils within earshot older than 3 weeks to stop all activity, i.e. eating or digging, and exhibit vigilance. To illustrate, in response to such a low-frequency sound gerbils either seek refuge in the gerbil shelters that are in each cage, go to the highest point in the cage and observe quietly, or also thump their hind legs in staccato bursts. This behavior can be readily triggered by mimicking the thumping sound while rapping in a similar rhythm on a wooden table (personal observations).

1.10 Developmental Changes

Neurobiological developmental changes are more profound in younger animals. Any physiological characterization of a neuron must take into account the developmental stage of the animal in order to determine whether a feature is most likely to be developmental or functional (Clerici & Coleman, 1998). Significant developmental changes occur in the gerbil nervous system in young animals (< 3 weeks) (Figure 1.5). Morphological studies have shown rapid developmental changes in cell size and density before 3 weeks of age in gerbils (Budinger, 2000). Concurrently, hearing onset occurs during this period. Older (4 - 5 weeks postnatal) animals were chosen for this study in order to better ascertain the functional physiological properties rather than a transient developmental phenomenon. Older animals were prohibitively difficult to do patch-clamp recordings due to the excessive myelination that exists in the thalamus after 5 weeks of age.

1.11 The Driver and Modulator Concept

In light of the driver and modulator concept (Sherman & Guillery, 1998) some interesting implications concerning the functional organization of the medial geniculate body neurons have arisen. The concept of "drivers" and "modulators" was coined by S.M. Sherman and R.W. Guillery (Sherman & Guillery, 1998) as a functional paradigm to describe

the differences in the thalamic nuclei and pathways based upon the sources of initial neural activity, connectivity, and the impact of the respective synaptic inputs. In general, neurons in the primary or first order thalamic nuclei are primarily involved in relaying "driver" information. Higher order thalamic nuclei are considered to consist of neurons relaying primarily "modulator" information. Some of the attributes that are ascribed to the driver designation are sparse convergence of input, relying instead upon input from a single or a small number of axons with strong synaptic input. Driver input represents the first relay or initial introduction of a particular kind of information. The driver or first order relay station in the auditory or visual thalamus are the ventral MGB and the lateral geniculate nuclei, respectively. Modulators integrate more converging inputs than drivers and are associated with converging facilitating weak synaptic input (Sherman et al., 1998). By using the driver and modulator paradigm, the physiology of two separate auditory regions are described and compared. The identification of parameters that can be attributed to either the driver or modulator designation may offer some insight on the role of intrinsic parameters in the type of information processed.

1.12 Objective

The output of a neuron is a product of the synaptic input, intrinsic physiology, leak conductances, and the proximal environment (eg. glial influences) of a neuron. Synaptic input is the sum impact of the excitatory and inhibitory input. The proximal external environment may be considered as a constant value in *in vitro* preparations. The focus in this study is the intrinsic properties of dMGB and vMGB neurons. In order to approximate the intrinsic response properties of neurons, rectangular-pulse current injections were administered to the soma at different amplitudes and polarities. Upon sufficient depolarizing current injection and time, action potential threshold is reached.

The resultant spike waveform entails a specific delay in the rise time to the action potential. The kinetics of this rise time is a benchmark to the conductances, both passive and active, that would be engaged in response to synaptic activity leading to threshold. The delay from the onset of the stimulus to the occurrence of a spike is a function of the subthreshold conductances, which is driven by the sum of the excitatory and inhibitory inputs. Essentially, the delay to fire a spike is a function of the integration capacity of a neuron. Shorter delays may be more appropriate for relaying discrete information. Longer delays may be more useful in relaying more integrated information.

The objective of this study is to contribute to the current understanding of the intrinsic response properties of neurons in the ventral and dorsal division of the medial geniculate body. Upon consideration of the following facts, this study clearly represents a novel approach. First, the gerbil has similar hearing frequency sensitivity as humans, in the lower frequency range. Secondly, the gerbil medial geniculate body is devoid of GABAergic interneurons therefore the response properties should exclusively reflect those of a relay neuron to the cortex. Also, patch-clamp electrophysiological recordings in the auditory thalamus of the gerbil have not been reported heretofore. Lastly, older animals (4-5 weeks) give a better estimation of the adult functional properties than younger animals.

2.0 METHODS AND MATERIALS

The experiments reported here comply with the ''Principles of Animal Care'' (publication No. 86-23, revised 1985 of the NIH) and also with current German laws.

2.01 Slice Preparation

Gerbils (*Meriones unguiculatus*) between 28-40 days old were anaesthetized with isoflourane (Forene, Abbott Gmbh & Co., Wiesbaden) and decapitated. Coronal slices (200-μm-thick) were cut using a Leica Vibratome (vibratome, Leica 1000S, Leica). Dissection and slices were done in cold (1-2°C) Ringer's solution containing: (in mM) 87 NaCl, 25 NaHCO$_3$, 10 Glucose, 2.5 KCl, 1.25 NaH$_2$PO$_4$, 7 MgCL$_2$, 0.5 CaCl$_2$, and 75 sucrose equilibrated with 95% O$_2$ and 5% CO$_2$. Slices were incubated at 34°C for 25 minutes and subsequently stored at room temperature (RT) for at least 20 minutes before being moved to the recording chamber.

2.02 Development of Slice Preparation Protocol

One of the most important limiting factors in slice electrophysiology is making adequate slices (Geiger et al., 2002). Several fundamental issues must be addressed in order to accomplish this task. Earlier patch-clamp work (Adamson & Reid et al., 2002a, b; Reid et al.2004) done by the author was done on cultured cells, not slices therefore a significant effort was undertaken to find the optimal method to procure adequate slices. The slice protocol for rats was adapted for the gerbil (Edwards et al., 1989). Succinctly, obtaining brain slices requires (a) removing the brain from the animal; (b) submerging the brain in cold (2 ° C) ringer solutions while maintaining adequate carbogen gas concentration; (c) slicing the brain with the proper vibratome settings for blade vibration (90 Hz) and slice speed (0.05 mm/s); (d) storing the brain slices carefully in warm (34°C) solution and subsequently in solution at

RT for the optimal amount of time; (e) determining how much time should be allowed for the slice to equilibrate in the recording chamber before recording; and (f) handling the slices properly in between all stages. These issues were further complicated by the fact that the area of interest, the MGB, is heavily myelinated after a certain age (4 - 5 weeks). Therefore, a compromise must be made about what age the animal should be. If the animal is too young (< 3 weeks) then significant developmental changes are still taking place (Figure 1.5; Budinger, 2000). If the gerbil is too old (> 5 weeks) then the density of myelinated fibers crossing through the thalamus makes patch recording prohibitively difficult. The thalamus is particularly difficult to do intracellular recordings because of the heavy myelination. Attempts at recordings in animals up to 8 weeks old were done, but were not successful.

The two initial challenges were the identification of the location of the appropriate brain region of interest and the determination of how thick a slice should be. In order to find the regions of interest, variations of slice angles (e.g. parasaggital, horizontal, and coronal) were tried. Coronal slices proved to have the best angle to find visually clear delineated borders between the ventral and dorsal divisions and because of the well established anatomical documentation of the borders in this view (Paxinos & Watson, 1986; Winer et al., 1999). Another challenge was determining the best slice thickness to obtain the vMGB and the dMGB in a single slice, with clearly delineated borders. Slice thicknesses of 400, 350, 325, 300, 275, 250, 225, and 200μm were tried and 200μm was chosen to be the best compromise for good visibility and cell viability. All of these issues had to be sorted out through meticulous trial and error.

2.03 Identification of the Area of Interest: MGB subdivisions

The dorsal and ventral MGB divisions are visually distinguishable under the microscope. The dorsal MGB division is dorsally located and has sparse cell density. The ventral MGB division is ventrally located and has a densely populated and laminated organization. The border between the two divisions was clearly identifiable in IR-DIC images by the stark contrast in light transmission (Figure 2.0). The laminated cell dense vMGB permitted very little light through and was, therefore, dark.
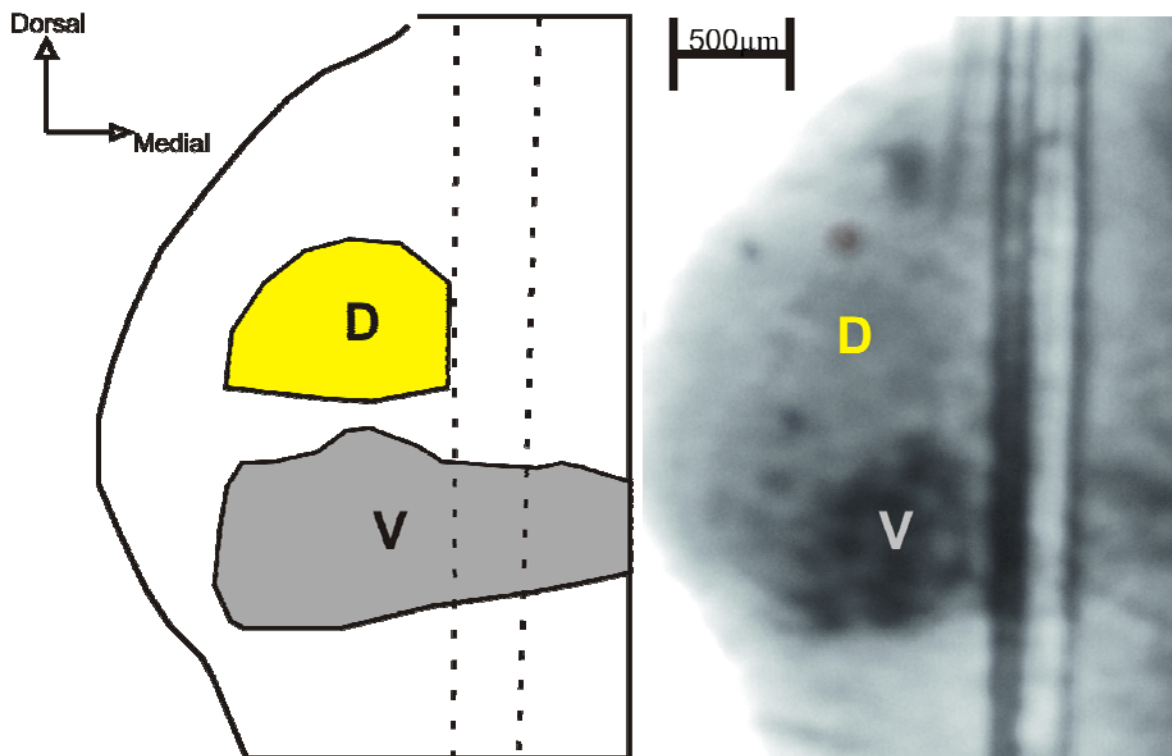
Figure 2.0 Low magnification (40x) IR-DIC image of a coronal slice through the thalamus displaying the medial geniculate body of a 5 week old gerbil shows that the dorsal (D) and the ventral (V) divisions are visually distinguishable. The MGB protrudes laterally from the thalamus. The cell dense ventral division is less transparent and larger in size than the cell sparse dorsal division. The cartoon is an overlay of the IR-DIC image, depicting the division borders. The dotted parallel vertical lines are traces of the wire, used to hold the brain slice securely to the recording chamber. The slice is a 200 μm coronal section through the main at approximately 6 mm caudal of Bregma.

2.04 Recording Solutions

Slices were superfused with a physiological extracellular solution, artificial cerebral spinal fluid (ACSF), containing (in mM): 125 NaCl, 25 NaHCO$_3$, 10 Glucose, 2.5 KCl, 1.25 NaH$_2$PO$_4$, 1 MgCl$_2$, and 2 CaCl$_2$ equilibrated with 95% O$_2$ / 5% CO$_2$; mOsm=315, pH=7.4. Pipette solutions contained (in mM) 105 K-Gluconate, 30 KCl, 10 HEPES, 5 EGTA, 2 MgCl, 0.1 CaCl, and 2 Na$_2$-ATP, mOsm=290; pH=7.3. All water used for solutions was prepared by a 3 step process: reverse osmosis, ion exchange, and UV radiation.

The appropriate solutions were critical. Physiological salt concentrations across the biological membrane, first proposed by Ringer (1882a,b; 1883a,b) and Nernst (1893), give the first approximation of the appropriate ion composition (Na$^+$, Ca^{2+}, K$^+$) to use and at what concentrations. Other standard metabolically important ingredients include glucose, NaH$_2$PO$_4$ and NaHCO$_3$, extracellularly; as well as ATP, EGTA, and HEPES, intracellularly. Cryoprotection during slicing in 2°C solution was accomplished with sucrose (75 mM). Calcium concentration was particularly important. Calcium is involved in many cellular processes, such as 2nd-messenger systems and channel gating. Thalamic neurons vary in their calcium binding capacity. Different cell groups may express parvalbumin or calbindin, which bind to Ca^{2+} with different kinetics (Müller et al., 2007). Also, thalamic cell functionality at low voltage levels is Ca^{2+} dependent. An extracellular Ca^{2+} concentration of 2 mM and an intracellular concentration of 0.1mM were chosen. Extracellular millimolar concentrations of Cl$^-$=134; Mg^{2+}=7; Na$^+$=151; K$^+$=2.5 and intracellular millimolar concentrations of Cl$^-$=154; Mg^{2+}=2; K$^+$=150 were determined to be most appropriate. In order to obtain the appropriate concentration of chloride, K$^+$-gluconate in addition to K$^+$Cl$^-$, instead of K$^+$Cl$^-$ alone, was used. K$^+$-gluconate was not used exclusively either because it may lower the resting membrane potential as much as 10 mV. The resultant solutions were a slight variation on the slice electrophysiology solutions commonly used (Edwards et al., 1989).
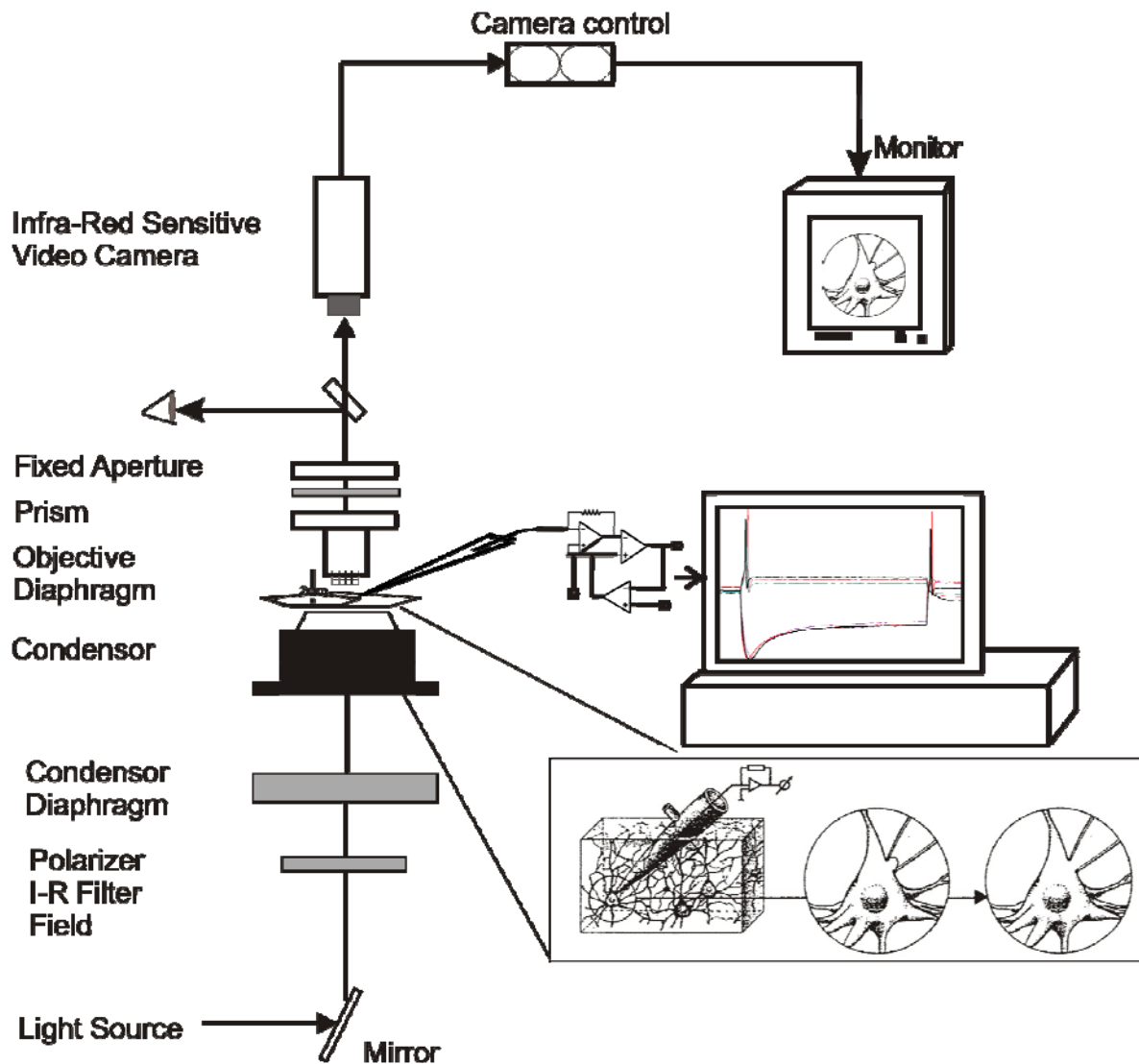
Figure 2.1. Electrophysiological set-up for patch-clamp slice recording. The standard slice recording setup including a microscope, patch-clamp amplifier, CCD camera, and monitor is displayed. IR-DIC microscopy is used to visualize neurons on the monitor via a CCD camera. Patch-clamp whole-cell recordings are then conducted. Schematic drawings in the box (lower right) depict a patch-clamp electrode tip ending that is submerged into a slice of brain tissue. The electrode is pressed upon a neuron and suction is applied. An opening is then created in the cell allowing the electrode to have access to the internal milieu of the neuron thereby permitting whole-cell patch-clamp recordings.

2.05 Holding Potential Dependent Firing Properties

The issue that this study focuses on is the question of the intrinsic properties of the MGB neurons that may be involved in sensory encoding. Any observation of thalamic

physiology must take into account the peculiarity that thalamic neurons may respond in one of two general firing modes, tonic or bursting firing mode (Sherman et al., 1998, 2001, 2005) depending upon the holding membrane potential and the timing of the stimulus. The tonic mode permits the cell to follow the stimulus input in a non-stereotyped, relatively linear fashion. The bursting mode restricts the response of the neuron to a stereotyped bursting response, irrespective of changes in input strength (Ramcharan et al., 2005). A neuron can respond in a tonic mode if held at a high resting membrane potential voltage. The same neuron can respond in a burst mode when held at a lower voltage membrane potential (Sherman et al., 1998). Brain slice patch-clamp recording is an ideal technique to explore the electrophysiology of thalamic neurons because it allows direct control of the membrane potential. The tonic mode is commonly held to serve in an "active or awake" role. The burst mode is considered to represent a "sleeping" or low activity state (Steriade et al., 2004.). For these reasons the tonic mode is better suited for a more faithful representation of behaviourally relevant information to be relayed.

2.06 Electrophysiology

Patch pipettes were pulled from thick-walled borosilicate glass tubing (1.05 x 1.50x 100 mm, GB-150TF) on a Sutter Instruments Company P-87 Puller. Signals were recorded with a Heka EPC-10 amplifier (HEKA Elektronik Lambrecht, Germany), digitized at 20 kHz, and low pass filtered at 10 kHz. Potential values were not corrected for liquid junction potentials, which could add +5 - 8 mV (Barry et al., 1991). MGB neurons were identified visually with infrared differential interference contrast (IR-DIC) video microscopy on a Zeiss (Oberkochen, Germany) inverted microscope with a 40x water immersion objective (Figure 2.1). Whole cell patch-clamp slice recordings were then performed (Hamill et al., 1981). Recordings were made at 30-32°C from the neuronal cell somata. Pipette offset current was zeroed immediately before contacting the cell membrane.

2.07 Recording Conditions

The resting membrane potential was measured in the current-clamp configuration, without any current injection, input at the membrane voltage level immediately after establishing a whole-cell patch clamp seal and checked intermittently during the experiment. Threshold voltage level was measured at the steady-state portion at the end of the stimulus response. Responses to hyperpolarizing current injections were evaluated by hyperpolarizing from the holding potential to a maximal level of -160 mV. Neurons were analyzed at resting membrane potential and during a hyperpolarized holding potential of either -60 mV, -70 mV, and/or -80 mV. Recordings adhering to the following criteria were used for further analysis: stable membrane potentials with less than a 3 mV fluctuation at the holding membrane potential, discernible membrane rise time on step current injection (i.e. no noticeable membrane voltage fluctuations in the response to the step current- less than 1 mV), and overshooting action potentials (clear inflection points and action potentials overshooting the 0 voltage level, with a magnitude of over 50 mV in the first spike). If any of these parameters changed during an experiment, indicating compromised cell health or metabolic failure, the remaining data were not analyzed.

2.08 Data Analysis and Parameter Definitions

Measurements were expressed as a function of voltage level attained, rather than injected current. The use of this physiological relevant parameter does not distort any of the physiological characteristics described. Measurements were made at the action potential threshold voltage level for all mean value comparisons of parameters in the current-clamp configuration. Threshold voltage level is the voltage that a neuron becomes functional therefore neurons were compared at their respective threshold levels. This threshold was defined as the lowest voltage level that an action potential can be elicited. The voltage level measurement was taken at the plateau of the steady-state level during the stimulus (Figure

3.15, single asterisk). Mean value measurements, for comparisons, were made at threshold. Threshold levels vary between neurons and a bias can be introduced into the analysis. Therefore, in addition to mean value measurements at threshold, comparisons were made throughout the full range of voltage levels attained for each parameter measured.

The rise time constant to the first action potential was measured with an exponential fit from the onset of the stimulus to the inflection point of the action potential (Figure 3.9). The first spike latency was defined as the time difference between the onset of stimulus to the peak of the spike. The offset time constant was measured with a decaying exponential from the end of the stimulus step. For all neurons, a voltage level of maximum excitation could be defined, at which a max number of spikes could be elicited. This maximum number of spikes fired in response to increasing current injections occurred at voltage levels between -35 and -25 mV. For the maximum number of spikes fired in response to depolarizing currents of 200 ms duration, two categories regarding neuronal adaptation were defined, slowly accommodating and rapidly accommodating neurons. Neurons that fired throughout the duration of the stimulus were characterized as slowly accommodating (Adamson & Reid, 2002a). The accommodation rate of slowly accommodating neurons was compared by measuring the interspike intervals between successive spikes ($Spike_{n+1}/Spike_n$). Neurons that did not fire throughout the duration of the stimulus were characterized as rapidly accommodating. Another parameter, the duration of the half-width of the spike, was measured at the half-way point between the peak and the threshold of the spike. The input resistance was measured close to 0-injected current for low-voltage measurements and above threshold level for high voltage measurements. The afterhyperpolarization was described with a decaying exponential fit at the time of the offset of stimulus to the end of the trace. Hyperpolarization activated current (I_h) responses were measured from the onset of stimulus to the plateau and the time constant was established with an exponential fit to the curve. Values are given as the mean and SEM. Error bars also indicate SEM.
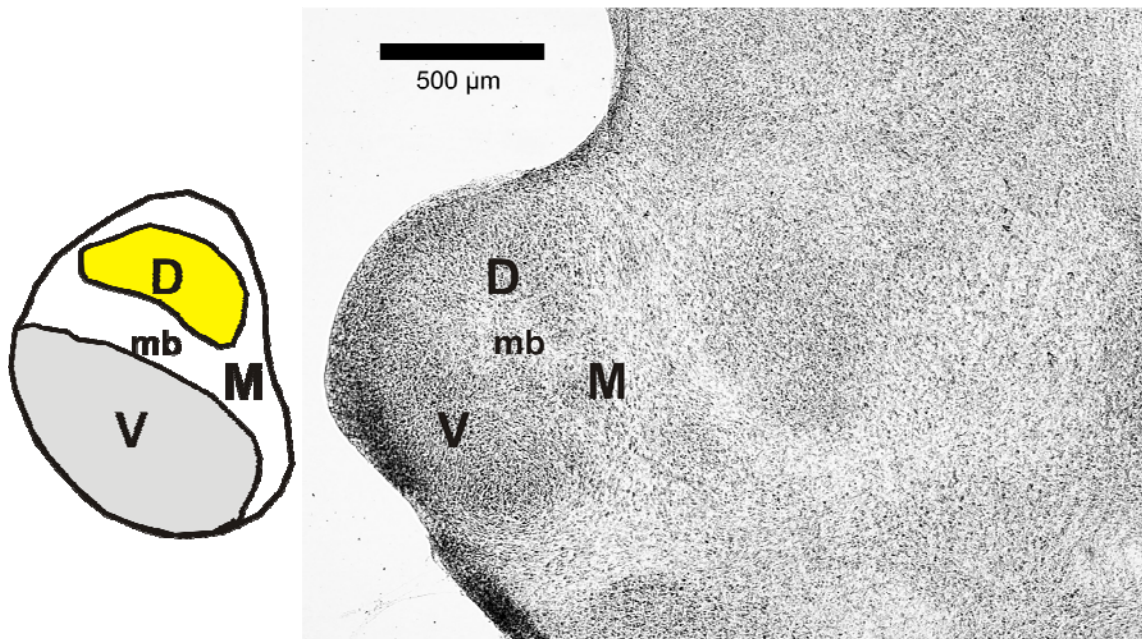
Figure 2.3. Nissl stained coronal slice of the right medial geniculate body. Cartoon of the medial geniculate body anatomy is to the left. A Nissl stained image of the right side of the thalamus is rendered in grey scale. Slice thickness is 200 μm. The medial geniculate body (MGB) protrudes laterally from the main body of the thalamus close to the midpoint of the MGB along the rostral-caudal axis. The rostral and caudal ends are more difficult to define because the protrusion of the medial geniculate body disappears; therefore recordings were concentrated on neurons in sections with prominent medial geniculate body protrusions. Recordings were done in the encircled regions labeled D and V. D- dorsal, V- ventral, M- medial, mb- midgeniculate bundle.

2.09 Nissl Staining

Conventional Nissl stains were done on all slices. All slices within a series from one brain were fixed in 4% paraformaldehyde over night after each experiment. Fixed slices were mounted onto slides, allowed to dry over night, and then processed on the slides. Slices were first defatted in 96% ethanol for at least 2 hours. Slices were then put into 70% ethanol for 5 minutes and then washed in distilled water for 5 minutes. Slices were then put into cresyl violet for 10 minutes. Afterwards, slices were dipped briefly in aqua dest. to reduce excessive cresyl violet staining. Further differentiation was done in 70% ethanol with a small amount ($^1/_4$ of a Pasteur pipette) of pure acetic acid (glacial acetic acid,"Eisessig") for 2-5 minutes, until the background was nearly without stain and the somata were clearly stained.

Slides were then put into 96% ethanol for 10 minutes, then 100% isopronanol for 10 minutes. Slides were then put into rotihistol for 3 x 10 minutes and coverslipped with DPX (Fluka).

2.10 Image Acquisition

Infra-red differential interference contrast (IR-DIC) images were acquired on a Zeiss microscope (Koehler aligned) with a charged-coupled device (CCD) camera coupled to a video monitor. In addition, photographs were taken with a digital camera (Casio 5700) for archival purposes. Nissl stains were photographed in light microscopy with a Zeiss microscope equipped with CCD camera.

3.0 RESULTS

Relay neurons of the dorsal and ventral divisions of the medial geniculate body are responsible for transmitting the bulk of auditory information to the cortex. Specifically, the vMGB and dMGB receive tonotopic and nontonotopic auditory information from the central nucleus and the cortex of the inferior colliculus along glutamatergic and GABAergic pathways. Neurons in the vMGB and dMGB also receive reciprocal input from layers V and VI projection neurons in their respective cortical areas. In addition, layer V projections send collaterals to the neurons in the reticular nucleus of the thalamus, which in turn sends inhibitory projections to the vMGB and dMGB. This study aimed to elucidate the functional distinction of the intrinsic firing properties of neurons in the vMGB and dMGB. The whole-cell configuration of the patch-clamp technique was employed to obtain current-clamp recordings for this purpose (Neher & Sakmann 1975; Sakmann & Neher, 1976). Electrophysiological recordings were conducted in coronal slice preparations of the medial geniculate body in older gerbils (P28 - P35). A total of 73 neurons were patched and included in the final analysis. Intrinsic properties were compared between neurons from the vMGB (n = 34) and the dMGB (n = 39) in response to rectangular-pulse depolarizing or hyperpolarizing current injection of varying lengths (50 - 250 ms). Neurons were held at resting membrane potential or a more hyperpolarized holding potential. All neuronal recordings underwent the same initial stimulus protocol and then, based upon the response properties, the stimulus protocol was subsequently adjusted to further elucidate the properties of interest.

3.01 General Response Properties

The average resting membrane potential levels were not significantly different between the vMGB and the dMGB (p > 0.05), with mean values of -62.9 ± 3.4 mV (n = 34) and -60.1 ± 2.9 mV (n = 39), respectively (Table 1). The RMP values ranged between -79 mV and -45 mV.
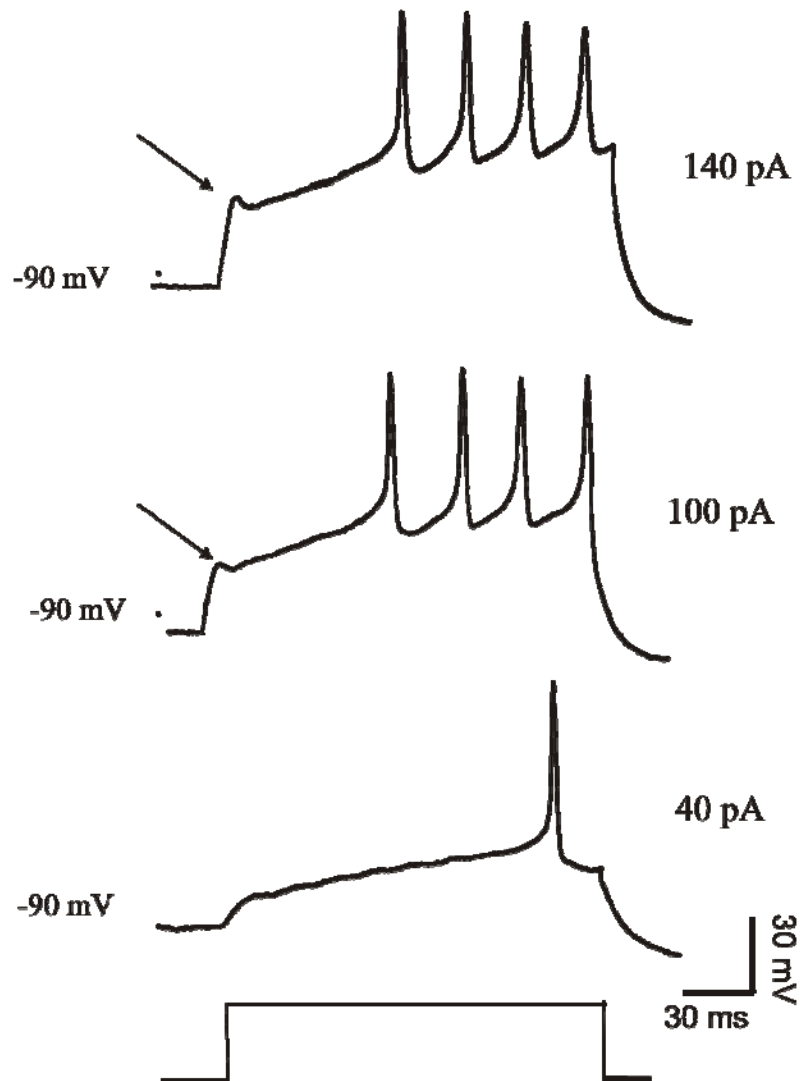
Figure 3.0. Low-voltage membrane potential dependent response properties. Example traces from one neuron of responses to current injections at the low voltage level (-90 mV) holding potential. Step current injections of 150 ms resulted in a stereotyped delay-like response. Three sweeps from the same neuron are shown at 3 different current injection levels of 40, 100, and 140 pA. The bottom trace is at the threshold voltage level. The middle and upper traces are at increased depolarized voltage levels. Arrows indicate subthreshold depolarization peak before delayed spike bursts.

Neurons stimulated with a rectangular pulse current injection from a more hyperpolarized (i.e. low) holding voltage (-80 to -120 mV) potential for a short period (40 - 100 ms) elicited a stereotyped delayed response of burst-like spike behaviour (Figure 3.0). Upon stimulation from a hyperpolarized holding potential the membrane potential increased to an initial peak (see arrows in Fig. 3.0), followed by a rapid repolarization caused by an apparent inward conductance. This rapid repolarization subsided as an ascending
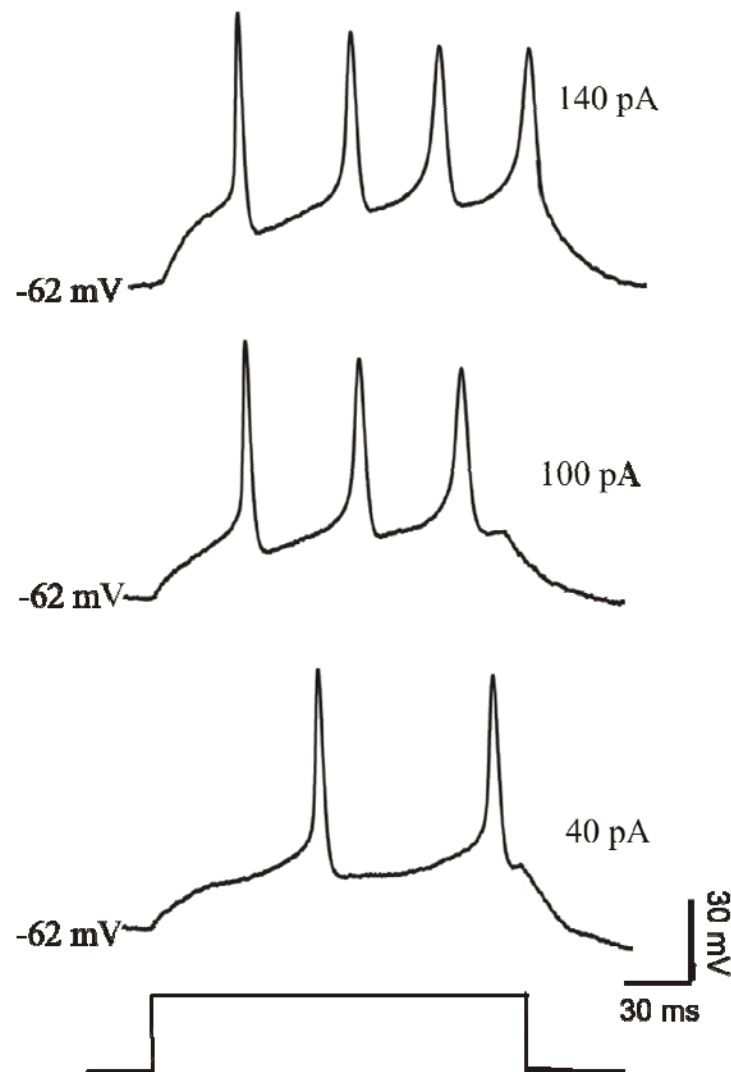
Figure 3.1. High Voltage membrane potential dependent response properties. Three current-clamp traces are shown from the same experiment as in Figure 3.2. Current injections from resting membrane potential (-62 mV) were done (150 ms duration). Medial geniculate body neurons responded in a linear fashion at voltages near resting membrane potential. The lower trace is at threshold. Increasing current injections resulted in responses with corresponding increases in kinetics and firing of 3 spikes (middle) and 4 spikes (top), respectively, with increasingly shorter interspike intervals and timing.

voltage ramp leading to a burst of action potentials. The same neurons were stimulated from resting membrane potential levels (Figure 3.1). Neurons stimulated from the more depolarized resting membrane potential levels elicited a corresponding rise in membrane potential, which culminated into firing at threshold voltage level.

3.02 Threshold

The threshold voltage level to evoke action potentials was compared between both groups. The average threshold values were -44.29 ± 2.92 mV for the dMGB and –42.91 ± 2.87 mV for the vMGB, which were not significantly different (Table 1). The values ranged between -54 mV and -32 mV.
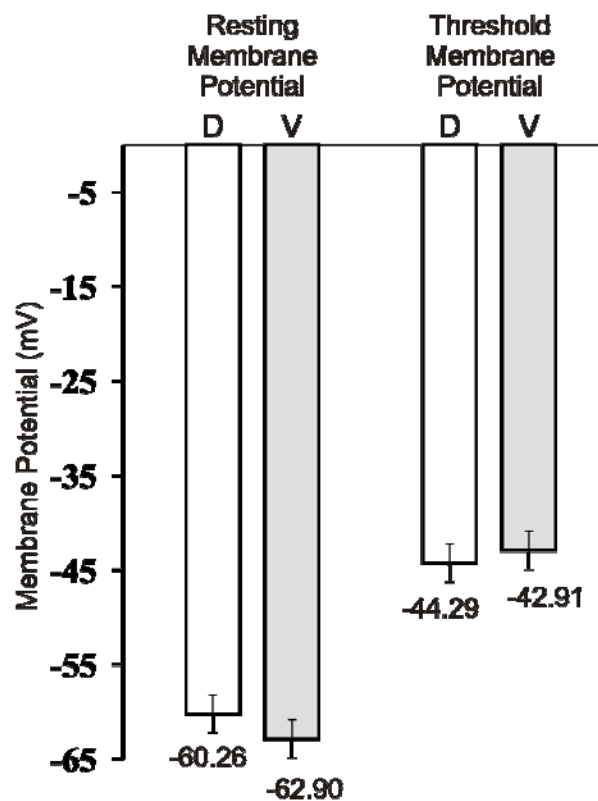
Figure 3.2. Membrane voltage potential measured at threshold and rest were not significantly different between the dorsal and ventral groups in the MGB. Shown are average membrane potentials for dMGB (open bars) and vMGB neurons (grey bars). The ventral group had a lower average resting membrane potential and a higher average threshold level than the dorsal group. Hence the ventral group has a greater voltage range to span between resting and threshold to fire a spike. The threshold, resting membrane voltage and the range between rest and threshold were not found to be significantly different ($P > 0.05$) between dMGB and vMGB. Error bars are S.E.M.
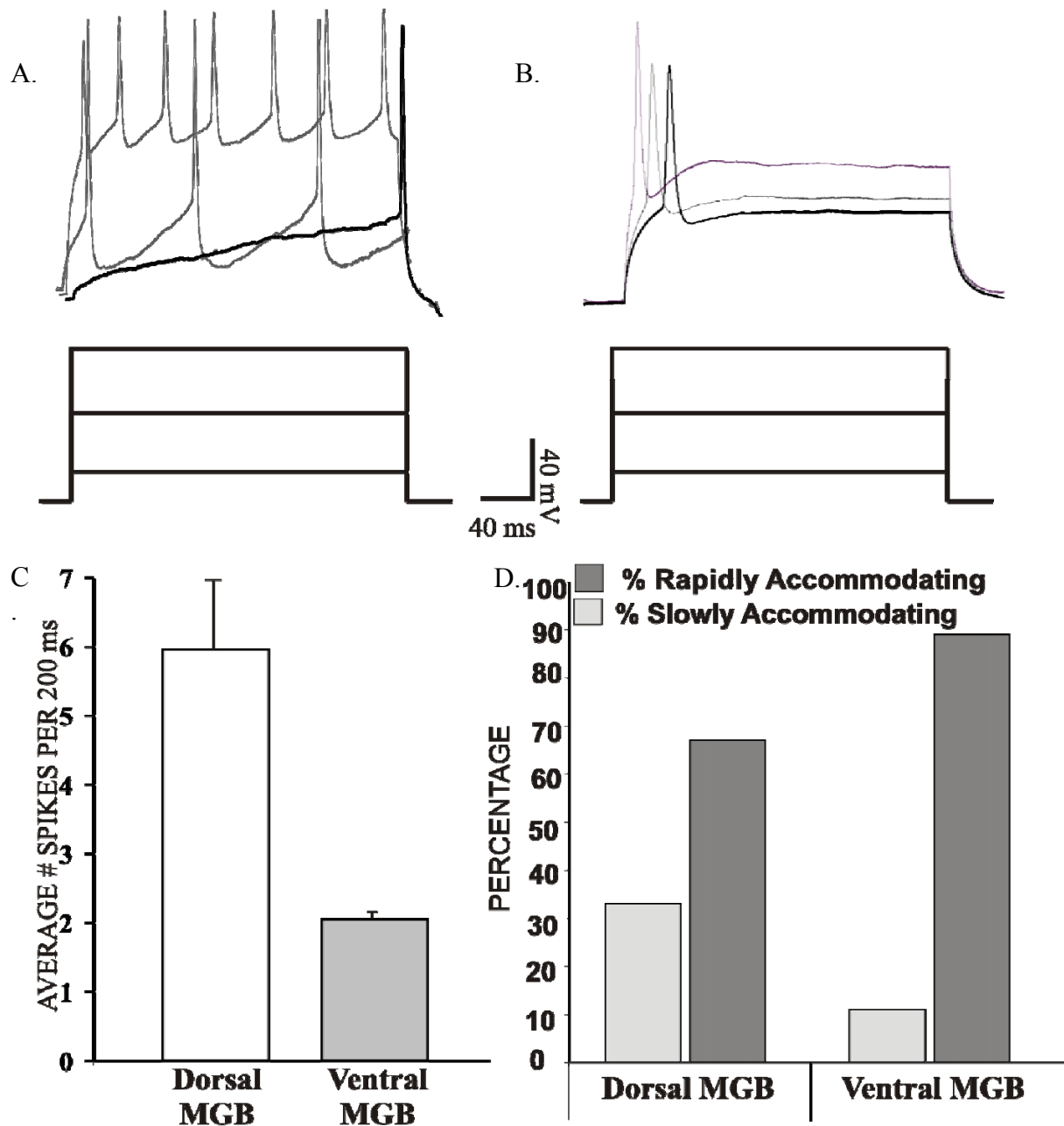
Figure 3.3. Slowly and rapidly accommodating neurons can be found in the gerbil MGB. (A) Example of a slowly accommodating neuron from the dMGB. In response to 3 depolarizing steps of 40 pA of current injection the neuron fired 7 action potentials maximally. (B) Example of a rapidly accommodating neuron. In response to similar stimuli the neuron fired only 1 spike maximally at a high voltage level. (C) Statistical comparisons of dMGB and vMGB slowly accommodating neurons revealed that the average number of spikes elicited in response to similar depolarizing stimuli (200 ms) was greater in the dMGB (6 ± 1.12 spikes) than the vMGB (2 ± 0.3 spikes). (D) Comparison of the distribution of neurons with different accommodation behavior between dMGB and vMGB. The percentage of slowly accommodating neurons was much larger in the dMGB than in the vMGB.

The greater differences between RMP and threshold voltage levels were seen in the dMGB group (average value = 22.65 ± 3.99 mV), whereas the average difference in the vMGB group was only 16.6 ± 3.90 mV (Figure 3.2). That is a 28% difference in RMP to threshold difference between the dMGB and vMGB groups. The difference did not prove to be significant ($p > 0.05$, Table 1).
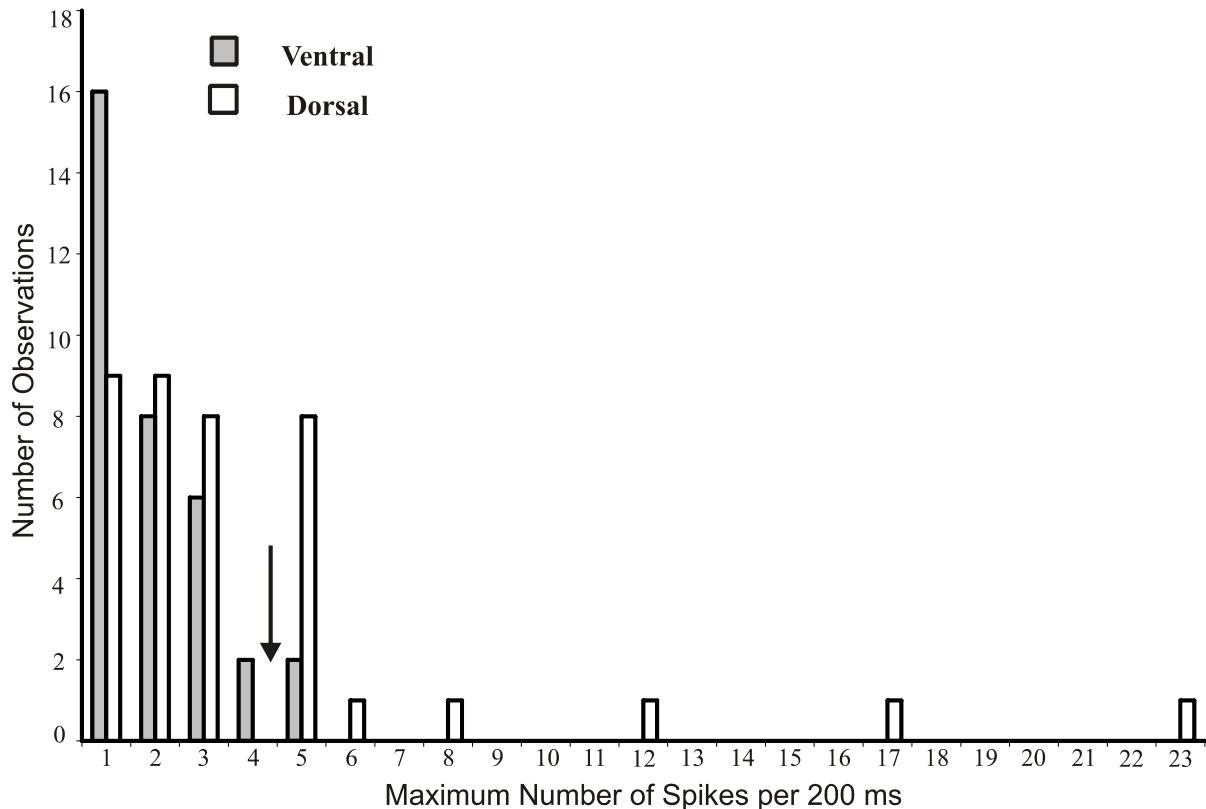
Figure 3.4. The maximum number of spikes was uses as a criterion for classification of slowly and rapidly accommodating neurons. Neurons were characterized based upon the maximum number of spikes that were fired during the 200 ms-stimulus, irrespective of the current injection level it occurred. Most of the neurons did not fire more than 5 spikes. Neurons in the dMGB were capable of firing more than 5 spikes maximally, whereas the vMGB neurons fired 5 or less spikes. The arrow indicates the dividing point between the class of slowly accommodating neurons that fired throughout the 200 ms stimulus and rapidly accommodating neurons that did not cease firing before the end of the stimulus. Slowly accommodating neurons were found mostly in the dMGB, whereas the vMGB neurons were almost exclusively rapidly accommodating.

3.03 Accommodation

The diminution of repetitive spikes in response to a sustained stimulus is known as accommodation. Depolarizing current step injections from RMP caused a corresponding

depolarization of membrane potential that culminated in a maximum number of action potentials. The spike number increased with depolarization, between -35 mV and -25 mV, and attenuated at higher voltage levels due to Na^+ channel inactivation, which does not subside until the membrane voltage is hyperpolarized (Fleidervish et al., 1996; Jung et al., 1997). The response behaviour of neurons was classified as "slowly accommodating" when the neurons did not stop firing action potentials before the end of a 200 ms rectangular pulse current injection stimulus. A typical example of a slowly accommodating neuron from the dMGB is given in Fig. 3.3A. As these neurons fired (maximally) 5 spikes or more, a measure of spike count (during 200 ms stimulus duration) was used as a quantitative criterion for classification (Figure 3.4). Neurons, on the other hand, that fired maximally 4 action potentials or less were also the neurons that stopped firing before the end of the stimulus. An example of such a neuron is given in Fig. 3.3B. These neurons were classified as "rapidly accommodating" (Figure 3.4). The distinction between slowly and rapidly accommodating neurons is based on a criterion that was applied in the peripheral auditory system (Mo & Davis, 1997, Adamson & Reid, et al., 2002a, b; Reid et al, 2004). Overall, most neurons in the gerbil MGB were found to be rapidly accommodating (76.5%, n = 56; Figure 3.4; Table 1).

Neurons from the dMGB and vMGB were found to display different degrees of accommodation in response to a rectangular pulse stimulus (200 ms duration). The average number of spikes fired during the 200 ms stimulus was greater in the dMGB (5.95 ± 1.12 spikes/ 200 ms) than in the vMGB (2.05 ± 0.3 spikes /200 ms) at comparable voltage levels (p < 0.01; Figure 3.3C). Accordingly, the percentage of neurons that showed slow accommodation was much larger in the dMGB (33%) than in the vMGB (11%), as shown in Figure 3.3D. The vast majority of slowly accommodating neurons (in absolute numbers) were found in the dMGB (13 of 17 neurons; open bars in Figure 3.4).
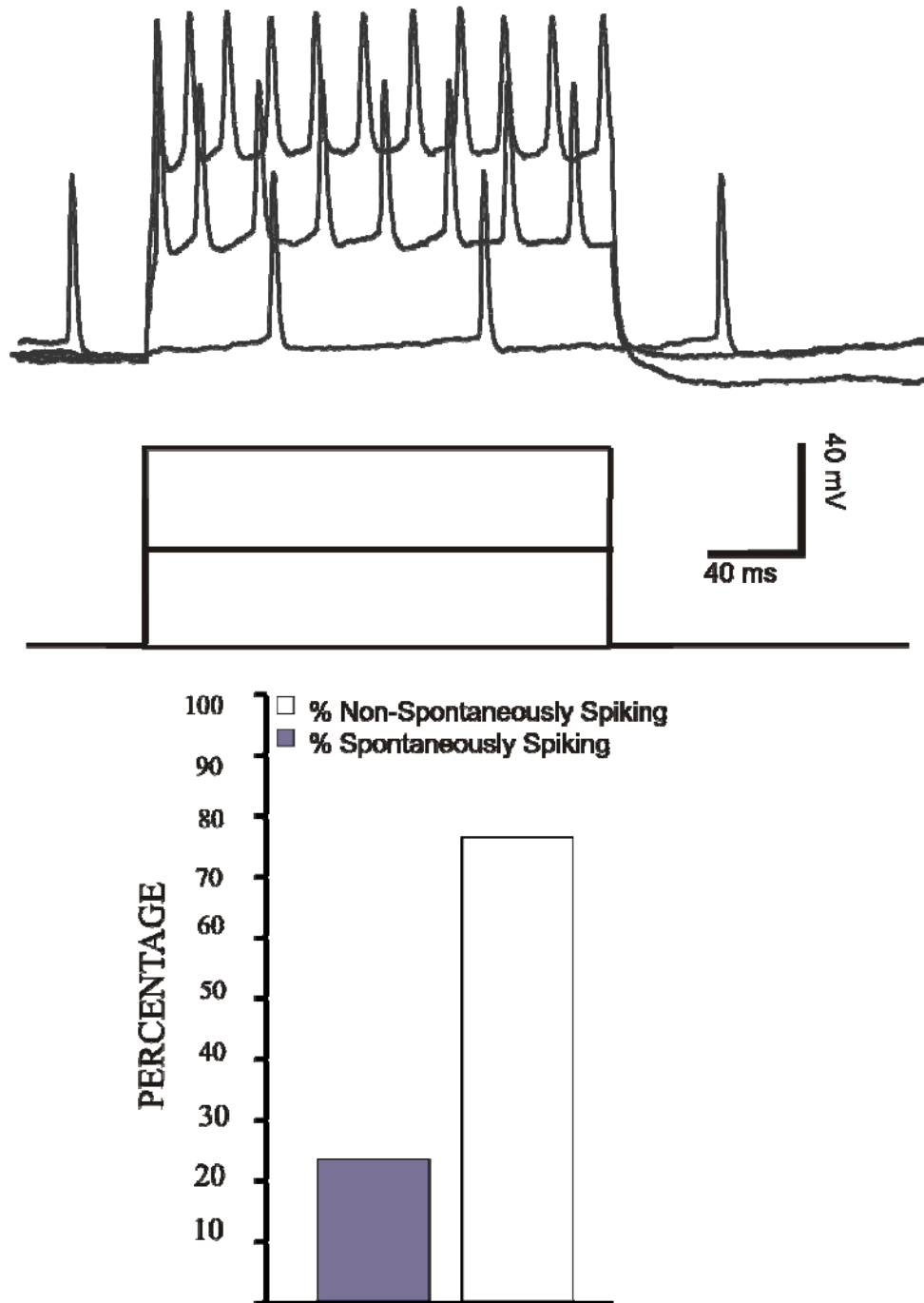
Figure 3.5. Spontaneously firing neuron from the dorsal MGB. Spontaneously firing neurons were found exclusively in the dorsal MGB. (Top) Traces from a dMGB neuron without stimulation (bottom trace) and in response to depolarizing current-injections in 10 pA increments. While at resting membrane potential voltage level spikes persisted throughout the entire time frame (spontaneous activity), the neuron increased firing frequency to a maximal point and decreased firing inactivation at higher voltage levels. (Bottom) The open and dark bars represent slowly accommodating neurons that fired spontaneously or at distinct higher threshold levels (non-spontaneously active), respectively
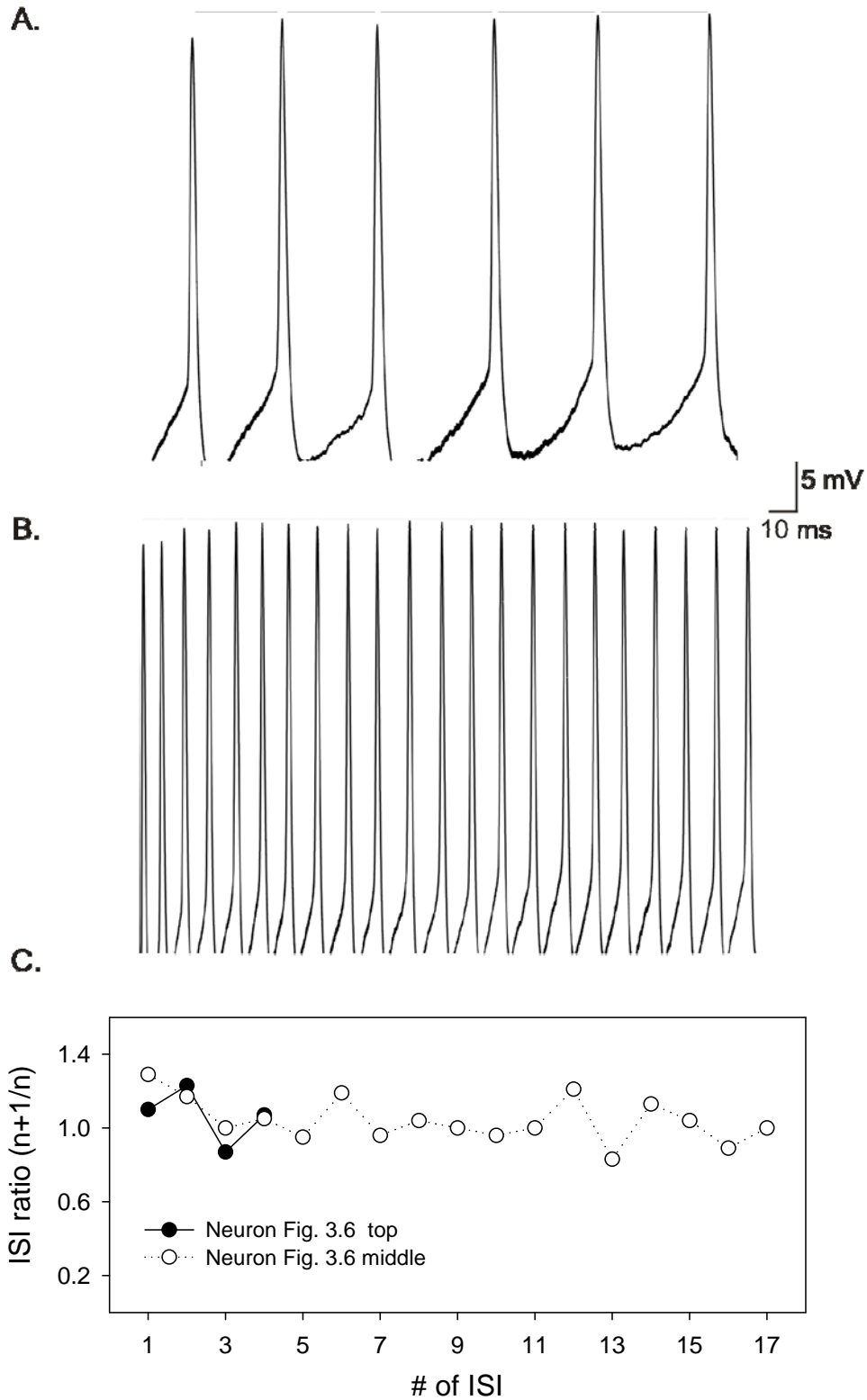
Figure 3.6 Inter-spike intervals of slowly accommodating neurons change over time. Example traces from slowly accommodating neurons with very different accommodation rates. (A) Example neuron displaying slow accommodation at a low firing rate. (B). Example neuron that displays slow accommodation at high firing rate. Both traces have S_{n+1}/S_n ratios close to 1. Both traces are from dorsal MGB neurons.

A subpopulation of slowly accommodating neurons fired at RMP, "spontaneously" (n=4), all of which were found in the dMGB (Figure 3.5). The family of traces in Fig. 3.5 (top) are an example of such a spontaneously firing neuron, spiking at RMP and higher membrane potentials. The firing rate of the spontaneously firing neurons was between 12 and 15 Hz at RMP but was similar to the other slowly accommodating neurons at the maximum firing rate (25 – 100 Hz). Overall percentage of spontaneously active and non-spontaneously active neurons among slowly accommodating neurons was 24% and 76%, respectively.

Changes in the interspike interval (ISI), the time difference between two action potentials, can in addition be used as an index to describe accommodation behaviour in slowly accommodating neurons. In this study the ratio of two successive ISIs (I_{n+1}/I_n, with n being any integer greater than 0) was used as a measure to quantify in detail the change in accommodation rate over time.

Figure 3.7. The interspike interval (ISI) of slowly accommodating neurons. The ISI changes over time but the average ratio of ISIs stays close to 1 for ISIs after the initial 3 – 4 spikes. The connected symbols represent ISI ratios (I_{n+1}/I_n) from individual recordings of different slowly accommodating neurons.

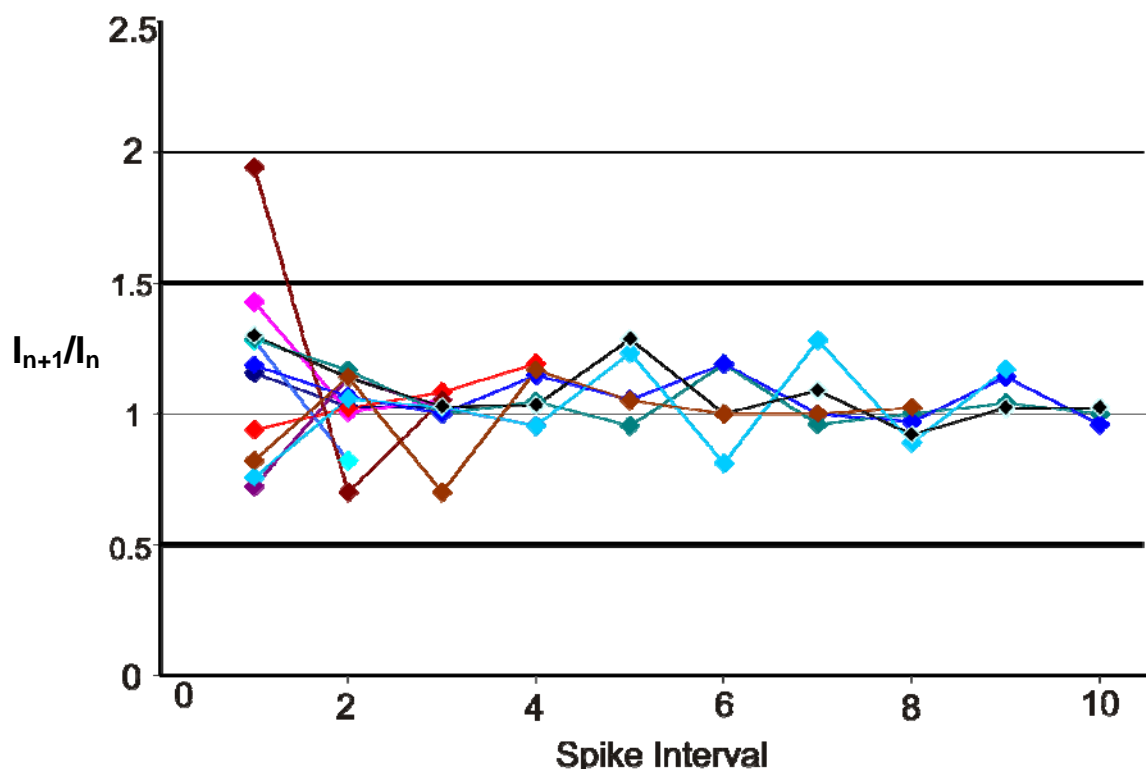Slowly accommodating neurons with ISI-ratios (I_{n+1}/I_n) of 2.0 between the first interspike interval and a subsequent interspike interval indicates a doubling of the interspike interval. Ratios close to 1.0 indicate little or no accommodation, i.e. a nearly unchanging or constant interspike interval.

Accommodating behavior in these slowly accommodating neurons was independent of the absolute values of interspike interval, i.e. independent of absolute firing rate. Figure 3.6A shows a neuron with different firing rate. ISI ratios in this recording ranged from 0.87 to 1.23 (Fig. 3.6C black dots). The measured ISI-ratios are well comparable to values from Fig. 3.6B which shows a neuron with high firing rate. ISI ratios in this case oscillated between 0.83 and 1.29 (Fig. 3.6C, open dots), a very similar range. Both traces in Figure 3.6 are from dorsal MGB neurons. The majority of slowly accommodating neurons displayed an accommodation pattern as shown in Figure 3.6B.

ISI ratios in slowly accommodating neurons usually oscillated around 1.0 ($\pm$ 0.2), examples are shown in Figure 3.7. Typically, the initial 3 - 4 spikes displayed a distinct trend that was different from the following spikes. The first ISI-ratios deviated stronger from 1 than later ratios with values up to 2.0 or down to 0.6. After the 4th spike, slowly accommodating neurons displayed ISI values that were concentrated near a mean as compared with the normal distribution of values (Fig. 3.7).

The slowly accommodating neurons in both the vMGB and dMGB possessed similar ISI properties (average ISI ratio: dMGB: 1.08, vMGB: 1.04). ISI ratios were also similar between those neurons that fired at RMP and at a distinct threshold, measured at their respective maximum firing rates.
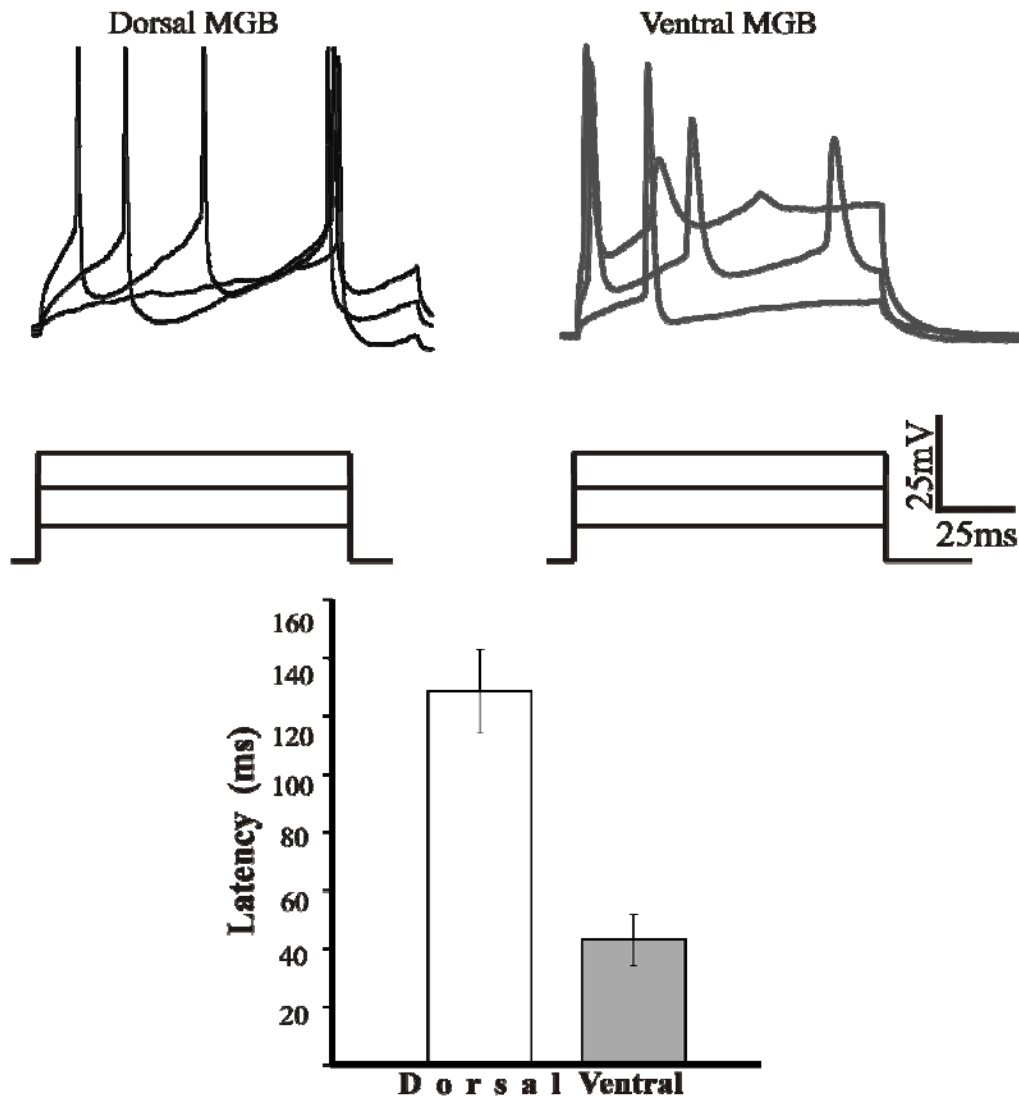
Figure 3.8. First spike latency in dorsal and ventral MGB groups. Three superimposed traces of a dorsal MGB (top left) and a ventral MGB (top right) are shown. The trace with a single action potential is at threshold level. The additional traces are responses to more depolarizing current injections, showing the maximal number of spikes the respective neurons could fire in response to the 100 ms rectangular-pulse stimulus. (Bottom) Average latency of first spike in dorsal MGB neurons (128.43 ± 16.28 ms, open bar) and ventral MGB neurons (41.50 ± 7.77 ms, grey bar). Error bars are S.E.M
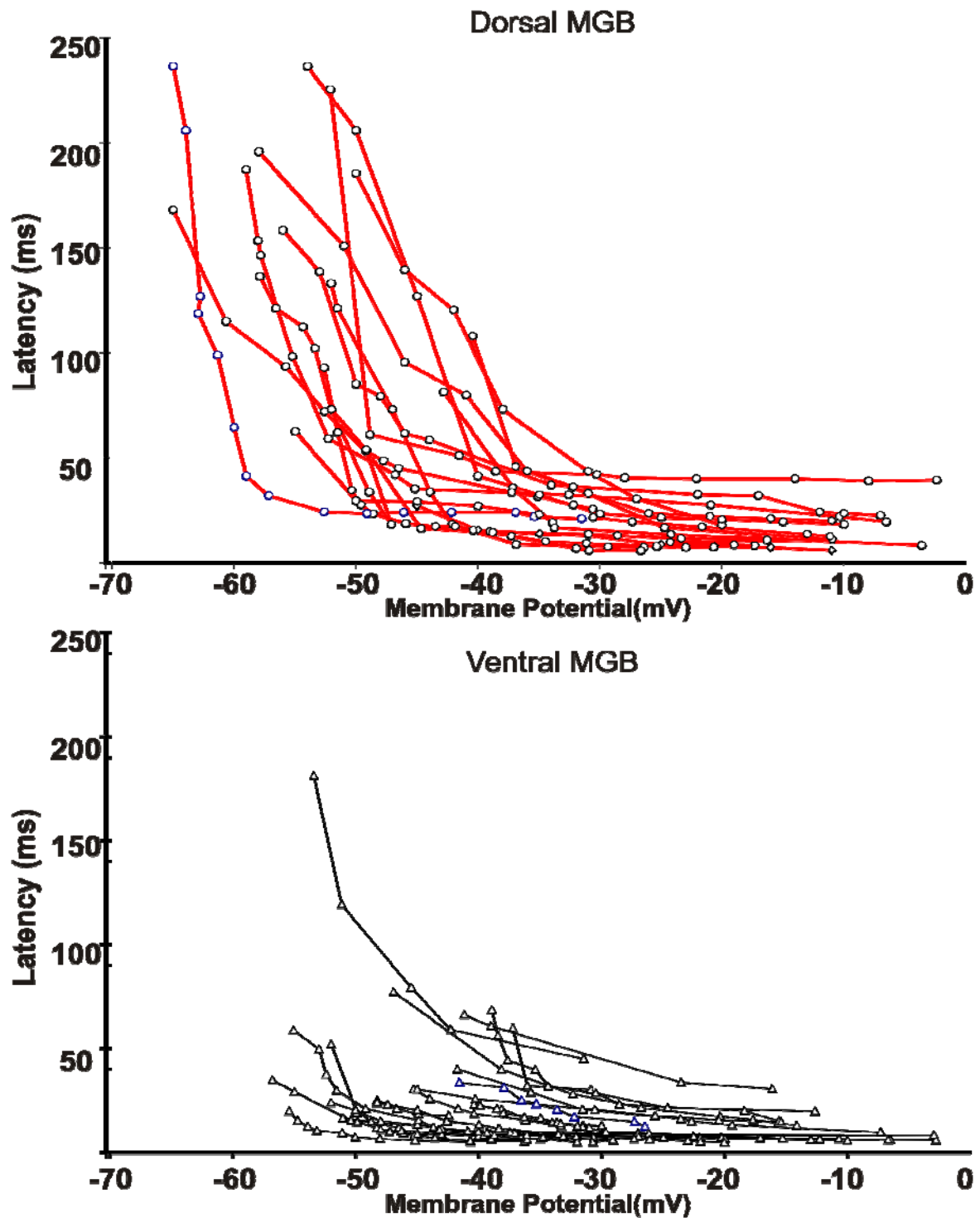
Figure 3.9. Voltage dependent changes in first spike latency in dMGB and vMGB neurons. Latency as a function of membrane potential values were plotted for dorsal MGB neurons (top) and ventral MGB neurons (bottom) to compare the voltage dependence of latency between both groups. Neurons that possessed longer latency values at threshold maintained longer latency values throughout the entire voltage range.

3.04 First Spike Latency

Neurons in the dMGB had a significantly longer average first spike latency at the spike threshold voltage level than neurons in the vMGB (dMGB = 128.4 ± 16.3 ms, n = 39: vMGB = 41.5 ± 7.8 ms, n = 34, p < 0.01, Figure 3.8; Table 1). The same was true throughout the full voltage range (Figure 3.9). Neurons in the vMGB had a wider range in latency values (20 – 250 ms) than the dMGB group (130 – 260 ms). It is not clear whether the broad range of latency values is associated with the tonotopic organization of the vMGB. The slowly accommodating neurons as a whole had significantly longer latencies, with an average latency of 100.5 ± 18.8 ms (dMGB 152.3 ± 17.6 ms; n=13; vMGB 48.7 ± 5.9 ms; n=4), than the rapidly accommodating neurons, which had an average latency of 58.5 ± 8.9 ms (dMGB 72.3 ± 16.5 ms, n=26; vMGB 44.7 ± 7.6 ms, n = 30 (p < 0.01).
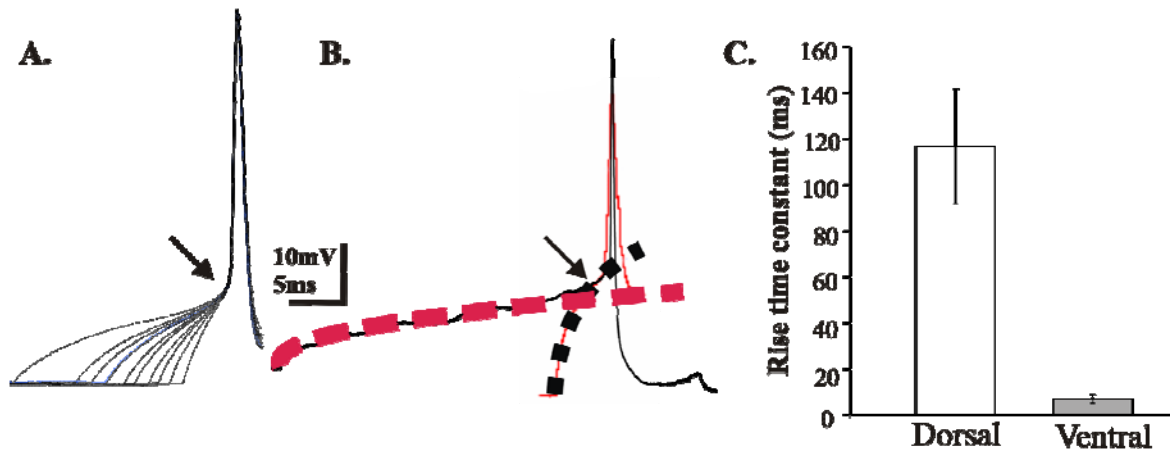
**Figure 3.10 Quantification of rise time to the first action potential (onset kinetics) revealed differences between neurons in the dorsal MGB and ventral MGB.** (A) Ten traces from the same neuron at different voltage levels were superimposed and normalized to the inflection point to show the changing rise times in response to depolarizing current injections. The left most rise time is at threshold to spiking. Rise time kinetics changed with voltage. (B) Time constant of the rise time to the first spike was quantified by means of an exponential fit from the point of the onset of stimulus to the inflection point (arrow) of the spike (dotted lines). This was done for a rapid (black) and a slow (red) time constant rise time. (C) Average rise time constant in dMGB neurons were found to be significantly slower than in vMGB neurons at spike threshold membrane potential. Error bars are S.E.M
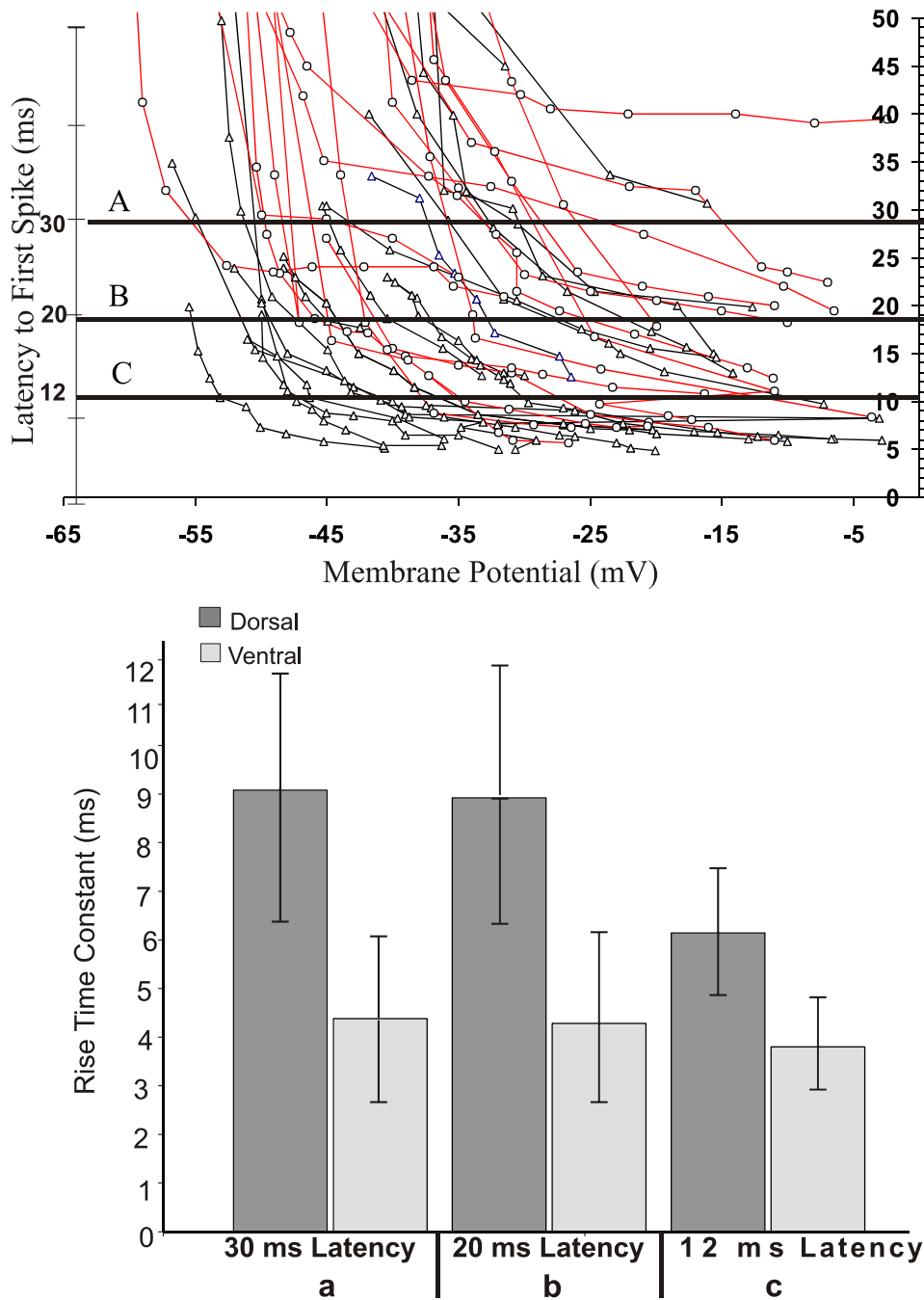
Figure 3.11 The rise time constant is related to first spike latency in MGB neurons.
(top) Shown is the first spike latency as a function of membrane voltage, as shown in Figure 3.9 but with an expanded y-axis (0 to 50 ms). Circles with connecting lines represent the dMGB recordings. Triangles with connecting lines represent the vMGB experiments. For comparison, latency values of (A) 30 ms, (B) 20 ms, and (C) 12 ms were chosen, as indicated by bold horizontal lines in the figure. The rise time constants were evaluated for each latency level (A, B, and C) at the data point that corresponds to the latency level for each experiment. (bottom) Comparison of average time constants for rise time of the ventral and dorsal MGB at different latency levels of 30, 20, and 12 ms.

Further comparisons at specific intermittent voltages were done to further confirm that the dMGB neurons had longer latencies than the vMGB neurons along the full voltage range of membrane potentials (Figures 3.9 and 3.11). The dMGB and vMGB group comparisons at intermittent voltage levels were made at the respective threshold voltage levels and at -30 mV, -20 mV, and -12 mV. The vMGB neurons were found to maintain shorter first spike latency values than the dMGB at the different voltage levels. Neurons that possessed longer latency values at threshold were found to maintain their longer time spans even at higher voltages. The latencies of dMGB neurons were found to be longer than those of the vMGB neurons throughout the entire voltage range tested and were averaged 128.43 ± 16.28 and 41.5 ± 7.77 ms at the spike threshold voltage level, respectively. The latency is a function of the sub-threshold conductances, threshold, and the resting membrane potential. Therefore, a delayed onset and a higher threshold/RMP difference should result in a longer first spike latency.

3.05 Quantification of Onset Rise Time Constant

The precise timing of the occurrence of the first spike (first spike latency) is determined by the delay of the rise time constant (Figure 3.10). This was quantified by fitting exponential fits to the rising voltage curve from stimulus onset to the inflection point of the first spike. Time constants read from these fits were strikingly different between dMGB and vMGB neurons, when measured at threshold level. The average rise time constants of the dorsal MGB neurons were much longer (tau = 116.7 ± 30.45 ms; n = 39) than from the ventral MGB neurons (tau = 6.9 ± 0.90 ms, n = 34) on average (Table 1). The difference in average time constant remained significant upon comparison of time constants at similar membrane voltage values.
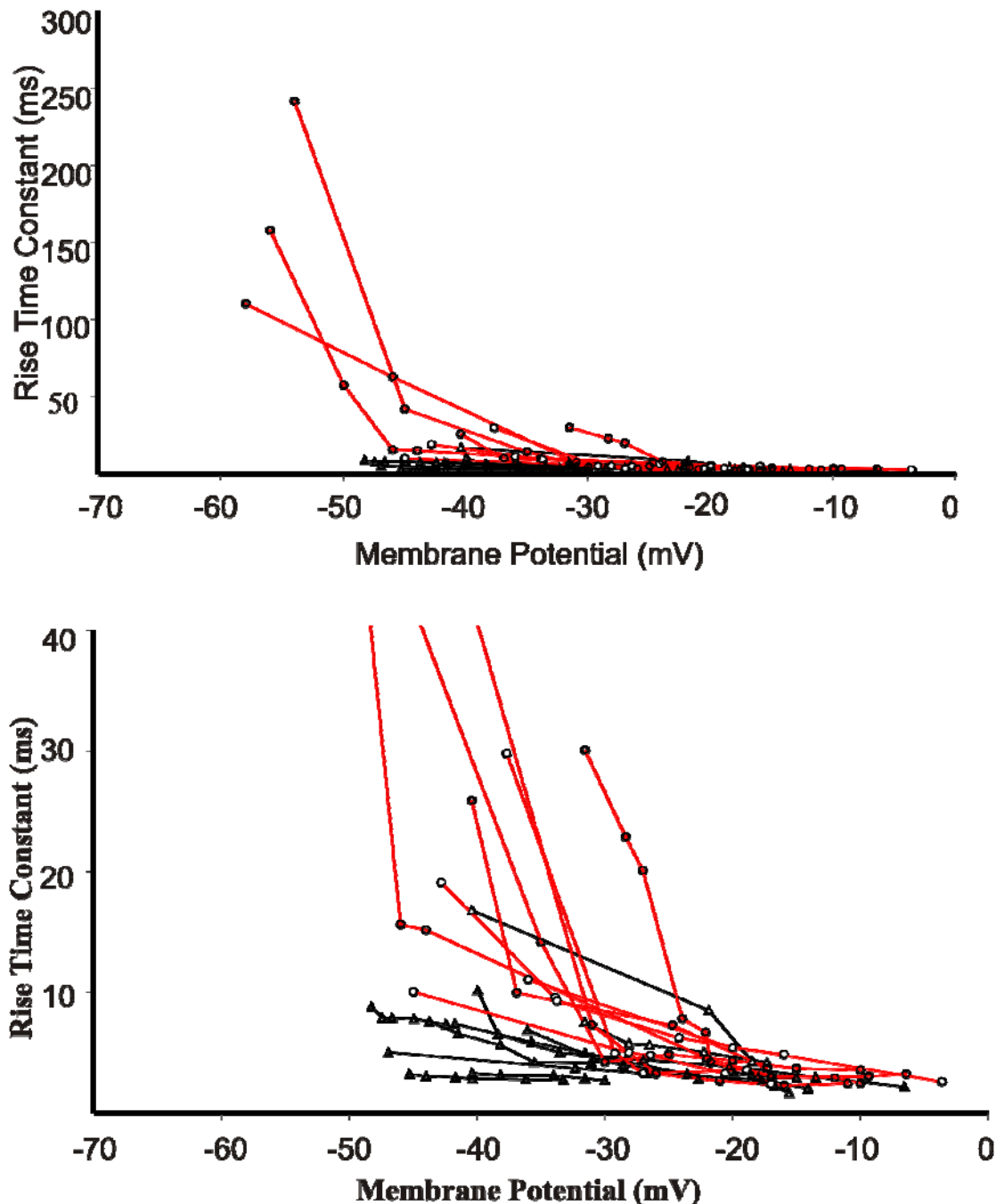
Figure 3.12 Differences in the kinetics of the delay to the first action potential were found between the dorsal and ventral MGB groups throughout the entire range of voltages tested. Rise time constants as a function of membrane potential values were plotted for dorsal (circles) and ventral (triangles) MGB neurons to compare the voltage dependence between both groups. Dorsal MGB neurons possessed slower kinetics than the ventral group throughout the full range of voltages. Both charts show the same data, only the y-axis is expanded in the bottom chart to show the data more clearly for time constants below 40 ms.

The majority of MGB neurons could be fitted with one exponential. MGB neurons that

required 2 exponentials to characterize a fast and slow component were average tau-weighed.

The rise time constant of the first spike of neurons that were shown to be slowly accommodating (93.2 ± 30.87 ms) were found to be significantly slower (p < 0.01) than those that rapidly accommodated (11.7 ± 0.94 ms), at threshold levels. The rise time constants decreased asymptotically with membrane potential (Figure 3.12). The ventral division maintained a more rapid time constant throughout the voltage range tested.

3.06 Relating Rise Time Constant to Membrane Potential and First Spike Latency

The rise time constants were not only compared at similar membrane voltage levels but were also compared at similar latency values to explore whether the rise time kinetics can be correlated to the latency values (Figure 3.11). The y-axis of the latency-voltage relationship from Figure 3.9 was expanded in Figure 3.11 thereby displaying the data from 0-50 ms more clearly. The x-axis remained unchanged. Latency values (30, 20, and 12 ms) were specified (a, b, and c). The corresponding traces for each data point were evaluated for rise time constant values. The rise time constants and the latency were then compared. Surprisingly, the average values of the rise time constants were not significantly different for short latency values (less than 12 ms) irrespective of membrane potential (p > 0.05). The time constants at the 30 ms latency level were 9.08 ms (dorsal) and 4.83 ms (ventral). The 20 ms latency level had 8.92 ms (dorsal) and 4.28 (ventral) time constant values. Rise time constants at the 12 ms latency level were 6.14 ms (dorsal) and 3.80 ms (ventral) The P values were (p = 0.088) for A, 30 ms; (p = 0.288) for B, 20 ms; and (p = 0.101) for C, 12 ms, for the Student's Two Tailed T-test.

The latency and rise time constant were fitted with regression linear trend lines (Figure 3.13). The linear regression analysis of the time constants and first spike latency in Figure 3.13 resulted in an average coefficient of determination of 0.9652 for the vMGB neurons and 0.8312 for the dMGB neurons, indicating that the regression lines were able to predict the normalized R from the latency values.
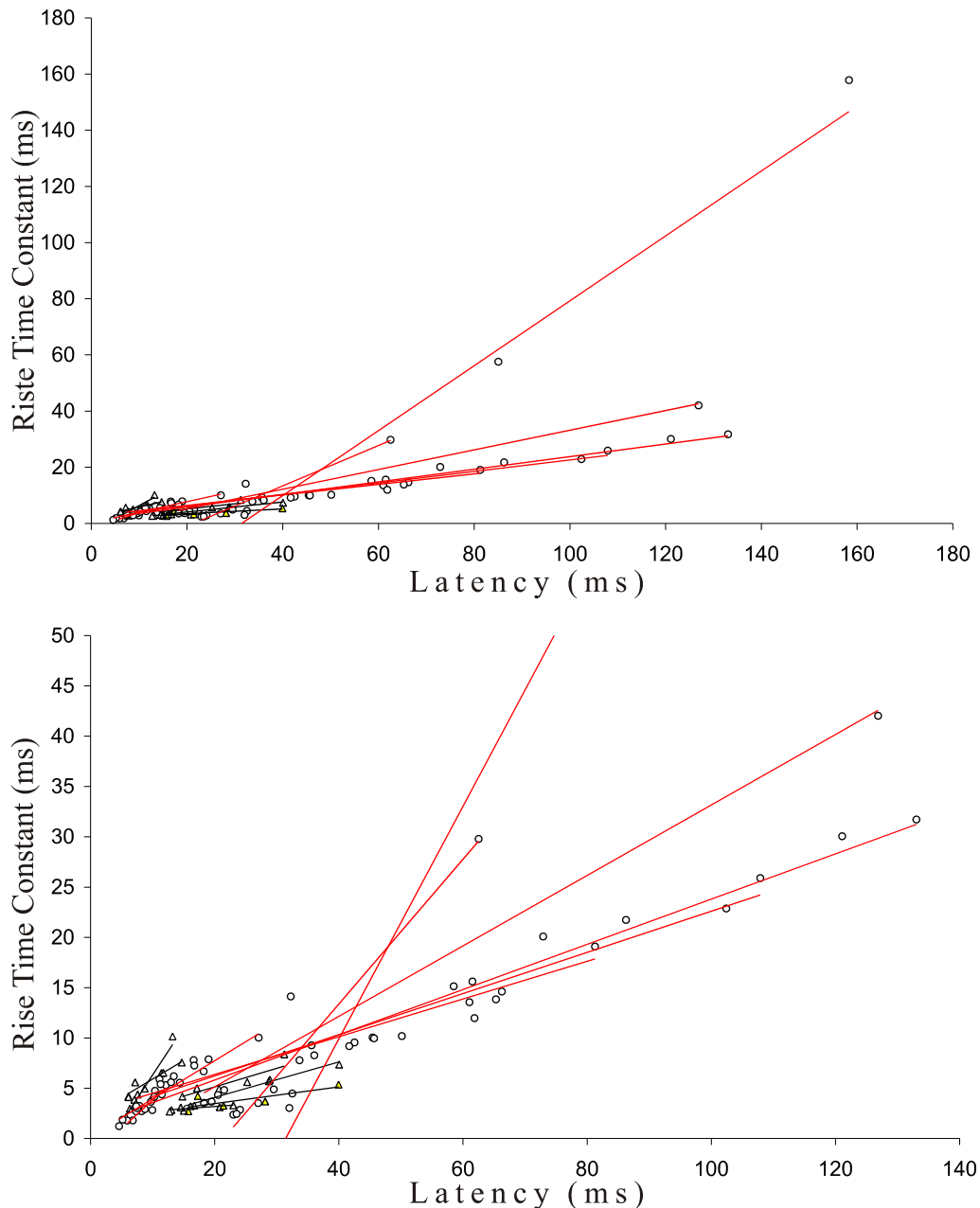
Figure 3.13 Onset kinetics versus first spike latency in dMGB and vMGB neurons.
The data points for different membrane potentials from each neuron were fitted with a linear function. The dorsal group (circles) is fitted with red lines and the ventral group (triangles) with black lines. Since the dorsal group had significantly longer latency and onset rise time constants, the scales of the top graph were reduced to show the ventral group more clearly in the bottom graph.

The rise time constant decayed asymptotically as a function of increasing depolarization of the membrane potential, similar to the latency. The latency and rise time constants are nearly linearly related (Figure 3.13).

A.

B.
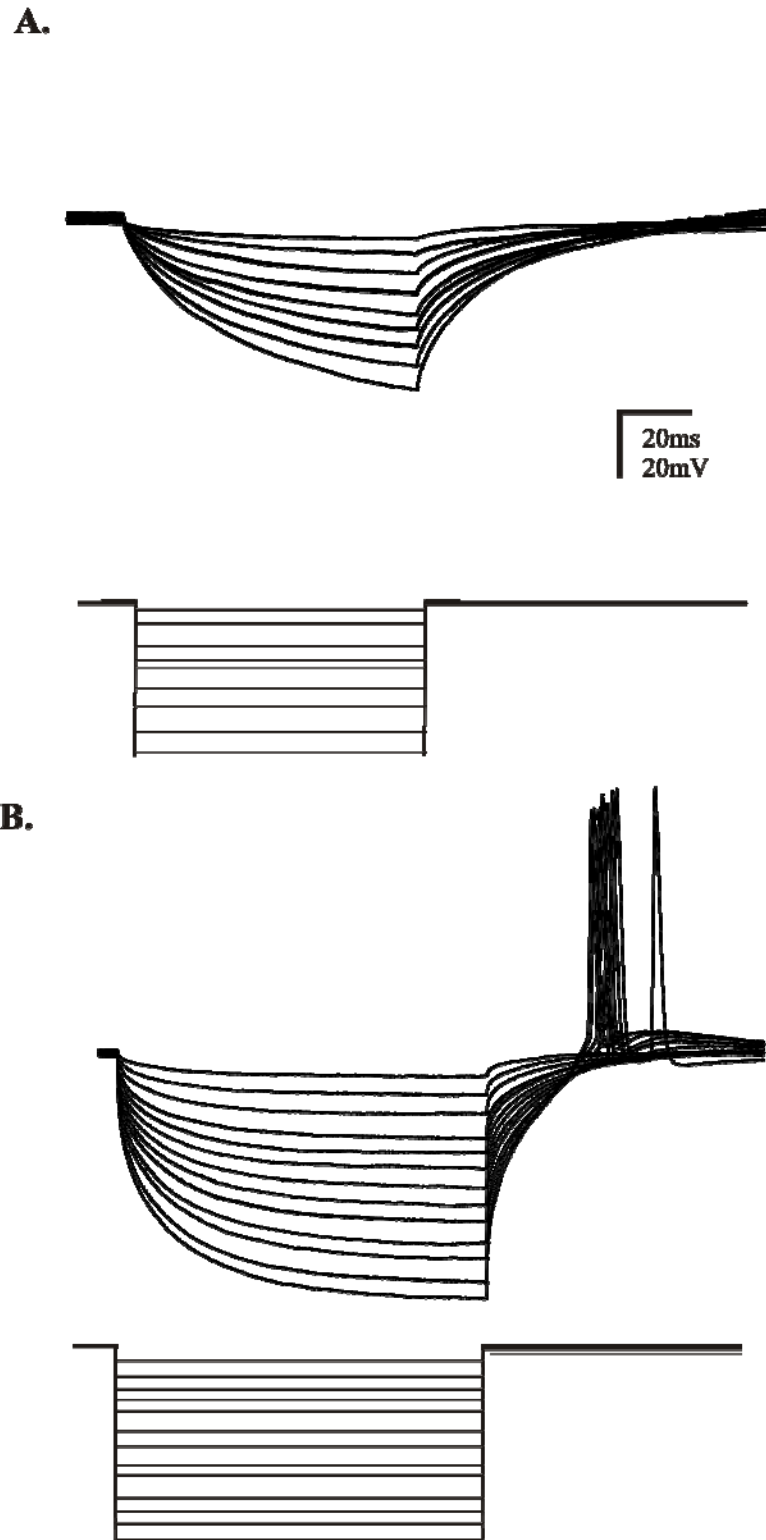
Figure 3.14. Current clamp recordings reveal similar inward rectification properties between dMGB and vMGB neurons in response to hyperpolarizing current injections. Neither group displayed a prominent hyperpolarizing activated inward rectifying "sag" (A) Superimposed sweeps of an example vMGB neuron that was held at RMP (-72 mV) and stepped to hyperpolarized voltages with 75 ms rectangular pulses. (B) Superimposed sweeps of an example dMGB neuron stepped to hyperpolarized voltages with 100ms rectangular pulses. Note the rebound spikes. Rectangular pulse stimulus protocols are depicted. (dMGB, tau = 6.4 ± 0.83 ms , n = 39; vMGB, tau= 4.9 ± 1.63 ms , n = 34, P > 0.05).
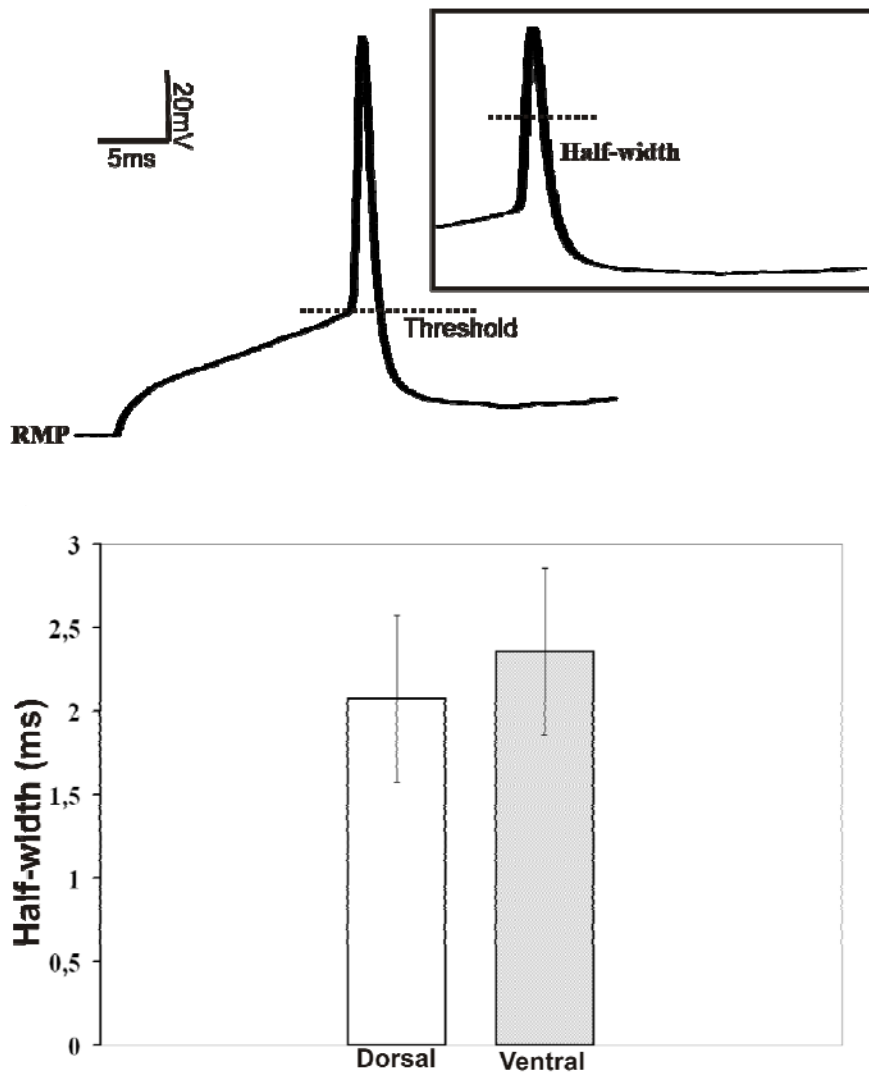
Figure 3.15. Significant differences in the action potential half-width were not found between the dorsal and ventral MGB groups. The length of time between the half-way point of the spike, "half-width", were measured and compared between the ventral (2.04 ± 0.16 ms) and dorsal (1.95 ± 0.13 ms) MGB groups. The groups were not found to have significantly different half-width values (p > 0.05).

3.07 Hyperpolarization- Activated Responses

Currents activated in response to hyperpolarizing current injections were investigated. Neurons from neither the dMGB or vMGB groups displayed a prominent inward rectifying 'sag'. Neurons may respond to a square pulse hyperpolarizing current with a pronounced inward rectification that has been variously described as a 'sag' because the resultant voltage trace has a sagging portion. Neurons hyperpolarized from RMP, e.g. -60 mV, displayed various degrees of inward rectification but the depolarizing 'sag' was not an apparent feature

67

of these neurons, under stated conditions (stimulus time < 200ms, holding at resting potential). Neurons of both the dorsal and ventral divisions failed to show the "sag" and the inward rectification but seemed to follow a slower activating conductance trajectory (Figure 3.14). Dorsal MGB (tau = 6.4 ± 0.8 ms) and ventral MGB (tau = 4.9 ± 1.6 ms) neurons displayed differences in time constant that were not significantly different (p > 0.05; Table 1). Both groups displayed rebound spikes. Rebound spikes possessed spike half-width times similar to the first spike duration at threshold level. No correlation between occurrence of rebound spikes and inward rectification was found
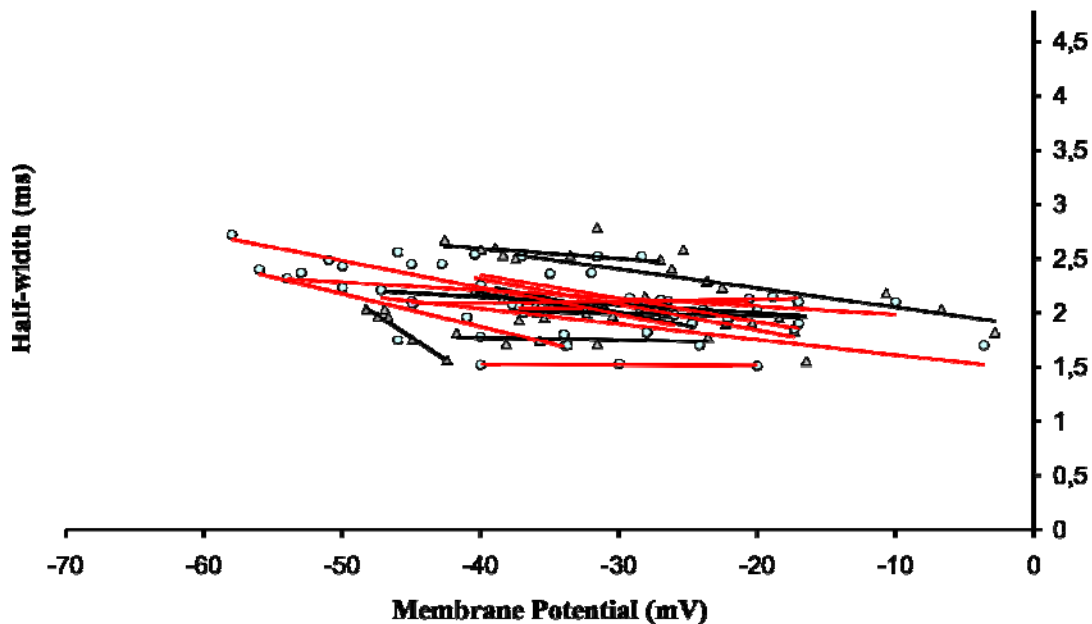
Figure 3.15 Action potential half-width in first spike of dMGB and vMGB neurons as a function of membrane potential. Half-width values of neurons from both groups exhibited a marginal decrease in the half-width time that changed linearly but not to a significant extent from threshold values (red-dMGB, black-vMGB).

3.08 Half-width of Initial Spike

The action potential duration was quantified by measuring the width of the action potential half-way between the peak of the spike and the beginning of the afterhyperpolarization (Figure 3.15, Table 1).
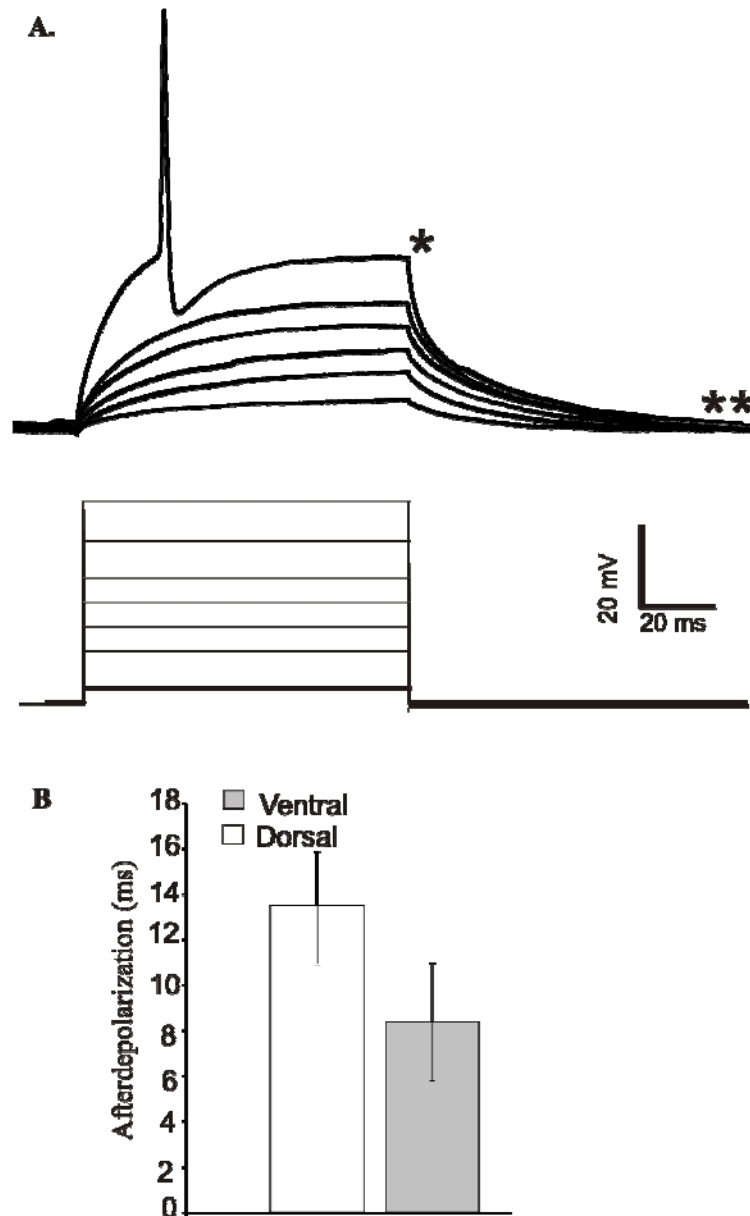
Figure 3.16. The time constant of afterdepolarization (ADP) of the dorsal and ventral divisions were compared. The time constant of ADP was measured from offset of stimulus (*), at the steady-state portion of the trace, along the decaying portion of the response (**). The ADP measurements were not found to differ significantly (P > 0.05) between the two groups.

Neurons in the dMGB (1.95 ± 0.13 ms, n = 39) and vMGB (2.04 ± 0.16 ms, n = 34) did not have significantly different spike durations at threshold level (p > 0.05, Table 1). Spike duration did not change much in response to increased depolarization in either group nor with respect to other parameters. Half-width values of neurons from both groups exhibited a marginal decrease in the half-width time with the increase of membrane potential.

TABLE 1	Ventral MGB	Dorsal MGB
First Spike Latency**	41.5 ± 7.7	128.4 ±16.2
Spike Half-width	2.0 ± 0.2	1.95 ± 0.1
Rise Time Constant**	7.0 ± 0.9	116.7 ± 30.5
Accommodation**	2.1 ± 0.03	5.95 ± 1.1
Threshold	42.9 ± 2.9	44.3 ± 2.9
% Spontaneous	0%	23.5%
RMP-Threshold	19.96	17.95
Ih Tau	4.9 ± 1.63	6.4 ± 0.83
Slow AHP	8.3 ± 3.8	13.2 ± 3.4
RMP	62.9 ± 3.4	60.1 ± 2.9
Low Voltage Rinput	307.0 ± 74.2	237.5 ± 48.9
High Voltage Rinput	61.0 ± 10.4	64.2 ± 16.2

Table 1. The Table compares the average values of the respective intrinsic properties between the dMGB (n = 39) and vMGB (n = 34) measured at spiking threshold, unless otherwise indicated. Asterisks indicate the statistical significance between dorsal and ventral MGB neurons (**$p < 0.01$, *$p < 0.05$). The latency, duration, onset tau, Slow AHP, and I_h tau are expressed in milliseconds; the threshold and resting membrane potential in millivolts; and the input resistances for the low voltage (Low R_{input}) and high voltage (High R_{input}) measurements are in megaohms. The accommodation comparison is of the number of spikes averaged for a 200 ms stimulus time.

3.09 Afterdepolarization (ADP) at the offset of the stimulus step

Cessation of steady depolarizing current injection not only allows Na^+ ion channels to loose their deactivation but the voltage response represents the activation of K^+ currents. Measurements of the time course of the response at the offset of depolarizing current injection, the afterdepolarization (ADP), were fitted with single decaying exponentials.

The ADP was not found to be significantly different between the two groups of neurons. Both the dMGB (13.2 ± 3.4 ms) and the vMGB (8.3 ± 3.8 ms) groups were fitted and exhibited a monophasic ADP that was able to be fitted with a single exponential. No significance differences were found ($p > 0.05$; Table 1) (Fig. 3.16).
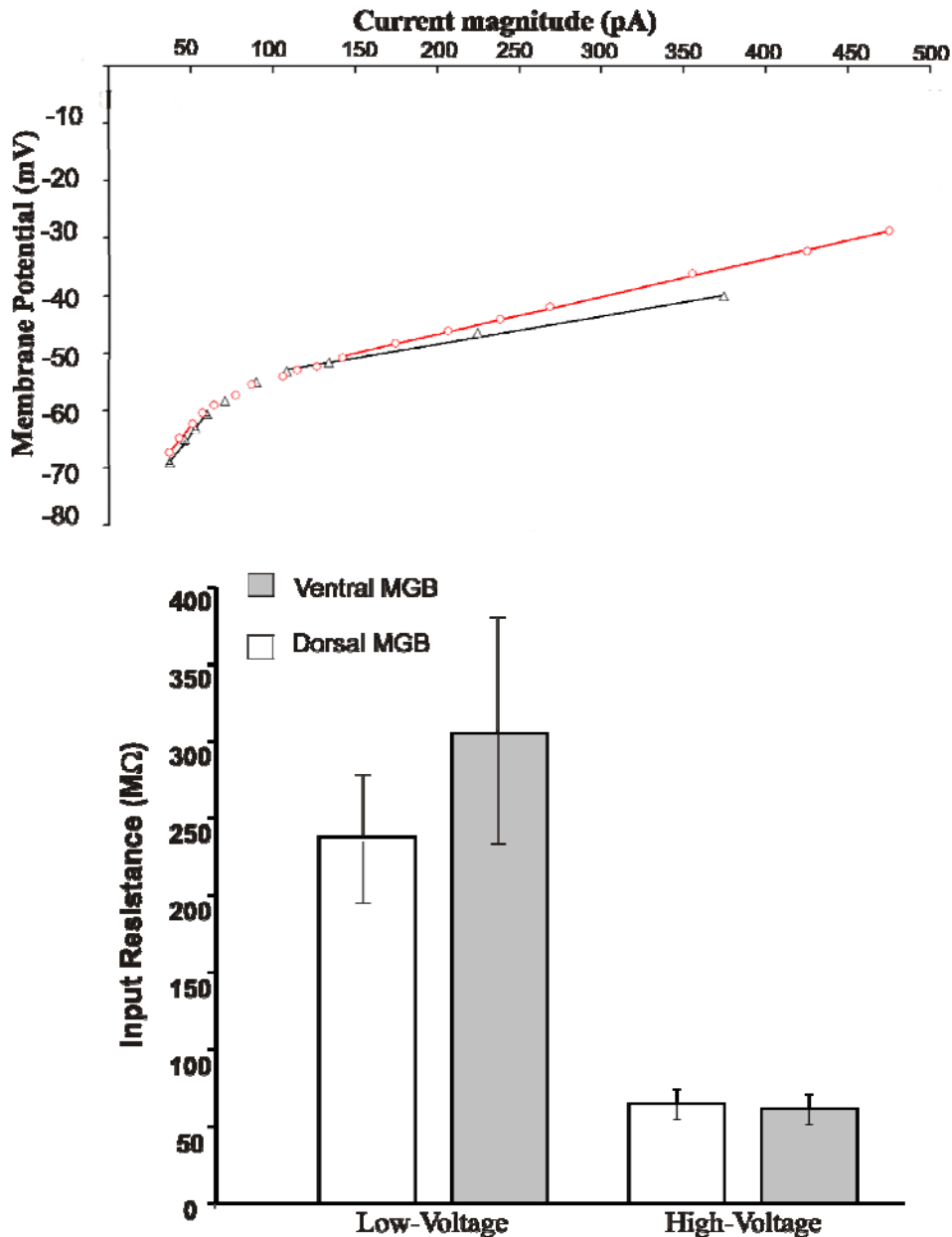
Figure 3.17 Input resistances at low and high voltage levels were similar. An example of comparisons of current-to-voltage relationships of the dMGB and vMGB groups were found to have similar values at low (below -55mV) and high (above -55 mV) voltage levels for input resistances. The current-to-voltage relationship of dMGB and vMGB neurons was used to calculate the input resistance. The input resistance was not found to be significantly different between both groups of neurons. Low-voltage input resistance was 237.5 ± 48.9 MΩ and 307 ± 74.2 MΩ and high-voltage input resistance was 64 ± 16.2 MΩ and 61 ± 10.4 MΩ for the dMGB and vMGB groups, respectively (dMGB n = 39, vMGB n = 34, P > 0.05).

3.10 Input Resistance

Neurons in the dMGB and the vMGB did not have significantly different input resistances at low or high voltage levels (Table 1). Input resistances were measured at low-voltage, near resting membrane potential, and at high voltage, suprathreshold levels. Input resistance values at low voltage levels were 237.5 ± 48.9 MΩ in the dMGB and 307.0 ± 74.2 MΩ in the vMGB. Input resistance at high voltage levels were 64.2 ± 16.2 MΩ in the dMGB and 61.0 ± 10.4 MΩ were found in the dMGB and vMGB groups ($p > 0.05$), respectively (Figure 3.17).

4.0 DISCUSSION

There are copious descriptions of the physiological properties of neurons, based upon intracellular electrophysiology, on most of the major groups of neuronal subtypes in the peripheral and central nervous system. Nonetheless, there still remains much to be learned about the functional implications and an elegant system to use as a model for a better understanding of neuronal physiology is the auditory system. Within the auditory nervous system there resides a topographic and physiological strategy to faithfully encode and preserve the sound properties that carry information about temporal and frequency properties of a sound stimulus with high fidelity.

4.01 The Auditory Peripheral Nervous System: A Model of Organization

Sound temporally varies in amplitude, the phase of oscillatory compounds, and in frequency. The auditory nervous system has the task of analyzing these time-varying features. The integration of the full spectro-temporal range of sounds into a spatio-temporal code of neural activity is the challenge that the auditory nervous system meets perpetually. Along the entire auditory processing axis, from the external ear to the cortex, sound frequencies are encoded tonotopically, a specific topological organization based upon frequency (Kiang, 1965; Spoendlin, 1973). Before sound reaches the nervous system, a real-time spectral decomposition is executed as the tonotopic segregation of sound begins biomechanically in the cochlea (see Dallos, 1992 for review). Once sound reaches the nervous system, at the level of the spiral ganglion neurons (SGN), the tonotopic order is established. A convenient feature of the auditory system is that the tonotopic organization

permits an investigator to identify the high and low frequency regions anatomically. One can compare the properties along the frequency axis thereby identifying parameters that may be involved with the neural encoding of sound (Liu 2007). In earlier studies it was shown that the SGNs possess intrinsic electrophysiological features that varied along the tonotopic axis of the cochlea (Adamson & Reid et al.,2002a,b, Reid et al., 2004) (Figure 4.1). Some of the intrinsic parameters compared were the action potential latency, duration, and rise time constant from the onset of stimulus. The neurons in the high frequency region possessed shorter response times than those in the low frequency region for the parameters studied. This organization exemplifies a system with heterogenous electrophysiogical properties orderly distributed along the tonotopic axis, an "ordered heterogeneity". Another significant electrophysiological distinction that was determined in the auditory periphery is between the two main groups of SGNs, the Type I and Type II spiral ganglion neurons. These two groups were known to differ in innervation pattern (Dallos, 1992) and intermediate filament protein distribution (Hafidi et al., 1998) and were later shown to differ in their electrophysiological properties in ways that may have bearing on other regions of the nervous system (Reid et al., 2004). Considering the auditory peripheral nervous system can set the stage for a clearer understanding of the relevance and implications of the physiology elsewhere in the auditory system.

4.02 Comparative Analysis of the Spiral Ganglion & Medial Geniculate Neurons

Parallels can be drawn between the spiral ganglion neurons and the neurons found in the medial geniculate nucleus of the thalamus, which may give some insight on neuronal encoding strategies. For instance, a comparative analysis of the innervation patterns and the firing properties between the spiral ganglion and the medial geniculate body neurons suggests a correlation between the firing characteristics and the innervation pattern.
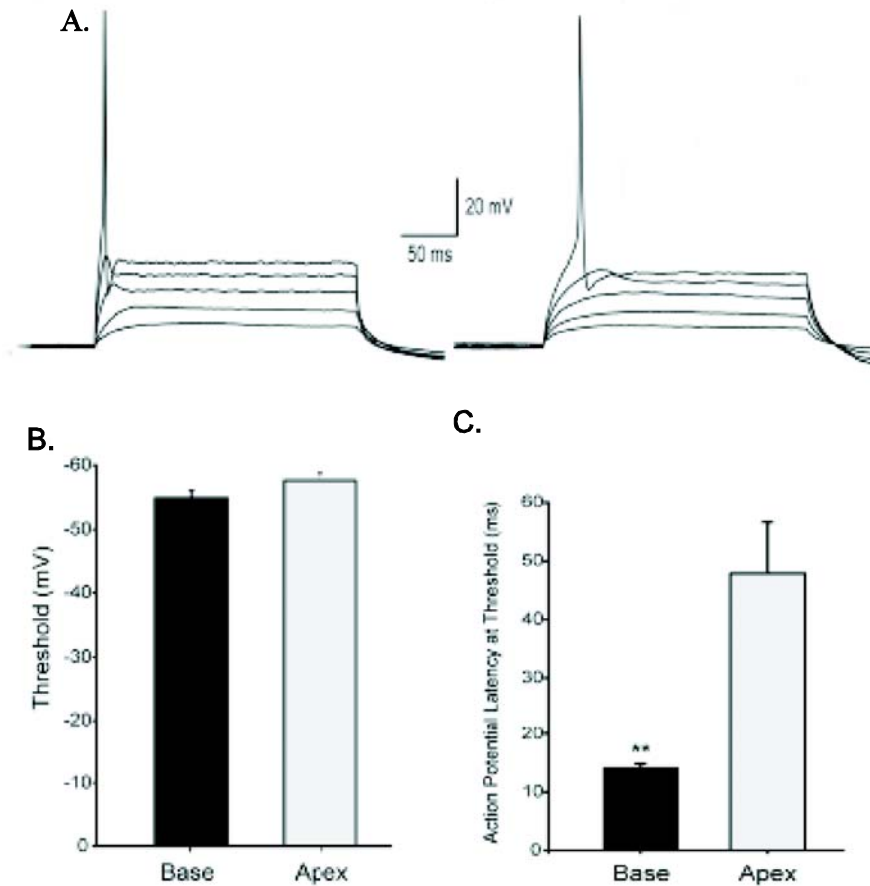
Figure 4.1 Differences in latency and rise time kinetics in the spiral ganglion neurons. (A) Two families of traces from current clamp recordings are shown to depict the differences in rise time kinetics and latency between neurons with different functional roles. The left and right family of traces are from Type I spiral ganglion neurons that encode high and low frequency sounds, respectively. (B) Average threshold values were not significantly different while (C) latency to the first spike values were found to be so.

4.02a Innervation Patterns

In the cochlea between 10,000 and 55,000 spiral ganglion neurons can be found in each ear, depending on the animal species. For instance, cats have 55,000 neurons, while rodents have 30,000. These neurons innervate the 2 categories of sensory receptors, the inner hair cells (IHC) and outer hair cells (OHC). One row of IHC and 3 rows of OHCs are in each ear. The Type I and Type II SGNs innervate the 2 categories of hair cells. The peripheral, also termed radial, fibers of the Type I SGNs innervate the IHCs. Those of the Type II SGNs innervate the OHCs. Type I SGNs make up 95% of the afferents, while Type IIs comprise

less than 5%. Although the Type II SGNs comprise less than 5% of the afferents they innervate all of the OHC. It has been shown that there may be another category rarer than the Type II variety, the Type III SGNs, which also innervate the OHC but they are much larger than the Type IIs and little is known about them (Webster & Webster, 1978).

The Type I and Type II SGNs do not only differ in which sensory receptors they innervate. There is also difference in their pattern of innervation. The Type I SGNs innervate the inner hair cells in a one to one fashion, with a non-branching dendrite, and each IHC is innervated by 10 - 70 Type I SGNs. In contrast, each Type II SGN innervates 5 - 50 OHCs (Spoendlin, 1979; Perkins & Morest, 1975; Ryugo, 1992). Therefore, the output of multiple OHCs converges onto an individual Type II dendritic tree and the individual IHC output diverges upon multiple Type I fibers. The axons of the Type I and Type II fibers comprise a part of the vestibulo-cochlear pathway (Cranial Nerve VIII) projecting to the cochlear nucleus complex in the brainstem. The cochlear nuclei project to the superior olivary complex (SOC), which not only projects forward to the inferior colliculus but feeds back to the cochlea. Processes from the lateral olivocochlear system of SOC project directly back to the OHC, thereby modulating the input to the Type II SGNs. Processes from the medial olivocochlear system of the SOC project back to the dendritic processes of the Type I radial fibers to modulate the dendritic conductance of the SGNs (Warr, 1997). The precise innervation of Type I SGNs from individual IHCs is reflected by their high selectivity for a narrow range of sound frequencies at low stimulus levels (Kiang, 1965; Liberman, 1978). The profuse innervation of the Type II SGNs from many OHCs predicts that they possess sensitivity for a broad range of frequencies and the capacity to integrate greater combinations of input (Reid, 2004). The differences in the innervation patterns and roles of the Type I and Type II SGNs bares similarity to the innervation patterns of the vMGB and dMGB neurons. The vMGB neurons derive precise frequency input from less sources than the dMGB neurons, which must integrate multi-modal and broad frequency input.

4.02b Firing Properties

The Type II neurons have significantly slower response properties (latencies = 121.9 ± 7.25 and rise time constants: 35.16 ± 4.1) than the Type I (latencies: 17.4 ± 0.7 and rise time constants: 15.6 ± 0.25) neurons (Reid et al., 2004). Type II neurons also have a greater percentage of slowly accommodating neurons. The distinction between firing properties, coupled with the differences in the pattern of innervation along the tonotopic axis, seem to suggest a link between intrinsic firing properties and neural encoding. The differences in firing responses between the Type I and Type II SGNs share similarities to the differences between the neurons of the vMGB and dMGB, qualitatively. The dMGB have significantly (p < 0.01) longer first spike latency (128.43 ± 16.28) and rise time constants (116.67 ± 30.45) than the vMGB (latency: 41.50 ±. 7.7, rise time: 6.95 ± 0.90). Additionally, the dMGB neurons also exhibit a greater amount of slow accommodation.

Although the vMGB and dMGB relationship was found to be qualitatively similar to the Type I and Type II relationship, there was no reason to expect that the latency and rise time constants of the dMGB and the Type II SGNs or the vMGB and the Type I SGNs to be statistically similar. The dMGB neurons possessed significantly different first spike latency (p < 0.01) and rise time (p < 0.05) values from the Type II group. The vMGB neurons differed from the Type I neurons in first spike latency (p < 0.001) but not in the rise time constant (p = 0.539). However, differences in experimental procedures make it difficult to make direct comparisons. The spiral ganglion neurons were stimulated from a holding potential of -80 mV, while the MGB neurons were stimulated from resting potential. The SGNs were patched in culture and the recordings from the MGB neurons were done in slices. The SGNs were from 6 - 10 day old mice and the MGB neurons were from 4 – 5 week old gerbils. What is being described is a conserved neuronal encoding strategy that may extend,

not simply across species, but at different stages of the auditory system. Hence, an added benefit of the present study is the opportunity to make a comparison at two stages of the auditory system to assess whether similar or conserved cellular properties can be found.

4.03 Membrane Voltage Dependent Spiking Behaviour

The thalamic nuclei are strongly suggested to have two membrane potential modes of operation when stimulated without any synaptic background conductances, the high voltage "active" state and the low voltage "sleep" state (Sherman & Guillery, 1998). Such a mechanism is not unique to neurons in the thalamus. For instance, cortical neurons may respond differently dependent upon the background conductances (Bal et al., 2004) or the timing of different conductances in the dendrites and soma (Larkum et al., 1998, 1999). Nonetheless, these two functional states have been demonstrated in some thalamic nuclei, including the MGB (Tennigkeit, 1998). Therefore, before any consideration of the functionality of neuronal physiology in the thalamus can be entertained, the implications of membrane voltage level must be determined.

4.03a Resting Membrane Potential

The resting membrane potential (RMP) was measured as the membrane voltage potential that the neuron maintained without hyperpolarizing or depolarizing current injection, e.g. 0 current input. The threshold voltage potential was determined by measuring the lowest membrane voltage that elicited an action potential. In the present study, the two MGB groups did not show significantly different resting membrane potentials, -60.1 mV and -62.9 mV for the dorsal and ventral group, respectively. This is supported by an *in vitro* study from Smith and Bartlett (Bartlett & Smith 1999). Smith and Bartlett reported RMP levels that were not significantly different between the dMGB and vMGB in the rat with RMP levels of -64.7 ± 6.4 mV and -64.3 ± 4.9 mV, respectively. However, Hu reported a significantly lower RMP

in the dMGB (-62 ± 4.6 mV) than the vMGB (-71 ± 4.7 mV) neurons in *in vivo* experiments (Hu, 1995; Yu, 2004).

Several reasons may account for the differences found in the resting membrane potential levels. The differences may reflect species specific differences. Others used rats or mice (Bartlett & Smith, 1999; Hu, 1995). The differences may be due to differences in the preparations. Synaptic connections were maintained in other studies whereas the cortical and subthalamic connections were not preserved in this study, in order to avoid any inadvertent synaptic activity. An *in vivo* preparation would leave intact several inhibitory circuits, which could lower the membrane potential. It is possible that the hyperpolarizing effects of the cholinergic input from the midbrain parabrachial region (Mooney et al., 2004) and the GABAergic input from the zona incerta (Bokor, 2005) and the inferior colliculus (Winer et al., 1996) account for the differences. The membrane potential differences may also be due to differences in recording solutions, i.e. the use of K^+-gluconate would lower the membrane potential more than KCl^-.

4.03b Threshold Voltage Level

The threshold levels between the two groups were not significantly different either. The dMGB was -44.29 ± 2.92 mV and the vMGB –42.91 ± 2.87 mV. Since the threshold voltage levels were not significantly different, it can be assumed that the threshold level is not the determining factor in the functional differences between the ventral and dorsal groups. Other groups did not report the specific spiking threshold levels, but rather stated that it lies above -55 mV (Schwartz, 1998; Tennigkeit et al., 1997 1998; Hu et al., 1994, 1995; He et al., 2002; 2004, Bartlett & Smith, 1999). The respective absolute voltage differences between the threshold and resting membrane potentials were compared and not found to be significantly different. This difference is a reflection of the requisite depolarizing conductance that must take place before a neuron can fire.

Thusly, the vMGB and dMGB neurons were stimulated from resting potential, instead of a hyperpolarized voltage level, and neither the RMP nor the threshold voltage level were significantly different from each other. Therefore, it can be assumed that the spike behavior differences were not due to differences in membrane voltage level and must be due to some other intrinsic physiological factor.

4.04 Some Varieties of Spiking Behaviour

Spiking behaviour has been variously characterized in cortical neurons and may offer some insights on the firing properties of thalamic neurons. Reports describing the electrophysiology of neocortical neurons have appeared since the early days of *in vivo* intracellular electrophysiology (Albe-Fessard & Buser, 1953; Calvin & Sypert, 1976; Li, 1959; Phillips, 1956; Takahashi, 1965; Tasaki, 1954). However, it was not until more recent studies on membrane properties of cortical neurons that we begin to gain our current, more extensive, perspective on electrophysiological distinctions (Connors et al, 1982; Llinas, 1988, 1990; McCormick et al, 1985; Victor 2000, 2005). Neocortical neurons have been classified into at least 5 main electrophysiological categories based upon firing patterns in response to intracellular current injection: regular spiking (RS), intrinsically bursting (IB), fast spiking (FS), fast repetitive bursting/chattering (FRB), and low-threshold spiking (LTS) (For review see Rieke et al 1997). One of the distinctions, the LTS category, is of particular interest here because neurons in the thalamus have been described as being of the LTS variety. LTS spiking is typified by short bursts of 2 - 3 spikes riding on a small depolarizing hump, which can only be elicited from a hyperpolarized membrane voltage level. The activation range is positive of -70 mV. The inactivation range is between -100 mV and -60 mV, with a time constant of 20 - 50 ms for complete inactivation. The spike generation is based on a small single channel conductance (8 pS) and it is calcium dependent (Hille, 2001). The LTS

spiking pattern is also attributed to tiny conductance Ca^{2+} channels and is, therefore, also referred to as I_T. I_T is normally found in the dendrites and plays a critical role in amplifying electrotonically distant inputs (de la Pena, 2000). LTS neurons respond linearly, with spikes, to synaptic input if they are stimulated from depolarized voltage level but are reported to respond with a stereotyped burst of spikes when stimulated from hyperpolarized voltage level, relative to RMP (Contreras et al., 2004). For instance, if an LTS neuron were stimulated by an inhibitory input reducing the membrane potential to below -65 mV for at least 50 ms just before (< 7 ms) an excitatory stimulus then the neuron would respond in the stereotyped bursting pattern. The duality of the spiking behaviour of the MGB neurons is most similar to the LTS neurons of the cortex. The different firing patterns, in the same neuron, found at depolarized or hyperpolarized stimulation voltage levels is aptly described as a tonic or bursting firing behaviour, respectively (Sherman et al, 1998).

The important functional distinction that has been drawn about thalamic relay neurons to be considered is that neurons either assume a tonic or burst firing modus operandi, dependent upon membrane potential level (Sherman et al., 1998). Neurons held at lower voltage levels are shown to have a stereotyped response mode, a LTS spike pattern. On the other hand, neurons held at depolarized voltage levels have tonic properties. The stereotyped mode is the firing pattern induced by holding a neuron at a hyperpolarized (below -65 mV) membrane voltage for approximately 100 ms before stimulating, similar to the cortical responses that have also been reported in many thalamic nuclei (Ramcharan et al., 2005). This protocol engages a voltage and time dependent inward Ca^{2+} current (I_T) (Sherman et al., 2001; Zhan et al., 2000; Jahnsen, 1984; Destexhe et al., 1998; Williams et al., 2000) resulting in a low threshold spike crowned with several Na^+ spikes. The tonic mode requires holding a neuron at high voltage levels (approximately -60 mV) before stimulation. The tonic mode is considered to be the most relevant mode for sensory encoding because it is the mode whereby stimulus input can have direct temporal and amplitude correlation to the response. It has been

further suggested that the low voltage is associated with sleep whereas the high voltage mode plays a functional or arousal role (Steriade et al., 1993; Crick et al., 1984; Hubel & Livington, 1981).

This study is concerned with the intrinsic response properties found in the depolarized or tonic mode of functionality within the gerbil thalamus that may have significant coding capacity. Therefore each neuron was characterized at or near RMP (-60 mV). In addition, neurons were subsequently held at hyperpolarized voltages and underwent a similar stimulus protocol. Upon comparison of dMGB and vMGB neurons that were characterized at or near RMP significant differences were found. Since the goal is to characterize the functional neuronal encoding mechanisms than it is was necessary to characterize the neurons at a higher voltage holding potential, e.g. RMP.

4.05 The Temporal Characteristics of Spiking

The time constant of the rise time, quantified by the time constant of one exponential fitted along the response at the onset of stimulation to the inflection of the spike, defines the specific timing of the action potential. This exponentially rising membrane voltage, in time, is the response to an "instantaneous" jump in membrane potential and is a simplified approximation of the complex process that entails the dynamics of the activation properties of different channel types, the quantity of the respective channels, and the various ionic conductances. The time constant is a cursory, yet definitive, approximation. The time constant of the rise time offers insight on the functional role of a neuron because of the direct relation to the spike latency and, additionally, the rise time waveform offers insight on the appropriate strength and timing of the ideal synaptic input required to elicit a spike.

The time constant of the rise time to an action potential occurs between the resting and threshold potential levels. In consideration of the fact that spike timing is a function of the

RMP, threshold level, and rise time constant combined then it should follow that one of these factors should significantly differ between the dMGB and vMGB groups. The dMGB and vMGB groups maintained similar resting and threshold voltage levels but differed in rise time constant values. This may be a hint to the functional role of rise time constants. The longer rise times between rest and threshold would allow for greater integration or convergence of input. Conversely, the faster rise time may afford the neuron greater resolution.

4.06 Action Potential Latency may be Critical for Encoding

Intracellular recording studies in the MGB have not reported action potential latency differences between the dorsal and ventral subnuclei. Latency changes in response to increased depolarization were described in general, but not comparatively (Bartlett & Smith, 1999). Additionally, other groups that have investigated medial geniculate body neuronal physiology used sharp electrodes which may have limited their ability to resolve the latency differences (Bartlett & Smith, 1999; Hu et al., 1994, 1995; He et 2004) due to the shunting or leakage resistance effect of impaling a neuron. Different parameters were the focus of these earlier studies, such as input resistance; RMP; rebound spikes and rectification in response to hyperpolarization; accommodation rate; and Ca^{2+}-dependent bursts; versus the primary considerations taken herein, e.g. first spike latency and rise time constant (Bartlett & Smith, 1999; Hu et al., 1995). Studies that have focused on the first spike latency have shown that the first spike is the most critical spike in a spike train for neuronal encoding (Panzeri, 2001) The authors quantified the contribution of 'information' in each spike in a spike train and were able to show that the bulk (83%) of information in a spike train resided in the first spike. The authors used an improvised (Panzeri et al., 2001; Panzeri & Schultz, 2001) Mutual Information (Shannon, 1963) information theoretic method, which quantifies the discrimination ability of an ideal observer of neuronal responses between all of

the different stimulation times, based on a single response trial. Therefore it is particularly important to concentrate on the first spike in a train when considering neuronal encoding.

It has been shown in the auditory periphery that first spike latency is associated with frequency encoding by correlating the latency of the first spike with the tonotopic organization of the cochlea in *in vitro* studies (Adamson & Reid et al., 2002a, b; Liu, 2007). It has also been shown in the same studies that first spike latency can be correlated to the amount of innervation a neuron receives (Reid et al., 2004). Additionally, it has been shown with *in vivo* studies that there is a more delayed response to auditory stimuli in the dMGB than the vMGB (Hu et al., 1995; He, 2002; Yu, 2004).

What might the purpose of this feature be? The functional significance may be indicative of the capacity of a neuron to integrate multiple inputs or respond to rapid inputs. In the auditory periphery, each Type II spiral ganglion neuron receives converging input from many outer hair cells and these neurons also have significantly longer latencies than their Type I primary auditory neuronal counterparts. This may be a case where many inputs are required to garner a response. Each Type I spiral ganglion neuron receives input from only one sensory receptor cell, permitting higher sensitivity and more resolution. Hence the longer latency of Type II neurons may imply a greater integration capacity, while a shorter latency of Type I neurons may suggest a greater capacity to derive discrete input. This idea does not imply that the dendritic tree in the respective neurons is not involved in the integration process. The role of the first spike latency in the computational capacity of a neuron does not negate the computational processes that occur in the dendritic tree (Larkum, 2005) but may shed further light on the complexity of interactions. An example of the complex interactions can be demonstrated by considering the role of spike latency in a backpropagating spike that is involved in coincident detection with dendritic Ca^{2+} spikes.

Upon consideration of the Type I group singularly, another functional purpose can be reasonably suggested. In the case of the Type I SGN group a latency difference is

tonotopically arranged, longer latencies are found in the low frequency area and shorter latencies are found in the high frequency area. The extensive range in latency values for the vMGB neurons may be related to the tonotopic organization of the ventral division although it was neither proven nor disproved herein. The tonotopy of the vMGB is arranged orthogonally along the rostro- caudal axis. In the periphery, the tonotopic order is arranged along one axis and is more accessible to investigation. Based upon the findings in the periphery, it was expected that the high frequency neurons would possess faster and the low frequency neurons slower response properties. The added difficulty however, lies in establishing the tonotopic axes in the slice preparation. The dMGB is not known to be organized tonotopically, although it projects tonotopically to the cortex (He et al., 2004), and has a narrower range in latency values. Therefore it came as no surprise to find that the response properties of the dMGB were not organized in any recognizable topography although the tonotopic organization is somehow be preserved.

4.07 Accommodation Rates

Rapidly and slowly accommodating neurons were found in both divisions but the dMGB possessed more slowly accommodating neurons, which is similar to the findings of others (Hu et al., 1994; Bartlett & Smith, 1999). The dMGB neurons possessed a significantly higher frequency of spikes per time period (200 ms bin). But not all properties of the slowly-accommodating neurons were the same, slowly accommodating neurons were found to exhibit two different firing characteristics in response to increasing stimulation. The majority of slowly accommodating neurons fired at threshold levels that were distinct from the resting membrane potential level but a subpopulation of 23.5 % fired at RMP, "spontaneous firing". Neurons that fired at RMP were found exclusively in the dMGB.

Spontaneously firing neurons were first described in invertebrates (Alving, 1968; Getting, 1989). It was shown that spontaneous firing arises from specific combinations of

intrinsic conductances (Llinas, 1988). In order for a neuron to fire spontaneously intrinsic conductances must depolarize the cell membrane to spiking threshold and then repolarize the membrane to a sufficiently negative membrane potential to elicit the next spike. Several currents have been found to be responsible for the subthreshold conductances that generate each spike spontaneously. Currents carried by I_h channels and T-type Ca^{2+} channels have been implicated (McCormick & Huguenard, 1992). Voltage-gated Na^+ currents and non-selective cation currents have also been shown to bring the membrane potential to threshold (Raman et al. 2000; Taddese & Bean, 2002; Jackson et al., 2004).

Spontaneous activity plays a role in transforming synaptic input into a specific spike output (Hausser et al, 2004). The role of spontaneously active neurons in the medial geniculate is clearly to regulate information flow to the cortex, since there are not any interneurons in the medial geniculate of the gerbil. These neurons were found only in the dorsal division and, therefore, may play a role in controlling non-auditory information flow to the cortex.

4.08 Not All Parameters Were Significantly Different

Other parameters that were compared in the auditory periphery (Reid et al., 2004) were also compared between the dMGB and vMGB. These parameters include the half-width of the first spike, the input resistance, and responses to hyperpolarizing current injections.

4.08a Half-width of the Spike

Unlike the parameters of latency, onset rise time, and accommodation rates, the spike half-width measurements were not significantly different between the dMGB and vMGB groups although the vMGB group was slightly longer. Similarly, the spiral ganglion neurons did not possess significantly distinct spike half width values between the Type I and Type II populations.

86

4.08b Input Resistance

Neurons in the dMGB and vMGB did not differ significantly in input resistance. Similarly, SGN groups did not possess significantly different input resistances. This finding suggests that the neuronal sizes between both groups were not significantly different. It can be then argued that the electrophysiological differences may not be a function of cell size differences. This is consistent with all other studies, which have not shown there to be a correlation between morphology or cell size and electrophysiological properties (Winer et al., 1999; Barltett & Smith, 1999).

4.08c Response to Hyperpolarizing Current

It has been reported that hyperpolarization-activated (I_h) cation channel activity is evident in a minority of vMGB neurons (Bartlett & Smith, 1997; Hu, 1995). Hyperpolarization-activated inward currents (Pape et al., 1996) have been reported extensively within the auditory nervous system (Davis et al., 1997b; Rogelis et al., 2006). It has been shown by in situ hybridization in the mouse that I_h genes (mHCN gene family) are expressed throughout the nervous system, including the relay nuclei of the thalamus (mHCN2, mHCN3, and mHCN4) (Franz et al., 2000; Santoro et al., 1998). I_h channel activity in various cell types have been well-documented (Yanagihara & Irisawa, 1980; DiFrancesco, 1981, 1986; Bader & Bertrand, 1984; Mayer & Westbrook, 1983; Spain et al., 1987). In the spiral ganglion neurons I_h activity is common, existing in most of the neurons (personal observations). These channel currents play a role in regulating synaptic transmission, setting the resting membrane potential, and contributing to the pacemaker depolarization in "spontaneous" firing neurons (McCormick & Bal, 1997). I_h channel activity can initiate rebound spikes after strong inhibition (McCormick & Pape, 1990; Pape et al., 1994, 1996; Lüthi & McCormick, 1998). Hyperpolarizing steps from resting membrane potential displayed a time-dependent slowly activating inward current in some neurons in the dMGB

and the vMGB (Figure 3.6) with rebound spikes. It has been suggested that I_h channels play a role in the sleep-wake cycle of the thalamus by regulating the transition from burst to tonic firing (Luthi, 1988).

Both the vMGB and dMGB were able to fire rebound spikes in response to hyperpolarizing stimuli. The ability for rebound spikes was not dependent upon latency, onset kinetics, accommodation rate, or any other measured parameter. Others have also reported rebound spikes in MGB neurons (Bartlett & Smith, 1999; Hu, 1995).

In response to hyperpolarizing current injection, neurons can respond in a variety of ways. A neuron may give a generic RC circuit response, displaying exponentially decaying charging voltage as a function of time, comparable to a Hodgkin-Huxley model (Hodgkin & Huxley, 1939, 1945, 1952a,b,c,d). Another common response to rectangular pulse stimulus is inward rectification, first characterized by Katz (1962) as a phenomenon whereby there existed a higher conductance for inward than outward current. Many neurons exhibit "inward rectification" in the hyperpolarizing direction (I_h), unlike the "inward rectification" described by Katz in several fundamental respects. The inward rectification described by Katz is a pure K^+ conductance. It is active mainly at voltage levels negative to the K^+ reversal potential, within several milliseconds, and is ohmic in nature. In contrast, I_h has a mixed Na^+/K^+ conductance and is dependent upon extracellular Cl^-. I_h has a reversal potential of approximately -20mV and very slow gating properties. Similar to Na^+, Ca^{2+}, and delayed rectifier K^+ channels, I_h has steep activation curves and activates with a sigmoidal time course but, in addition, I_h also deactivates with a sigmoidal time course in response to a rectangular-pulse stimulus. The I_h currents start activating between -45 and -60 mV, with a $^1/_2$ –activation between -75 and -85mV and a maximal conductance level at membrane potentials below -110 mV. I_h can also be regulated by the second-messenger signal cyclic adenosine monophosphate (cAMP), which can shift the gating along the voltage axis. I_h also affects resting membrane potential, input resistance, and afterhyperpolarization and, therefore, could

have a profound impact on the integrative capacity of a neuron. Ten to 15% of I_h is active at RMP, resulting in an estimated 30% addition to the resting conductance (Maccaferri et al., 1993; Pape et al., 1994). This depolarizing resting conductance makes the membrane potential positive to the K^+ equilibrium potential, which is at -90 mV. Establishment of the RMP allows the I_h to lower the apparent input resistance at membrane potentials negative to rest (Edman et al., 1989). An increase in I_h conductance and a lowered input resistance will result in a reduced period of hyperpolarization after a Na^+/ K^+ action potential. Although Na^+/ K^+ spike activity is out of the range of I_h activation, the rate of repolarization will be also enhanced by I_h. I_h has been implicated in rhythmic and burst firing and the initiation of rebound spikes (McCormick & Pape et al., 1990, 1996; Lüthe & McCormick, 1998). In the heart I_h plays a role in setting the pace of firing, in combination with several other prominent currents (I_{K+}, I_{Ca2+}, and leaky inward currents). The I_h current can play a role in shaping synaptic potentials to improve signal processing, which could be particularly advantageous in the auditory system (Banks M. et al, 1993). Indeed, in the SGN many neurons exhibited prominent I_h currents. I_h has also been reported in the auditory brainstem (Banks et al., 1993; Oertel et al., 1997). I_h currents have been demonstrated in a subpopulation of vMGB neurons but not in the dMGB. Under the conditions compared herein, higher voltage "tonic" resting membrane potential levels (-65 mV), I_h would be detected as a slowly activated inward current, possibly with a rebound spiking behaviour, but a prominent inwardly rectifying current was not obvious.

Bartlett and Smith (1999) showed a very slow mild inward rectification which rectifies to steady-state after several hundred milliseconds in response to hyperpolarizing current injections from a RMP of -63mV in the vMGB.

The inward rectification properties found in the present study displayed response properties that may be consistent with findings reported for thalamic relays neurons (Franz et

al., 2000), which showed evidence that slowly-activated inward rectification was due to low HCN1 and high HCN2, HCN3, and HCN4 expression, but a clear I_h sag could not be found.

4.09 The Driver and Modulator Hypothesis Applied

Sherman and Guillery (Sherman & Guillery et al., 1996, 1998, 2001) have proposed a theory on the functional organization of the sensory nervous system. According to their theory, sensory input is either of the driver or modulator variety. Drivers are inputs that carry primary information. The driver input carries the information that is qualitatively preserved. An example of driver input would be the projection from the retina to the lateral geniculate nucleus, which then continues as a driver pathway to the primary visual cortex. Another would be the Type I spiral ganglion input relayed through the subthalamic structures and then to the vMGB and the primary auditory cortex. Modulators are inputs that carry information that has been subsequently integrated. The modulator input carries information that has been converged upon by other pathways. An example of modulator input may be the layer VI cortico-thalamic pathway from a secondary auditory cortical area to the dMGB. Another would be the olivocochlear input to the OHC, which modulates the OHC activity that is relayed to the Type II spiral ganglion neurons. The modulatory input is essentially neural information that has been integrated with other neural information thereby fundamentally changing the qualitative nature of the code.

The primary, driver, input to the auditory system must travel through the vMGB. The projection neurons of the vMGB carry the precisely derived driver input to the primary auditory cortex. Thalamic nuclei that relay primary information are termed "first order". Secondary thalamic nuclei are termed "higher order" nuclei. The vMGB is considered a first order nucleus and the dMGB is considered a higher order nucleus. Additionally, higher-order thalamic neurons receive cholinergic inputs from the midbrain parabrachial region that cause

greater hyperpolarization than in the first-order neurons (Mooney, 2004) and a GABAergic input from the zona incerta targets higher order subnuclei predominately (Bokor, 2005). Therefore, in principle the higher order neurons are expected to have lower resting membrane potential levels, which were not found to be the case in this study. Regarding the other electrophysiological characteristics (e.g. action potential rise time constant, latency, and accommodation rates) distinguishing higher and first order relays, the dMGB and vMGB intrinsic neuronal responses were consistent with the driver-modulator theory.

Neurons in the dMGB and vMGB possess several physiological and anatomical characteristics that suggest a primary role in relaying primarily modulator or driver information, accordingly. Neurons in the dMGB have been consistently shown to exhibit longer delays and fire more spikes than vMGB neurons (Yu et al., 2004; Hu et al., 1995, 2003; Bartlett & Smith, 1999). It has been strongly suggested that higher-order neurons, presumably such neurons that relay modulator information predominately, burst more than first-order neurons (Sherman et al., 2001). Although neurons in both the dMGB and vMGB may respond with fast excitatory synaptic potentials, mediated by glutamate acting on N-methyl-D-aspartate (NMDA) and non-NMDA receptors, neurons exclusively found in the dMGB display a predominant slow synaptic potential that is associated with NMDA receptors (Hu, 1995). The multi-modal dMGB also sends efferents more broadly than the vMGB neurons and, thusly, receives reciprocal innervation from each of the respective structures such as the amygdala and association auditory cortical regions (Shinonaga, 1994; Deschenes et al., 1998; Doron & Ledoux, 2000). These synaptic properties are consistent with the respective intrinsic properties of the dMGB and vMGB. As such, the dMGB is thought to play a more prominent role in cortico-thalamo-cortical processing of information further downstream (Sherman, 2001). Similar to the auditory periphery, the neurons that receive more converging inputs, the dMGB or Type II spiral ganglion neurons, possess longer spike latency, rise time constants, and higher firing rates.

According to Sherman and Guillery's definition, the vMGB and the dMGB would then possess neurons that are intrinsically predisposed to relay "driver" and "modulator" information, respectively.

4.10 Conclusion

The question is of functionality, to the extent that it is based upon intrinsic physiological characteristics. An intracellular approach looking at intrinsic properties "reflects a closed reference system" (Llinas et al., 1988). Such a system affords us the opportunity to ascertain the integrative capacity, thereby defining the inherent limits or the physiological boundaries, of a particular neuron.

Upon comparison of the firing properties, innervation patterns, and roles of neurons in the auditory periphery and the thalamus, two functional organizational structures are suggested. Firstly, the Sherman and Guillery paradigm of modulator and driver organization may be correlated to the response differences. The neurons in the vMGB (and the Type I SGN) have shorter latency and rise time kinetics to spiking, are along the primary path to the cortex, and exhibit more rapid accommodation. These properties may be more useful in relaying driver input. The neurons in the dMGB (and Type II SGN) have longer latency and rise time constants to spiking, are along a secondary path, and exhibit slower and more variable accommodation rates. These properties may be better for relaying modulator information.

Secondly, the role of action potential latency and rise time constant may be determinants of a functional organizational structure, in and of themselves. They help determine the spike timing and are therefore the axial that turns the wheel with the spikes as the spokes, determining precisely when and where each spoke or spike will occur in time.

Spike timing is regulated by specific intrinsic physiology, i.e. action potential latency and rise time constantss.

In the cochlea and in the thalamus, two separate processing stages in the auditory system, an "ordered heterogeneity" of intrinsic electrophysiological properties have been explored. In the SGNs, the action potential latency, rise time constant, accommodation rates, and other parameters were found to be heterogeneous in the temporal component of their response. This heterogeneity is ordered along the tonotopic axis and suggests a functional role for these properties in the cochlea. As a further exploration into the significance of these electrophysiological properties as functional, experiments were done centrally, in the vMGB and dMGB, and the results indicate that the former proposed functional organization of "ordered heterogeneity" for the encoding of the modality of sound may not apply in this case but it could not be unequivocally ruled out. Interestingly, a modality related ordered heterogeneity along the tonotopic axis was not the only ordered heterogeneity to be found.

In addition to this ordered heterogeneity for the encoding of the modality of sound the Type I and Type II SGN groups, which have established functional distinctions, can also be correlated to an ordered heterogeneity of firing properties. Type I SGNs (and vMGB neurons) relay diverging information precisely and with high resolution whereas Type II SGNs (and dMGB neurons) relay converging input from many sources with low specific frequency resolution. The vMGB and the Type I SGNs relay a specific derivative of information. The dMGB and Type II SGNs relay an integrated input of information.

The latter suggested organization of a derivative or integration distinction evident in the subthreshold kinetics and organized by location is the primary theme of this dissertation. The vMGB must relay precisely resolved information from a specific frequency source, hence the precise tuning properties, implying a role in relaying discrete frequency information. This does not suggest that the vMGB dendrites receive input from one synaptic partner like the Type I SGNs, which receive input from a single inner hair cell. Yet it is suggested that the

vMGB relay cells' role may be to derive, irrespective of how it is received, a more discrete input for relay. The dMGB possesses broad tuning properties, implying a relay of multiple frequency sources, at least, and a greater integrative demand. The two groups do not have significantly different resting or threshold membrane potential but they differ in their intrinsic integrative capacity. The respective derivation or integration is a function of the kinetics of the subthreshold conductances that take place between the resting and threshold membrane potential before culminating in the all-or-nothing spike signal. Therefore the intrinsic physiology may be a critical component to understanding the information processing of individual neurons and the organizational structure of various nerve groups. Future studies on the functional relationship between intrinsic subthreshold kinetics and the presynaptic input should reveal new vistas for the elucidation of neural encoding,

5.0 REFERENCES

ADAMSON C., REID M., and DAVIS R. (2002a) Opposite actions of brain-derived neurotrophic factor and neurotrophin-3 on firing features and ion channel composition of murine spiral ganglion neurons. J. Neurosci. 22: 1385 - 1396.

ADAMSON C., REID M., MO Z., and DAVIS R. (2002b) Firing features and potassium channel content of murine spiral ganglion neurons vary with cochlear location. J. Comp. Neurol. 447: 331 - 350.

AITKIN L., DICKHAUS H., SCHULT W., and ZIMMERMANN M. (1978) External nucleus of inferior colliculus: auditory and spinal somatosensory afferents and their interactions. J. Neurophysiol. 41: 837 - 847.

ALBE-FESSARD D. and BUSER P. (1953) Exploration of certain activities of the motor cortex in cat with microelectrodes; endo-somatic leads. J. Physiol. (Paris) 45: 14 – 16.

ALVING B. (1968) Spontaneous activity in isolated somata of Aplysia pacemaker neurons. J. Gen. Physiol. 51: 29 - 45.

ANDERSON P. and ECCLES J. (1962) Inhibitory phasing of neuronal discharge. Nature 196: 645 - 647.

BADER C. and BERTRAND D. (1984) Effect of changes in intra- and extracellular sodium on the inward (anomalous) rectification in salamander photoreceptors. J. Physiol. (Lond) 347: 611 - 631.

BAJO V., ROUILLER E., WELKER E., CLARKE S., VILLA A., DE RIBAUPIERRE Y., and DE RIBAUPIERRE F. (1995) Morphology and spatial distribution of corticothalamic terminals originating from the cat auditory cortex. Hear. Res. 83: 161 - 74.

BAL R. and OERTEL D. (2000) Hyperpolarization-activated, mixed-cation current (I_h) in octopus cells of the mammalian cochlear nucleus. J. Neurophysiol. 84: 806 – 817.

BANKS M., PEARCE R., and SMITH P. (1993) Hyperpolarization-activated cation current (I_h) in neurons of the medial nucleus of the trapezoid body: voltage-clamp analysis and enhancement by norepinephrine and cAMP suggest a modulatory mechanism in the auditory brain stem. J. Neurophysiol. 70: 1420 - 32.

BARBARESI P., SPREAFICO R., FRASSONI C., and RUSTIONI A. (1986) GABAergic neurons are present in the dorsal column nuclei but not in the ventroposterior complex of rats. Brain Res. 382: 305 - 26.

BARRY P. and LYNCH B. (1991) Liquid junction potentials and small cell affects in patch-clamp analysis. J. Membr. Biol. 121: 101 - 117.

BARTLETT E. and SMITH P. (1999) Anatomic, intrinsic, and synaptic properties of dorsal and ventral division neurons in rat medial geniculate body. J. Neurophysiol. 81: 1999 - 2016.

BARTLETT E., STARK J., GUILLERY R., and SMITH P. (2000) Comparison of the fine structure of cortical and collicular terminals in the rat medial geniculate body. Neuroscience 100: 811 – 828.

BENTIVOLGIO M., SPREAFICO R., ALVAREZ-BOLADO G., SANCHEZ M., and FAIREN A. (1991) Differential expression of the GABA$_A$ receptor complex in the dorsal thalamus and reticular nucleus: An immunohistochemical study in the adult and developing rat. Eur. J. Neurosci. 3: 118 - 125.

BLUMERG-FELDMAN H. and EILAM D. (1995) Postnatal development of sychronous stepping in the gerbil (Gerbillus Dasyurus). J. Exper. Biol. 198: 363 - 372.

BOKOR H., FRERE S., EYRE M., SLEZIA A., ULBERT I., LUTHI A., and ACSADY L. (2005) Selective GABAergic control of higher order thalamic relays. Neuron 45: 929 - 940.

BORDI F. and LEDOUX J. (1994) Response properties of single units in areas of rat auditory thalamus that project to the amygdala. I. Acoustic discharge patterns and frequency receptive fields. Exp. Brain Res. 98: 261 - 274.

BRECHT M. and SAKMANN B. (2006) Cortex is driven by weak but synchronously active thalamocortical synapses. Science 312: 1622 – 1627.

BRUMBERG J., NOWAK L., and MCCORMICK D. (2000) Ionic mechanisms underlying repetitive high-frequency burst firing in supragranular cortical neurons. J. Neurosci. 20: 4829 – 4843.

BUDINGER E., HEIL P., and SCHEICH H. (2000) Functional organization of auditory cortex in the mongolian gerbil (Meriones unguiculatus). IV. Connections with anatomically characterized subcortical structures. Eur. J. Neurosci. 12: 2452 - 74.

CALFORD M. (1983) The parcellation of the medial geniculate body of the cat defined by the auditory response properties of single units. J. Neurosci. 3: 2350 - 2364.

CALFORD M. and WEBSTER W. (1981) Auditory representation within principal division of cat medial geniculate body: An electrophysiological study. J. Neurophysiol. 45: 1013 - 1028.

CALVIN W. and SYPERT G. (1976) Fast and slow pyramidal tract neurons: An intracellular analysis of their contrasting repetitive firing properties in the cat. J. Neurophysiol. 39: 420 – 434.

CASSEDAY J., EHRLICH D., and COVEY E. (2000) Neural measurement of sound duration: control by excitatory-inhibitory interactions in the inferior colliculus. J. Neurophysiol. 84: 1475 – 1487.

CLERICI W. and COLEMAN J. (1998) Postnatal cytoarchitecture of the rat medial geniculate body. J. Comp. Neurol. 399: 110 - 124.

CONNORS B., GUTNICK M., and PRINCE D. (1982) Electrophysiological properties of neocortical neurons in vitro. J. Neurophysiol. 48: 1302 – 1320.

CONTRERAS D. (2004) Electrophysiological classes of neocortical neurons. Neural Netw. 17: 633 - 646.

COREY D. and HUDSPETH A. (1983) Kinetics of the receptor current in bullfrog saccular hair cells. J. Neurosci. 3: 962 – 76.

CRICK F. (1984) Memory and molecular turnover. Nature 312: 101.

DALLOS P. (1992) The active cochlea. J. Neurosci. 12:4575 - 85.

DEBAY D., WOLFART J., LE FRANC Y., LE MASSON G., and BAL T. (2004) Exploring spike transfer through the thalamus using hybrid artificial-biological neuronal networks. J. Physiol. (Paris) 98: 540 - 58.

DE LA PENA E. and GEIJO-BARRIENTOS E. (2000) Participation of low threshold calcium spikes in excitatory synaptic transmission in guinea pig medial frontal cortex. Eur. J. Neurosci. 12: 1679 – 1686.

DE RIBAUPIERRE F. (1997) Acoustical information processing in the auditory thalamus and cerebral cortex. In: The Central Auditory System, edited by Ehret G and Romand R. New York: Oxford, Chapt. 5: 317 – 397.

DESCHENES M., PARADIS M., ROY J., and STERIADE M. (1984) Electrophysiology of neurons of lateral thalamic nuclei in cat: Resting properties and burst discharges. J. Neurophysiol. 55: 1196 - 1219.

DESCHENES M., VEINANTE P., and ZHANG Z. (1998) The organization of corticothalamic projections reciprocity versus parity. Brain Res. Rev. 28: 286 - 308.

DESTEXHE A., NEUBIG M., ULRICH D., and HUGUENARD J. (1998) Dendritic low threshold calcium currents in thalamic relay cells. J. Neurosci. 18: 3574 – 3588.

DIAMOND I., FITZPATRICK D., and SCHMECHEL D. (1993) Calcium binding proteins distinguish large and small cells of the ventral posterior and lateral geniculate nuclei of the prosimian galago and the tree shrew (Tupaia belangeri). Proc. Natl. Acad. Sci. U S A. 90:1425-9 (REID M).

DIFRANCESCO D. (1981) A study of the ionic nature of the pace-maker current in calf Purkinje fibers. J. Physiol. (Lond) 314: 377 - 393.

DIFRANCESCO D., FERRONI A., MAYYANTI M., and TROMBA C. (1986) Properties of the hyperpolarizing-activated current (i_f) in cells isolated from the rabbit sino-atrial node. J. Physiol. (Lond) 377: 61 - 88.

DORON N. and LEDOUX J. (2000) Cells in the posterior thalamus project to both amygdala and temporal cortex: a quantitative retrograde double-labeling study in the rat. J. Comp Neurol. 425: 257 - 274.

EDMAN A. and GRAMP W. (1989) Ion permeation through hyperpolarization-activated membrane channels (Q-channels) in the lobster stretch receptor neurone. Pflügers Arch. 413: 249 - 55.

EDWARDS F., KONNERTH A., SAKMANN B., and TAKAHACHI T. (1989) A thin slice preparation for patch clamp recordings from neurones of the mammalian central nervous system. Pflugers Arch. 414: 600 - 12.

FLEIDERVISH I., FRIEDMAN A., and GUTNICK M. (1996) Slow inactivation of Na^+ current and slow cumulative spike adaptation in mouse and guinea-pig neocortical neurones in slices. J. Physiol. 493: 83 - 97.

FOELLER E., VATER M., and KOSSL M. (2001) Laminar analysis of inhibition in the gerbil primary auditory cortex. J. Assoc. Res. Otolaryngol. 2: 279 - 96.

FRANZ O., LISS B., NEU A., and ROEPER J. (2000) Single-cell mRNA expression of HCN1 correlates with a fast gating phenotype of hyperpolarization-activated cyclic nucleotide-gated ion channels (I_h) in central neurons. Eur. J. Neurosci. 12: 2685 - 2693.

GATES G. and AITKIN L. (1982) Auditory cortex in the marsupial opossum, *Trichosurus vulpecula*. Hear. Res. 7: 1 - 11.

GEIGER J., BISCHOFBERGER J., VIDA I., FROBE U., PFITZINGER S., WEBER H., HAVERKAMPF K., and JONAS P. (2002) Patch-clamp recording in brain slices with improved slicer technology. Pflugers Arch. 443: 491 - 501.

GETTING P. (1989) Emerging principles governing the operation of neural networks. Ann. Rev. Neurosci. 12: 185 – 204.

GLIMCHER P. and LAU B. (2005) Rethinking the thalamus. Nat. Neurosci. 8: 983 - 984.

GRAY C. and MCCORMICK D. (1996) Chattering cells: Superficial pyramidal neurons contributing to the generation of synchronous oscillations in the visual cortex. Science 274: 109 – 113.

HAFIDI A. (1998) Peripherin-like immunoreactivity in type II spiral ganglion cell body and projections. Brain Res. 805: 181 – 190.

HAMILL O., MARTY A., NEHER E., SAKMANN B., and SIGWORTH F. (1981) Improved patch-clamp techniques for high-resolution current recording from cells and cell-free membrane patches. Pflugers Arch. 391: 85 - 100.

HE J. (2002) OFF responses in the auditory thalamus of the guinea pig. J. Neurophysiol. 88: 2377 - 2386.

HE J. (2004) Corticofugal modulation of the auditory thalamus. Exp. Brain Res.153: 579 - 90.

HERTZ J., KROGH A., and PALMER R. (1991) Introduction to the theory of neural computation. Addison-Wesley, Redwood City, California.

HILLE B. (2001) Ion Channels of Excitable Membranes. Third Edition. Sinauer Associates Publishers.

HODGKIN A. and HUXLEY A. (1939) Action potentials recorded from inside a nerve fiber. Nature (Lond) 104: 710 - 711.
.
HODGKIN A. and HUXLEY A. (1945) Resting and action potentials in single nerve fibres. J. Physiol. 104: 176 - 195.

HODGKIN A. and HUXLEY A. (1952a) Currents carried by sodium and potassium ions through the membrane of the giant axon of Loligo. J Physiol. 116: 449 - 72.

HODGKIN A. and HUXLEY A. (1952b) A quantitative description of membrane current and its application to conduction and excitation in nerve. J. Physiol. 117: 500 - 544.

HODGKIN A. and HUXLEY A. (1952c) Movement of sodium and potassium ions during nervous activity. Cold Spring Harb Symp Quant Biol. 17: 43 - 52.

HODGKIN A., HUXLEY A., and KATZ B. (1952d) Measurement of current-voltage relations in the membrane of the giant axon of Loligo. J. Physiol. 116: 424 - 48.

HU B., SENATOROV V., and MOONEY D. (1994) Lemniscal and non-lemniscal synaptic transmission in rat auditory thalamus. J. Physiol. (Lond) 479: 217 – 231.

HU B. (1995) Cellular basis of temporal synaptic signalling: an in vitro electrophysiological study in rat auditory thalamus. J. Physiol. (Lond) 483: 167 – 182.

HU B. (2003) Functional Organization of lemniscal and nonlemniscal auditory thalamus Exp. Brain. Res.153: 543 - 549.

HUBEL D. and LIVINGSTON M. (1981) Effects of sleep and arousal on the processing of visual information in the cat. Nature 291: 554 - 61.

JAHNSEN H. and LLINAS R. (1984a) Ionic basis for the electro-responsiveness and oscillatory properties of guinea-pig thalamic neurones in vitro. J. Physiol. (Lond.) 349: 227 – 247.

JAHNSEN H. and LLINAS R. (1984b) Electrophysiological properties of guinea-pig thalamic neurones: an in vitro study. J. Physiol. (Lond.) 349: 205 – 226.

JACKSON A., YAO G., and BEAN B. (2004) Mechanism of spontaneous firing in dorsomedialsuprachiasmatic nucleus neurons. J. Neurosci. 24: 7985 – 7998.

JONES E. (1975) Some aspects of the organization of the thalamic reticular complex. J. Comp. Neurol. 162: 285 – 308.

JONES E. (1985) The Thalamus. New York, Plenum Press.

JONES E. (2003) Chemically defined parallel pathways in the monkey auditory system. Ann. N.Y. Acad. Sci. 999: 218 - 233.

JUNG H., MICKUS T., and SPRUSTON N. (1997) Prolonged sodium channel inactivation contributes to dendritic action potential attenuation in hippocampal pyramidal neurons. J. Neurosci. 17: 6639 - 46.

JUUSOLA M., ROBINSON H., and POLAVIEJA G. (2007) Coding with spike shapes and graded potentials in cortical networks. Bioassays 29: 178 - 187.

KATZ L. (1962) The Croonian Lecture. The transmission of impulses from nerve to muscle, and the subcellular unit of synaptic action. Pro. R. Soc. Biol. 155: 455 - 477.

KAAS J. and HACKETT T. (2000) Subdivisions of auditory cortex and processing streams in primates. Proc. Natl. Acad. Sci. U S A. 97:11793 -11799.

KIANG N., WATANABE T., THOMAS E., and CLARK L. (1965) Discharge patterns of single fibers in the cat's auditory nerve. M.I.T. Press, Cambridge.

KIMURA A., DONISHI T., SAKODA T., HAZAMA M., and TAMAI Y. (2003) Auditory thalamic nuclei projections to the temporal cortex in the rat. Neuroscience 117: 1003 – 1016.

KOCH C. and SEGEV I. (2000) The role of single neurons in information processing. Nat. Neurosci. 3: 1171 - 1177

KÖSSL M., CORA F., SEYFARTH E., and NÄSSIG W. (2007) Otoacoustic emissions from insect ears having just one auditory neuron. .J Comp. Physiol. A Neuroethol. Sens. Neural Behav. Physiol. 193: 909 – 915.

KUDO M., TASHIRO T., HIGO S., MATSUYAMA T., and KAWAMURA S. (1984) Ascending projections from the nucleus of the brachium of the inferior colliculus in the cat. Exp. Brain Res. 54: 203-211.

LARKUM M., LAUNEY T., DITYATEV A., and LÜSCHER H. (1998) Integration of excitatory postsynaptic potentials in dendrites of motoneurons of rat spinal cord slice cultures. J. Neurophysiol. 80: 924 - 35.

LARKUM M., ZHU J., and SAKMANN B. (1999) A new cellular mechanism for coupling inputs arriving at different cortical layers. Nature 398: 338 - 41.

LARKUM M. (2004) Top-down dendritic input increases the gain of layer 5 pyramidal neurons. Cereb. Cortex 14: 1059 - 1070.

LAY D. (1972) The anatomy, physiology, functional significance and evolution of specialized hearing organs of gerbilline rodents. J. Morphol. 138: 41 - 120.

LE GROS CLARK W. (1932) Structure and connections of the thalamus. Brain 55: 406 – 470.

LEDOUX J., RUGGIERO D., and REIS D. (1985) Projections to the subcortical forebrain from anatomically defined regions of the medial geniculate body in the rat. J. Comp. Neurol. 242: 182 - 213.

LEDOUX J., RUGGIERO D., FOREST R., STOMETTA R., and REIS D. (1987) Topographic organization of convergent projections to the thalamus from the inferior colliculus and spinal cord in the rat.J. Comp. Neurol. 264: 123 - 146.

LI C. (1959) Cortical intracellular potentials and their responses to strychnine. J. Neurophysiol. 22: 436 – 450.

LIBERMAN M. (1978) Auditory-nerve response from cats raised in a low noise chamber. J. Acoust. Soc. Am. 63: 442 – 455.

LIBERMAN M. and OLIVER M. (1984) Morphometry of intracellularly labeled neurons of the auditory nerve: correlations with functional properties. J. Comp. Neurol. 223: 163 - 176.

LIU X., HONDA C., and JONES E. (1995) Distribution of four types of synapse on physiologically identified relay neurons in the ventral posterior thalamic nucleus of the cat. J. Comp. Neurol. 352: 69 – 91.

LIU X. and JONES E. (1999) Predominance of corticothalamic synaptic inputs to thalamic reticular nucleus neurons in the rat. J. Comp. Neurol. 414: 67 – 79.

LLINAS R. (1988) The intrinsic electrophysiological properties of mammalian neurons: insights into central nervous system function. Science 242:1654-64.

LLINAS R. (1990) Intrinsic electrical properties of nerve cells and their role in network oscillation. Cold Spring Harb. Symp. Quant Biol. 55: 933 - 8.

LUI Q. and DAVIS R. (2007) Regional specification of threshold sensitivity and response time in CBA/CaJ mouse spiral ganglion neurons. J. Neurophysiol. 98: 2215 – 2222.

LUTHI A. and MCCORMICK D. (1988) H-current: properties of a neuronal and network pacemaker. Neuron 21: 9 – 12.

MACCAFERRI G., MANGONI M., LAZZARI A., and DI FRANCESCO D. (1993) Properties of the hyperpolarization-activated current in rat hippocampal CA1 pyramidal cells. J. Neurophysiol. 69: 2129 - 36.

MANIS P. (1990) Membrane properties and discharge characteristics of guinea pig dorsal cochlear nucleus neurons studied in vitro. J. Neurosci. 10: 2338 - 51.

MASTERTON B., HEFFNER H., and RAVIFFA R. (1969) The evolution of human hearing. J. Acoust. Soc. Am. 45: 966 - 85.

MAYER M. and WESTBROOK G. (1983) A voltage-clamp analysis of inward (anomalous) rectification in mouse spinal sensory ganglion neurones. J. Physiol. (Lond) 340: 19 - 45.

MCCORMICK D. and BAL T. (1997) Sleep and arousal: thalamocortical mechanisms. Ann. Rev. Neurosci. 20: 185 – 215.

MCCORMICK D., CONNORS B., LIGHTHALL J., and PRINCE D. (1985) Comparative electrophysiology of pyramidal and sparsely spiny stellate neurons of the neocortex. J. Neurophysiol. 54: 782 – 806.

MCCORMICK D. and HUGUENARD J. (1992) A model of the electrophysiological properties of thalamocortical relay neurons. J. Neurophysiol. 68: 1384 - 1400.

MCCORMICK D. and PAPE H. (1990) Properties of a hyperpolarization activated-cation current and its role in rhythmic oscillation in thalamic relay neurones. J. Physiol. (Lond) 431: 291 – 318.

MERZENLICH M. and SCHREINER C. (1992) Mammalian auditory cortex- some comparative observations- In: Webster DB, Fay RR, Popper AN (eds) The evolutionary biology of hearing, pp 673 - 689. Springer, Berlin Heidelberg New York.

MILLER J., CHI D., O'KEEFE L., KRUSZKA P., RAPHAEL Y., and ALTSCHULER R. (1997) Neurotrophins can enhance spiral ganglion cell survival after inner hair cell loss. Int. J. Dev. Neurosci. 15: 631 - 643.

MILLER J., ESCABI M., READ H., and SCHREINER C. (2001a) Functional convergence of response properties in the auditory thalamocortical system. Neuron 32: 151 - 60.

MILLER J., ESCABI M., and SCHREINER C. (2001b) Feature selectivity and interneuronal cooperation in the thalamocortical system. J. Neurosci. 21: 8136 - 44.

MILLER J. and SCHREINER C. (2000) Stimulus-based state control in the thalamocortical system. J. Neurosci. 20: 7011 - 6.

MO Z. and DAVIS R. (1997a) Endogenous firing patterns of murine spiral ganglion neurons. J. Neurophysiol. 77: 1294 - 305.

MO Z. and DAVIS R. (1997b) Heterogeneous voltage dependence of inward rectifier currents in spiral ganglion neurons. J. Neurophysiol. 78: 3019 - 2.

MOONEY D., ZHANG L., BASILE C., SENATOROV V., NQSEE J., OMAR A., and HU B. (2004) Distinct forms of cholinergic modulation in parallel thalamic sensory pathways. Proc. Nat. Acad. Sci. 101: 320 - 324.

MOREST D. (1964) The neuronal architecture of the medial geniculate body of the cat. J. Anat. Lond. 98, 4, 611 - 630.

MOREST D. (1965) The lateral tegmental system of the midbrain and the medial geniculate body: study with Golgi and Nauta methods in cat. J. Anat. 99: 611 - 634.

MOREST D. and WINER J. (1986) The comparative anatomy of neurons: Homologous neurons in the medial geniculate body of the opossum and the cat. Adv. Anat. Embryol. Cell. Biol. 97: 1 – 94.

MOONEY D., ZHANG L., BASILE C., SENATOROV V., NGSEE J., OMAR A., and HU B. (2004) Distinct forms of cholinergic modulation in parallel thalamic sensory pathways. Proc. Natl. Acad. Sci. U S A 101: 320 – 324.

MOORE R. and GOLDBERG J. (1963) Ascending projections of the inferior colliculus in the cat. J. Comp. Neurol. 121: 109 - 135.

MOUNTCASTLE V., TALBOT W., SAKATA H., HYVARINEN J. (1969) Cortical neuronal mechanisms in flutter-vibration studied in unanesthetized monkeys. Neuronal periodicity and frequency discrimination. J. Neurophysiol. 32: 452 - 84.

MÜLLER M., FELMY F., SCHWALLER B., SCHNEGGENBURGER R. (2007) Parvalbumin is a mobile presynaptic Ca^{2+} buffer in the calyx of held that accelerates the decay of Ca^{2+} and short-term facilitation. J. Neurosci. 27: 2261 - 71.

NADOL J., BURGESS B., and REISSER C. (1990) Morphometric analysis of normal human spiral ganglion cells. Ann. Otol. Rhinol. Laryngol. 99: 340 - 348.

NEHER E. and SAKMANN B. (1975) Voltage-dependence of drug-induced conductance in frog neuromuscular junction. Proc. Nat. Acad. Sci. 72: 2140 - 2144.

NERNST W. (1893) *Theoretische Chemie vom Standpunkte der Avogadro'schen Regel und der Thermodynamik* (Theoretical chemistry from the standpoint of Avogadro's rule and thermodynamics) Stuttgart, F. Enke, 1893 [5th editon, 1923]

NUNEZ A., AMZICA F., and STERIADE M. (1993) Electrophysiology of cat association cortical cells *in vivo*: Intrinsic properties and synaptic responses. J. Neurophysiol. 70: 418–430.

OJIMA H. (1994) Terminal morphology and distribution of corticothalamic fibers originating from layers 5 and 6 of cat primary auditory cortex. Cereb. Cortex 4: 646 – 663.

OERTEL D. (1997) Encoding of timing in the brain stem auditory nuclei of vertebrates. Neuron. 19: 959 - 62.

OERTEL D. (1999) The Role of Timing in the Brainstem Auditory Nuclei of Vertebrates. Annu. Rev. Physiol. 61: 497 – 519.

OERTEL D. (1991) The role of intrinsic neuronal properties in the encoding of auditory information in the cochlear nuclei. Curr. Opin. Neurobiol 1: 221 - 8.

OERTEL D. (2006) Hyperpolarization-activated currents regulate excitability in stellate cells of the mammalian ventral cochlear nucleus. J. Neurophys. 95: 76 - 87.

OVERSTREET E., RICHTER C., TEMCHIN A., CHEATHAM M., and RUGGERO M. (2003) High-frequency sensitivity of the mature gerbil cochlea and its development. Audiol Neurootol. 8: 19 - 27.

PANZERI S., PETERSEN R., SCHULTZ S., LEVEDEV M., and DIAMOND M. (2001) The role of spike timing in the coding of stimulus location in rat somatosensory cortex. Neuron 29: 769 - 277.

PANZERI S. and SCHULTZ S. (2001) A unified approach to the study of temporal, correlational, and rate coding. Neural Comput. 13: 1311 -1349.

PAPE H. (1994) Specific bradycardic agents block the hyperpolarization-activated cation current in central neurons. Neuroscience 59: 363 - 73.

PAPE H. (1996) Queer current and pacemaker: the hyperpolarization activated cation current in neurons. Ann. Rev. Physiol. 58: 299 – 327.

PAXINOS G. and WATSON C. (1986) The Rat Brain in Stereotaxic Coordinates. San Diego. Academic Press.

PENNY G., CONLEY M., SCHMECHEL D., and DIAMOND I: (1984) The distribution of glutamic acid decarboxylase immunoreactivity in the diencephalon of the opossum and rabbit. J. Comp. Neurol. 228: 38 - 56.

PERUZZI D., BARTLETT E., SMITH P., and OLIVER D. (1997) A monosynaptic GABAergic input from the inferior colliculus to the medial geniculate body in rat. J. Neurosci. 17: 3766 - 3777.

PERKINS R. and MOREST K. (1975) A study of cochlear innervation patterns in cats and rats with the Golgi method and Nomarkski Optics. J. Comp. Neurol. 163: 129 - 58.

PHILLIPS C. (1956) Intracellular records from Betz cells in the cat. Quart. J. Exper. Physiol. Cogn. Med. Sci. 41: 58 – 69.

RAMEN I., GUSTAFSON A., PADGETT D. (2000) Ionic currents and spontaneous firing in neurons isolated from the cerebellar nuclei. J. Neurosci. 20: 9004 – 9016.

RAMCHARAN E., GNADT J., and SHERMAN S. (2005) Higher order thalamic relays burst more than first-order relays. Proc. Nat. Acad. Sci. USA 34. 12236 - 12241.

RAPHAEL Y. and ALTSCHULER R. (2003) Structure and innervation of the cochlea. Brain Res. Bull: 60: 397 - 422.

RIEKE F., WARLAND D., DE RUYTER V., STEVENINCK R., and BIALEK W. (1997) Spikes Exploring the Neural Code, pp. 121 – 127. MIT Press.

RINGER S. (1882a) Concerning the influence exerted by each of the constituents of the blood on the contraction of the ventricle. J. Physiol. 3: 195 - 202.

RINGER S (1882b) Concerning the influence exerted by each of the constituents of the blood on the contraction of the ventricle. J. Physiol. 3: 380 - 393.

RINGER S (1883a) A further contribution regarding the influence of the different constituents of the blood on the contraction of the heart. J. Physiol. 4: 29 - 42.

RINGER S. (1883b) A third contribution regarding the influence of the inorganic constituents of the blood on the ventricular contraction J. Physiol. 4: 222 - 225

ROGELIS A. and OERTEL D. (2006) Hyperpolarization-Activated Currents Regulate Excitability in Stellate Cells of the Mammalian Ventral Cochlear Nucleus J. Neurophysiol. 95: 76 – 87.

ROMANSKI L. and LEDOUX J. (1993) Information cascade from primary auditory cortex to the amygdala: corticocortical and corticoamygdaloid projections of temporal cortex in the rat. Cereb. Cortex. 3: 515 - 32.

ROSE J. and WOOSLEY C. (1958) Cortical connections and functional organization of the thalamic audiotry system of the cat. In Biological and Biochemical Bases of Behavior, p.127. Ed. H.F. Harlow and C.N. Woolsey, Madison: University Wisconsin Press.

ROUILLER E. and WELKER E. (1991) Morphology of corticothalamic terminals arising from the auditory cortex of the rat: a *Phaseolus vulgaris*leucoagglutinin (PHA-L) tracing study. Hear. Res. 56: 179 – 190.

ROGER M. and ARNAULT P. (1989) Anatomical study of the connections of the primary auditory area in the rat. J. Comp. Neurol. 287: 339 – 356.

ROUILLER E., COLOMB E., CAPT M., and DE RIBAUPIERRE F. (1985a) Projections of the reticular complex of the thalamus onto physiologically characterized regions of the medial geniculate body. Neurosci. Lett. 53: 227 – 232.

ROUILLER E. AND DE RIBAUPIERRE F. (1985b) Origin of afferents to physiologically defined regions of the medial geniculate body of the cat: ventral and dorsal divisions. Hear. Res. 19: 97 – 114.

RYAN A. (1976) Hearing sensitivity of the Mongolian gerbil, *Meriones unguiculatis*. J. Acoust. Soc. Am. 59: 5.

RYUGO D. (1992)''The auditory nerve: Peripheral innervation, cell body morphology, and central projections,'' in The Mammalian Auditory Pathway:Neuroanatomy, edited by D.B. Webster, A.N. Popper, and R.R. Fay, pp. 23–65.Springer-Verlag, New York.

SAKMANN B. and NEHER E. (1976) Patch clamp techniques for studying ionic channels in excitable membranes. Annu. Rev. Physiol. 46: 455 - 72.

SANTORO B., LIU D., YAO H., BARTSCH D., KANDEL E., SIEGELBAUM S., and TIBBS G. (1998) Identification of a gene encoding a hyperpolarization activated pacemaker channel of brain. Cell 93: 717 – 729.

SCHEICH H., HEIL P., and LANGER G. (1993) Functional organization of auditory cortex in the mongolian gerbil (Meriones unguiculatus). II. Tonotopic 2-deoxyglucose. Eur. J. Neurosci. 5: 898 - 914.

SCHNITZLER H. and HENSON O. (1980) Performance of airborne animal sonar systems. I. Microchiroptera. In: Busnel RG, Fish JF (eds) Animal sonar systems. , pp 109–181. Plenum Press, New York.

SCHNITZLER H. and KALKO E. (1998) How echolocating bats search and find food. In: Kunz TH, Racey PA (eds) Bats: hylogeny, morphology, echolocation, and conservation biology, pp 183–196. Smithsonian Institution Press, Washington, DC.

SCHWARZ D., TENNIGKEIT F., ADAM T., FINLAYSON P., and PUIL E. (1998) Membrane properties that shape the auditory code in three nuclei of the central nervous system. J Otolaryngol. 27: 311 - 7.

SEYFARTH E. and PEICHL L. (2002) A Hundred Years Ago: Julius Bernstein (1839-1917) Formulates His "Membrane Theory". Neuro*forum* 4: 274-276.

SHERMAN S. and GUILLERY R. (1996) The functional organization of thalamocortical relays. J. Neurophysiol. 76: 1367 – 1395.

SHERMAN S. and GUILLERY R. (1998) On the actions that one nerve cell can have on another: Distinguishing "drivers" from "modulators." Proc. Natl. Acad. Sci. USA 95: 7121 – 7126.

SHERMAN S. and GUILLERY R. (2001) Exploring the Thalamus. San Diego, CA: Academic Press.

SHANNON C. and WEAVER W. (1963) The Mathematical Theory of Communication. Illinois Books.

SHI C. and CASSELL M. (1997) Cortical, thalamic, and amygdaloid projections of rat temporal cortex. J. Comp. Neurol. 382: 153 – 175.

SHINONAGA Y., TAKADA M., MIZUNO N. (1994) Direct projections from the non-laminated divisions of the medial geniculate nucleus to the temporal polar cortex and amygdala in the cat. J. Comp. Neurol 340: 405 - 426.

SCHEEL M. (1988) Topographic organization of the auditory thalamocortical system in the albino rat. Anat. Embryol. 179: 181 – 190.

SIMMONS J. (1989) A view of the world through the bat's ear: the formation of acoustic images in echolocation, pp. 155 – 99. Neurobiology of Cognition.

SIMONS D. and WOOSLEY T. (1979) Functional organization in mouse barrel cortex. Brain Res. 165: 327 - 332.

SPAIN W., SCHWINDT P., and CRILL W. (1987) Anomolous rectification in neurons from cat sensorimotor cortex in vitro. J. Neurophysiol. 57: 1555 - 1576.

SPOENDLIN H. (1979) Sensory neural organization of the cochlea. J. Laryngol. Otol. 93: 853 – 877.

SPREAFICO R., SCHMECHEL D., ELLIS C., and RUSTIONI A: (1983) Cortical relay neurons and interneurons in the N. ventralis posterolateralis of cats: a horseradish peroxidase, electron-microscopic, Golgi and immunocytochemical study. Neuroscience 9: 491 - 509.

SPREAFICO R., FRASSONI C., ARCELLI P., and DE BIASI F. (1994) GABAergic interneurons in the somatosensory thalamus of the guinea-pig: a light and ultrastructural immunocytochemical investigation. Neuroscience 59: 961 - 73.

STERIADE M., NUNˇEZ A., and AMZICA F. (1993) A novel slow (1 Hz) oscillation of neocortical neurons in vivo: depolarizing and hyperpolarizing components. J. Neurosci. 13: 3252 – 3265.

STERIADE M., TIMOFEEV I., DURMULLER N., and GRENIER F. (1998) Dynamic properties of corticothalamic neurons and local cortical interneurons generating fast rhythmic (30–40 Hz) spike bursts. J. Neurophysiol. 79: 483 – 490.

STERIADE M. (2004) Neocortical cell classes are flexible entities. Nat. Rev. Neurosci. 5, 121 – 134.

SUGA N. (1988) Auditory neruoetholgoy an dspeech processing. Complex/sound processing by combination-sensitive neurons, pp. 679-720 In G. M. Edelman, W.E. Gall, and W. M. Cowan (eds), Auditory Function: Neurobiological Bases of Hearing, New York: Wiley.

TADDESE A. and BEAN B. (2002) Subthreshold sodium current from rapidly inactivating sodium channels drives spontaneous firing of tuberomammillary neurons. Neuron 33: 587 – 600.

TAKAHASHI K. (1965) Slow and fast groups of pyramidal tract cells and their respective membrane properties. J. Neurophysiol. 28: 908 – 924.

TASAKI I., POLLEY E., and ORREGO F. (1954) Action potentials from individual elements in cat geniculate and striate cortex. J. Neurophysiol. 17: 454 – 474.

TENNIGKEIT F., SCHWARZ D., and PUIL E. (1998) Modulation of bursts and high-threshold calcium spikes in neurons of rat auditory thalamus. Neuroscience 83:1063 - 73.

TENNIGKEIT F., SCHWARZ D., and PUIL E. (1997) Firing modes and membrane properties in lemniscal auditory thalamus. Acta Otolaryngol.117: 254 -257.

THOMAS H., TILLEIN J., HEIL P., and SCHEICH H. (1993) Functional organization of auditory cortex in the mongolian gerbil (*Meriones unguiculatus*). I. Electrophysiological mapping of frequency representation and distinction of fields. Eur. J. Neurosci.5:882-897.

VICTOR J. (2005) Spike Train Metrics. Curr. Opin. Neurobiol. 15: 585 - 592.

VICTOR J. (2000) How the Brain Uses Time to Represent and Process Visual Information. Brain Res. 886: 33 - 46.

WANG S., EISENBACK M., DATSKOVSKAIA A., BOYCE M., and BICKFORD M. (2002b) GABAergic pretectal terminals contact GABAergic interneurons in the cat dorsal lateral geniculate nucleus. Neurosci. Lett. 323: 141 – 145.

WARR W., BOCH J., and NEELY S. (1997) Efferent innervation of the inner hair cell region: origins and terminations of two lateral olivocochlear systems. Hear. Res. 108: 89 - 111.

WINER J., WENSTRUPP J., and LARUE D. (1992) Patterns of GABAergic immunoreactivity define subdivisions of the mustached bat's medial geniculate body.J. Comp. Neurol. 319: 172 - 90.

WINER J., SAINT MARIE R., LARUE D., and OLIVER D. (1996) GABAergic feedforward projections from the inferior colliculus to the medial geniculate body.Proc. Natl. Acad. Sci. USA 93: 8005 - 10.

WINER J., KELLY J, and LARUE T. (1999) Neural architecture of the rat medial genculate body. Hear. Res. 130: 19 – 41.

WEBSTER D. and PLASSMAN W. (1992) Parallel evolution of low-frequency sensitivity in old world and new world desert rodents. In R. R. Fay and A. N. Popper (eds.), The evolutionary biology of hearing, pp. 633-636. Springer, New York.

WEBSTER D. and WEBSTER M. (1978) Cochlear nerve projections following organ of corti destruction. Otolaryngology. 86: 342 - 353.

WILLIAMS S. and STUART G. (2000) Action potential backpropagation and somatodendritic distribution of ion channels in thalamocortical neurons. J. Neurosci. 20: 1307 − 1317.

WINER J., SAINT MARIE R., LARUE D., and OLIVER D. (1996) GABAergic feedforward projections from the inferior colliculus to the medial geniculate body. Proc. Natl. Acad. Sci. USA 93: 8005 - 8010.

WINER J, KELLY J., and LARUE D. (1999) Neural architecture of the rat medial geniculate body. Hear. Res. 130: 19 - 41.

WOLFART J., DEBAY D., LE MASSON G., DESTEXHE A., and BAL T. (2005) Synaptic background activity controls spike transfer from thalamus to cortex. Nat. Neurosci. 8: 1760 - 7.

YANAGIHARA K. and IRISAWA H. (1984) Inward Current activated during hyperpolarization in the rabbit sinoatrial node cell. Pflugers Arch. 385: 11 - 19.

YAU K., MATTHEWS G., and BAYLOR D. (1979) Thermal activation of the visual transduction mechanism in retinal rods. Nature 279: 806 - 807.

YU Y., XIONG Y., CHAN Y., and HE J. (2004) *In vivo* intracellular responses of the medial geniculate neurons to acoustic stimuli in anaesthetized guinea pigs. J. Physiol. 560: 191 - 205.

ZADOR A. (2000) The basic unit of computation. Nat. Neurosci. 3: 1167.

ZADOR A. (2001) Synaptic connectivity and computation. Nat. Neurosci. 4: 1157-8.

ZHAN X., COX C., and SHERMAN S. (2000) Dendritic depolarization efficiently attenuates low-threshold calcium spikes in thalamic relay cells. J. Neurosci. 20: 3909 − 3914.

ZHOU Q. (1997) Visualization of Calcium Influx Through Channels That Shape the Burst and Tonic Firing Modes of Thalamic Relay Cells J. Neurophysiol. 77: 2816 − 2825.

ZOHARY E., SHADLEN M., and NEWSOME W. (1994) Correlated neuronal discharge rate and its implication for psychophysical performance. Nature 370:140 - 143.

Curriculum Vitae

MICHAEL A. REID

70-A Siesmayer Strasse, Frankfurt, D-60323
michaelreid01@yahoo.com

WORK EXPERIENCE

HUMAN ACADEMY OF SCIENCES
Nov/2003-Present

Founder — **N**ew York, New York

Board member, created Charter (with input from Pontifical Academy of Sciences), appointed Board, Officers, Committee, and administrative support. Activities: Awards; initiatives to make science more relevant to laypeople; to serve humanity; security issues in biological research.

RESEARCH ASSOCIATE
Aug/99-March/03

Rockefeller University/ RutgersUniversity — *New York, New York /Piscataway, New Jersey*

Electrophysiology: In vivo and in vitro. Extra/intracellular. Patch-clamp technique, single-channel, voltage or current-clamp, slice work, injections, toxins. Molecular biology: RT-PCR, transfections, immunocytochemistry. General laboratory maintenance, cell cultures, microscopy, various analyses of data.

RESEARCH ASSOCIATE
Jan/98-Jan/00

Albert Einstein College of Medicine — *New York, New York*

Various genetic, molecular biological, or neurobiological projects focusing on the C. elegans utilizing the electron microscope, light microscope (i.e. DIC, epi- flourescence), immunocytochemistry, and various computer applications.

SMARTT TECH INC.
(1993-1997) Incorporated Jan/97-Present

Customized software development. — *New York, New York*

MONITOR
Apr/94-May/94

International Electoral Commission — *Eastern Cape, South Africa*

Monitored and observed the 1994 South African Elections in conjunction with the United Nations.

EDUCATION

B.S. BIOLOGY
1988-93

North Carolina Central University — *Durham, North Carolina*

NEUROBIOLOGY
1993-94

Duke University — *Durham, North Carolina*

Ph.D. NEUROBIOLOGY
2005-

J.W. Goethe University of Frankfurt — *United States & Germany*

TECHNICAL SKILLS

Electrophysiology, patch-clamp and extracellular. Immunocytochemistry. Western Blots. RT-PCR. Software development.

PUBLICATIONS

Reid, M.A. and Davis, R.Tonotopic distribution of voltage-gated ion currents in spiral ganglion neurons
ARO Abstract February 6, 2001

Reid, M.A. and Davis, R Opposite actions of BDNF and NT-3 on spiral ganglion electrophysiology
ARO AbstractFebruary 6, 2001

Reid, M.A., Adamson, C., and Davis, R **Firing Features and Potassium Channel Content of Murine Spiral Ganglion Neurons J. Comparative Neurology 447 : 331-350 2002**

Reid, M.A. and Davis, R Characterization of Peripherin-Positive Spiral Ganglion Neurons ARO Abstract
January 28, 2002

Reid, M.A., Adamson, C. and Davis, R **Opposite Actions of BDNF and NT-3 on Firing Features and Ion Channel Composition COVER ARTICLE J. Neuroscience February 15, 2002 22(4) 1385-1396**

Reid, M.A. and Davis, R Firing Properties of Putative Type II Spiral Ganglion NeuronsARO Abstract
February 26, 2003

Reid, M.A. and Davis, R European Inner Ear Conference Abstract September 2003

Reid, M.A., Flores, J. and Davis, R **Firing Features of Type II Spiral Ganglion Neurons in vitro. J. Neuroscience January 21, 2004 24 (3) 733-42.**

Reid, M.A. Functional Relevance of Intrinsic Response Properties of Neurons in the Gerbil (*Meriones unguiculatus*) Auditory Thalamus. Ph.D. Dissertation 2007.

MEETINGS/ AWARDS/ PRESENTATIONS
Physiologische Institute (Bern, Schweiz), ETH-Zurich (Zurich, Schweiz),Brain Mind Institute (Lausanne, Schweiz), J. W. Goethe Universitat Frankfurt Am Main (Frankfurt, Germany); Association for Research in Otolaryngology (ARO) Travel Award 2006; Centre National De La Recherche Scientifique (Paris, France) 2005; Infineon (Munchen, Germany) 2005; Darmstadt Technische Universitat (Darmstadt, Germany) 2005; Mount Sinai Med. Center (NY) 2005; Cornell Univ. Med. Center (NY) 2005; University of Heidelberg 2004; European Inner Ear Meeting (Spain) 2003; Eastern Auditory Regional Conference (Univ.Penn) 2002, 2003; Max Planck Institute for Medical Research (Heidelberg, Germany) 2002; Rutgers University Newark 2003; ARO Mid-Winter Meetings 2001, 2002, 2003.